

**REPUBLIC OF TURKEY
MUĞLA SITKI KOÇMAN UNIVERSITY
GRADUATE SCHOOL OF NATURAL AND APPLIED
SCIENCES**

DEPARTMENT OF CIVIL ENGINEERING

**POST-FIRE RESPONSE OF DIFFERENT STEEL
GRADE MATERIALS**

MASTER OF SCIENCE

VEYSEL POLAT

JUNE 2024

MUĞLA

MUĞLA SİTKİ KOÇMAN UNIVERSITY

Graduate School of Natural and Applied Sciences

APPROVAL OF THE THESIS

The thesis entitled **POST-FIRE RESPONSE OF DIFFERENT STEEL GRADE MATERIALS** is submitted by **VEYSEL POLAT** in partial fulfillment of the requirements for the degree of Master of Science in Civil Engineering Department by,

EXAMINING COMMITTEE MEMBERS

Assoc. Prof. Dr. Mutlu SEÇER (**Head of Committee**)

Civil Engineering Department,
İzmir Katip Çelebi University, İzmir

Asst. Prof. Dr. Özer ZEYBEK (**Supervisor**)

Civil Engineering Department,
Muğla Sıtkı Koçman University, Muğla

Assoc. Prof. Dr. Yasin Onuralp ÖZKILIÇ (**Co-Supervisor**)

Civil Engineering Department,
Necmettin Erbakan University, Konya

Asst. Prof. Dr. Süleyman Bahadır KESKİN (**Member**)

Civil Engineering Department,
Muğla Sıtkı Koçman University, Muğla

APPROVAL OF THE HEAD OF THE DEPARTMENT

Assoc. Prof. Dr. Altuğ SAYGILI

Head of Civil Engineering Department,
Muğla Sıtkı Koçman University, Muğla

Asst. Prof. Dr. Özer ZEYBEK

Supervisor, Civil Engineering,
Muğla Sıtkı Koçman University, Muğla

Assoc. Prof. Dr. Yasin Onuralp ÖZKILIÇ

Co-Supervisor, Civil Engineering,
Necmettin Erbakan University, Konya

Date: 28/06/2024

I hereby declare that all information in this document has been obtained and presented in accordance with academic rules and ethical conduct. I also declare that, as required by these rules and conduct, I have fully cited and referenced all materials and results that are not original to this work.



Veysel Polat

28/06/2024

ÖZET

FARKLI KALİTEDEKİ ÇELİK MALZEMELERİN YANGIN ETKİSİ SONRASINDAKİ DAVRANIŞI

Veysel POLAT

Yüksek Lisans Tezi

Fen Bilimleri Enstitüsü

İnşaat Mühendisliği Anabilim Dalı

Tez Yöneticisi: Dr. Öğr. Üyesi Özer ZEYBEK

Ortak Tez Yöneticisi: Doç. Dr. Yasin Onuralp ÖZKILIÇ

Haziran 2024, 66 sayfa

Geleneksel düşük karbonlu yapısal çelik, düşük karbon içeriği ile bilinen ve genellikle yapı sektöründe kullanılan çelik türüdür. Kolay şekillendirilebilir ve kaynak kullanılabilir özellikleri bu çeliği, binalar, köprüler ve çeşitli inşaat projelerinde yaygın olarak tercih edilen bir malzeme yapar. Düşük maliyeti ve iyi mekanik özellikleri nedeniyle, düşük karbonlu çelik yaygın bir şekilde kullanılmaktadır. Yüksek dayanımlı çelikler, yüksek dayanım/ağırlık oranı ve iyi deprem dayanımı gibi üstün özelliklere sahip olduklarıdan köprülerde ve yüksek binalarda yaygın olarak kullanılmaktadır. Yüksek sıcaklıklara maruz kalmak bu malzemelerin mukavemetini ve rijitliğini etkiler. Yangın sırasında çelikler, yüksek sıcaklıkların etkisiyle önemli mikroyapısal değişikliklere uğrar. Çeliklerin mekanik özellikleri, yüksek sıcaklıkların etkisiyle genellikle zayıflar. Bu amaçla düşük karbonlu çelik ile yüksek dayanımlı çeliklerin yanın sonrası davranışlarının değerlendirilmesi güvenlik açısından önemli bir konudur. Bu amaçla yapı alanının önemli bir konusu olan çelik binaların yanın hasarlarını değerlendirmek için deneysel ve parametrik birleştirilmiş bir çalışma yapılmıştır. Öncelikle kalınlıkları 2,5 mm ile 15 mm arasında değişen yüksek dayanımlı S700MC çelik saclardan kesilen çekme testi kuponları ile kalınlıkları 6 mm ile 12 mm arasında değişen düşük karbonlu S235JR çelik çekme testi kuponları 1200 °C'ye kadar farklı sıcaklıklara maruz bırakılmıştır. Bu numuneler daha sonra test edilmeden önce doğal hava soğutması yoluyla normal oda sıcaklığına soğumaya bırakılmıştır. Elastisite modülü, akma mukavemeti ve nihai çekme mukavemeti gibi yanın sonrası mekanik davranış parametrelerini belirlemek için bu kuponlar üzerinde bir dizi çekme testi gerçekleştirildi. Test sonuçları, yüksek mukavemetli S700MC çeliği ile düşük mukavemetli S235JR çeliğinin yanına maruz kaldıktan sonraki mekanik davranışlarının, ısıtma sıcaklığı 600 °C'yi aşığında önemli ölçüde değiştigini göstermiştir. S700MC çeliğinin akma dayanımı kaybı kalınlıkla birlikte artma eğiliminde olsa da kalınlığın S235JR çeliği üzerinde önemli bir etkisinin olmadığı tespit edilmiştir. En yüksek akma dayanımı kaybı S235JR çeliğinde 8 mm kalınlıkta ve 1200 °C sıcaklıkta %50, S700MC çeliğinde ise 12 mm kalınlık ve 1200 °C sıcaklıkta %70 olarak ölçülmüştür. Kalınlığın en yüksek çekme dayanım kaybına etkisi her iki çelik için de sınırlı olduğu gözlemlenmiştir. Yüksek sıcaklıklara maruz kalma durumunda nihai dayanım kaybı S235JR çeliği için genellikle %30 civarında olurken, S700MC çeliği için bu oran değişmekte birlikte %50'ye kadar çıktıığı tespit

edilmiştir. Deneysel bulgulara dayanarak, S700MC ile S235JR çeliklerinin mekanik parametrelerindeki değişiklikleri tahmin etmek için yeni bir denklem seti geliştirilmiştir. Bu yeni tahmin denklemleri, yüksek dayanımlı S700MC çeliği ile geleneksel düşük karbonlu S235JR çeliğinden yapılmış binaların yanın olaylarına maruz kaldıktan sonra doğru şekilde değerlendirilmesine olanak tanır. Ayrıca önerilen bu empirik denklemler geneldir ve akma dayanımı 235 MPa - 420 MPa aralığındaki düşük karbonlu çelikler ile 700 MPa'ya kadar olan yüksek dayanımlı çelikler için geçerlidir. Önerilen denklemler, pratik tasarım standartlarına hemen uyarlanabilecek bir biçimde sunulmuştur.

Anahtar Kelimeler: Yüksek mukavemetli yapısal çelik, geleneksel düşük karbonlu yapısal çelik, S700 MC, S235JR, mekanik davranış, yanın sonrası, empirik denklemler

ABSTRACT
POST-FIRE RESPONSE OF DIFFERENT STEEL GRADE MATERIALS
Veysel POLAT

Master of Science (M.Sc.)
Graduate School of Natural and Applied Sciences
Department of Civil Engineering
Supervisor: Asst. Prof. Dr. Özer ZEYBEK
Co-Supervisor: Assoc. Prof. Dr. Yasin Onuralp ÖZKILIÇ
June 2024, 66 pages

Conventional carbon mild steel is a type of steel known for its low carbon content and generally used in the construction industry. Its easily formable and weldable properties make this steel a widely preferred material for buildings, bridges and various construction projects. Due to its low cost and good mechanical properties, low-strength steel is commonly employed. High-strength steels are widely utilized in bridges and high-rise buildings since they have superior properties such as a high strength/weight ratio and good earthquake resistance. However, exposure to high temperatures affects the strength and stiffness of these materials. During fire, steels undergo significant microstructural changes under the influence of high temperatures. The mechanical properties of steels generally weaken under the influence of high temperatures. For this purpose, evaluating the post-fire behavior of conventional structural mild steel and high-strength steel is an important issue in terms of safety. For this purpose, a combined experimental and parametric study was conducted to evaluate fire damage of steel buildings, which is an important issue in the construction field. Tensile test coupons were cut from high-strength S700MC steel sheets (thicknesses: 2.5 mm to 15 mm) and conventional structural S235JR mild steel sheets (thicknesses: 6 mm to 12 mm). These samples were exposed to varying temperatures up to 1200 °C. After exposure, the specimens were allowed to cool to room temperature naturally through air cooling before being tested. A series of tensile tests was conducted on these coupons to identify the parameters of post-fire mechanical behavior such as the elastic modulus, yield strength and ultimate tensile strength. Test results demonstrated that the mechanical behavior of high-strength S700MC steel and conventional structural S235JR mild steel after exposure to fire changed significantly when the heating temperature exceeded 600 °C. It was observed that while the yield strength loss of S700MC steel tends to increase with thickness, thickness has no significant effect on the yield strength loss of S235JR steel. The highest yield strength loss for S235JR steel was measured as 50% for a thickness of 8 mm at 1200 °C. For S700MC steel, the highest yield strength loss was measured as 70% for a thickness of 12 mm at 1200 °C. The effect of thickness on the ultimate tensile strength loss is limited for both steels. In the case of exposure to high temperatures, the ultimate strength loss is generally around 30% for S235JR steel, while for S700MC steel, it varies but can reach up to 50%. Based on experimental findings, a new set of equations has been developed to estimate changes in the mechanical parameters of S700MC and S235JR steels. These

novel predictive equations allow the accurate evaluation of buildings made of high strength S700MC and conventional structural S235JR mild steel after exposure to fire events. Furthermore, these proposed empirical equations are general and valid for low-strength steels with yield strengths in the range of 235 MPa - 420 MPa and high-strength steels up to 700 MPa. The proposed equations are presented in a form that is immediately useful for adoption into practical design standards.

Keywords: High strength structural steel, conventional structural mild steel, S700MC, S235JR, mechanical behavior, post-fire, empirical equations





To my wife Asya
and
My son Adar

PREFACE

I would like to express my deep gratitude to my thesis advisor, Asst. Prof. Dr. Özer ZEYBEK, for all his support and guidance in this thesis. He became an invaluable mentor for me with his patience, positive outlook and efforts during this process.

I would like to thank Assoc. Prof. Dr. Yasin Onuralp ÖZKILIÇ for his unwavering support during the experiment process.

I would like to express my special thanks to Assoc. Prof. Dr. Mehmet Rıfat KAHYAOĞLU for his support before and during the thesis process.

I would like to thank Prof. Dr. Deniz ÜLGEN, and the head of department, Assoc. Prof. Dr. Altuğ SAYGILI for helping me without hesitation in all kinds of problems and encouraging me.

I would like to thank the examining committee members, Asst. Prof. Dr. Süleyman Bahadır KESKİN, and Assoc. Prof. Mutlu Seçer for invaluable their contributions and sparing their valuable time.

Furthermore, I would like to express my endless gratitude to my entire family, especially my parents, who supported me throughout this process.

Finally, I would like to give the biggest thank you to my lovely wife and sweet son for their patience and support.

CONTENTS

PREFACE.....	vii
CONTENTS.....	viii
LIST OF TABLES	ix
TABLE OF FIGURES.....	x
ABBREVIATIONS	xi
1. INTRODUCTION.....	1
2. EXPERIMENTAL STUDY	11
2.1. Test Specimens.....	12
2.1.1. High strength steel S700MC.....	12
2.1.2. Conventional carbon mild steel S235JR	12
2.2. Test Setup and Instrumentation	13
3. EXPERIMENTAL RESULTS.....	17
3.1. Modulus of Elasticity	21
3.2. Yield Strength and Ultimate Tensile Strength.....	27
3.2.1. Yield strength for S700MC	27
3.2.2. Yield strength for S235JR	37
3.2.3. Ultimate strength for S700MC.....	40
3.2.4. Ultimate strength for S235JR	43
4. COMPARISON OF EXPERIMENTAL RESULTS WITH AVAILABLE RESULTS IN THE LITERATURE AND PROPOSED PREDICTIVE EQUATIONS.....	46
5. CONCLUSIONS AND FUTURE RESEARCH NEEDS.....	61
REFERENCES.....	63

LIST OF TABLES

Table 2.1. Chemical composition of high strength S700MC steel	12
Table 2.2. Chemical composition of conventional carbon mild steel S235JR.....	13
Table 4.1. Constants for the S700MC modulus of elasticity used in Equation (4.1).47	47
Table 4.2. Constants for the S235JR modulus of elasticity used in Equation (4.2)...48	48
Table 4.3. Constants for the S700MC yield strength of $(f_{y,0.2})_T$ used in Equation (4.2).....	48
Table 4.4. Constants for the S700MC yield strength of $(f_{y,0.5})_T$ used in Equation (4.2).....	49
Table 4.5. Constants for the S700MC yield strength of $(f_{y,1.5})_T$ used in Equation (4.2).....	49
Table 4.6. Constants for the S700MC yield strength of $(f_{y,2.0})_T$ used in Equation (4.2). ..	50
Table 4.7. Constants for the S235JR yield strength of $(f_y)_T$ used in Equation (4.2)..50	50
Table 4.8. Constants for the S700MC ultimate tensile strength of $(f_u)_T$ used in Equation (4.2).....	50
Table 4.9. Constants for the S235JR ultimate tensile strength of $(f_u)_T$ used in Equation (4.2).....	51
Table 4.10. Statistics for the ratio of estimated to test values for $t = 2.5$ mm specimens	51
Table 4.11. Statistics for the ratio of estimated to test values for $t = 3.0$ mm specimens	51
Table 4.12. Statistics for the ratio of estimated to test values for $t = 4.0$ mm specimens	51
Table 4.13. Statistics for the ratio of estimated to test values for $t = 5.0$ mm specimens	52
Table 4.14. Statistics for the ratio of estimated to test values for $t = 6.0$ mm specimens	52
Table 4.15. Statistics for the ratio of estimated to test values for $t = 8.0$ mm specimens	52
Table 4.16.. Statistics for the ratio of estimated to test values for $t = 10.0$ mm specimens	52
Table 4.17. Statistics for the ratio of estimated to test values for $t = 12.0$ mm specimens	52
Table 4.18. Statistics for the ratio of estimated to test values for $t = 15.0$ mm specimens	53
Table 4.19. Statistics for the ratio of estimated to test values for $t = 6.0$ mm specimens of CCMS S235JR	53
Table 4.20. Statistics for the ratio of estimated to test values for $t = 8.0$ mm specimens of CCMS S235JR	53
Table 4.21. Statistics for the ratio of estimated to test values for $t = 10.0$ mm specimens of CCMS S235JR	53
Table 4.22. Statistics for the ratio of estimated to test values for $t = 12.0$ mm specimens of CCMS S235JR	54

TABLE OF FIGURES

Figure 2.1. Test specimens with plate thicknesses of 2.5 mm and 8 mm for S700MC.....	11
Figure 2.2. Test specimens with different thicknesses for S235JR.....	12
Figure 2.3. View of heating furnace.....	14
Figure 2.4. Heating and cooling procedures	15
Figure 2.5. Tensile testing machine	16
Figure 3.1. Stress-strain curves for 8 mm specimen.....	18
Figure 3.2. Symbols to identify mechanical properties of S700MC.....	19
Figure 3.3. Symbols to identify mechanical properties of S235JR.....	19
Figure 3.4. Failure modes of tension test specimens	20
Figure 3.5. RFDA machine and test samples for S235JR steel grade.....	21
Figure 3.6. Changes in the modulus of elasticity of HSS S700MC at different temperatures	24
Figure 3.7. Changes in the modulus of elasticity of CCMS S235JR at different temperatures	26
Figure 3.8. Assessment of modulus of elasticity of different CCM steels at different temperatures	26
Figure 3.9. Assessment of YS (or 0.2% proof strength) of different HSS	31
Figure 3.10. Assessment of YS of different (0.5% proof strength) HSS	36
Figure 3.11. Assessment of the YS of different (1.5% proof strength) HSS	36
Figure 3.12. Assessment of the YS of different (2.0% proof strength) HSS	37
Figure 3.13. Assessment of the YS of conventional carbon mild steel.....	39
Figure 3.14. Assessment of YS of different CCM steels at different temperatures ...	39
Figure 3.15. Assessment of Ultimate Tensile Strengths of Different HSS	43
Figure 3.16. Assessment of Ultimate Tensile Strengths of CCMS	45
Figure 3.17. Assessment of ultimate strength of different CCM steels at different temperatures	45
Figure 4.1. Comparison of yield strength of S235JR and S700MC for different thickness.....	57
Figure 4.2. Comparison of elasticity modulus of S235JR and S700MC for different thickness.....	59
Figure 4.3. Comparison of elasticity modulus of S235JR and S700MC for different thickness.....	60

ABBREVIATIONS

CCMS	conventional carbon mild steel
CCM	conventional carbon mild
CIA	cooling in air
CIW	cooling in water
E	the modulus of elasticity of steel for normal temperature design
HSS	high strength steel
LSS	low strength steel
P-F	post-fire
UHS	ultra high strength
UTS	ultimate tensile strength
YS	yield strength
f_u	the ultimate strength of steel, MPa
f_y	Yield Strength, MPa
$(f_u)_T$	the ultimate strength of steel at temperature T, MPa
$(f_u)_{RT}$	the ultimate strength of steel at room temperature, M MPa pa
$(f_{y0.2})_T$	the yield strength of steel at temperature T based on 0.2% non-proportional strain, MPa
$(f_{y0.5})_T$	the yield strength of steel at temperature T based on 0.5% non-proportional strain, MPa
$(f_{y1.5})_T$	the yield strength of steel at temperature T based on 1.5% non-proportional strain, MPa
$(f_{y2.0})_T$	the yield strength of steel at temperature T based on 2.0% non-proportional strain, MPa
$(f_{y0.2})_{RT}$	the yield strength of steel at room temperature based on 0.2% non-proportional strain, MPa
$(f_{y0.5})_{RT}$	the yield strength of steel at room temperature based on 0.2% non-proportional strain, MPa
$(f_{y1.5})_{RT}$	the yield strength of steel at room temperature based on 0.2% non-proportional strain, MPa
$(f_{y2.0})_{RT}$	the yield strength of steel at room temperature based on 0.2% non-proportional strain, MPa

1. INTRODUCTION

Steel is a common construction material utilized in different applications such as residential, commercial and industrial structures. The development of new design procedures and architectural demands have led to the production of steels having high strength. In addition, with the improvement in steel making and welding techniques, steel producers offer high grade steels in the steel market (Shi et al., 2014; Tankova et al., 2021). Steels with a nominal yield strength (f_y) under 460 MPa are generally categorized as conventional mild or low-carbon structural steels, including grades such as ASTM A36, ASTM A572 (Grades 42 and 50), ASTM A992, S235JR, S275, and S355, while those with a nominal yield strength above 460 MPa are considered high strength steels. (Qiang et al., 2012; Shi et al., 2014). The conventional carbon mild steel (CCMS) is widely used in the construction of buildings, bridges, industrial machinery, pipelines, and various structural components. Low-carbon structural steels are commonly employed in a variety of structures owing to their affordability and simplicity of construction. These steels are commonly utilized in low to mid-rise residential buildings, serving as primary structural elements such as columns and beams. Industrial structures like warehouses and hangars often employ low-strength steels providing an economical solution. Small-scale bridges and pedestrian bridges incorporate low-strength steels as these structures do not require high load-bearing capacities. Agricultural buildings such as barns, greenhouses, and poultry houses frequently use low-strength steels, suitable for their large spans and minimal load requirements. Prefabricated steel buildings and light steel frame systems also benefit from the rapid and economical construction offered by low-strength steels. Examples of such applications include small-scale rural bridges, various company warehouses and logistics centers, and local sports halls and sports complexes. However, highly renowned and iconic structures typically do not extensively use low-strength steels, as these buildings often require high-strength steels and other high-performance materials. Despite this, some historically significant structures or parts of larger buildings may have utilized low-strength steels. For instance, the Eiffel Tower, built

in 1889, used steel that can be considered low strength by today's standards but remains an iconic landmark. Many factories and warehouses constructed during the Industrial Revolution employed low-strength steels and are preserved as industrial heritage sites, with some still in use today. Additionally, several old railway bridges built with low-strength steels, designed for lower load capacities, are still in existence. Thus, while low-strength steels are not typically used in modern high-profile projects, their historical and practical significance remains evident in numerous structures worldwide. The usage of high strength steel (HSS) is increasing in engineering applications such as stadiums, transmission towers, offshore platforms, long-span bridges and high-rise buildings, since it provides a higher strength-to-weight ratio and good earthquake resistance, compared to CCMS (Li and Young, 2018; Wang et al., 2018). With introduction of HSSs into structures, steel markets began to supply higher performance steel materials through more efficient material production and manufacturing process. The S690 ($f_y=690$ MPa) grade was employed for the roof trusses in the Sony Center in Berlin, Germany. On the other hand, S960 ($f_y=960$ MPa) and S1100 ($f_y=1100$ MPa) were preferred for use in a military bridge in Sweden. Thus, the increasing demand led to manufacturing of HSS with yield strengths of above 1000 MPa. However, the current version of European standard EN 1993-1-12 (2007) proposes rules for building structures made of steel grades with up to a yield strength of 700 MPa. On the other hand, a working group (WG12) planned to develop new rules for high strength steels up to the steel grade S960 (Kuhlmann et al., 2021). Other advantages of HSSs are that they could result in less total steel amount and carbon dioxide emission in engineering practice (Collin and Johansson, 2005). This would lead to environmental benefit, saving energy and less consumption of raw materials (Qiang et al., 2012; Shi et al., 2014; Qiang et al., 2016). Despite the existence of HSSs today, low-strength CCMSs are extensively utilized in the construction industry, especially in the load-bearing columns and beams of buildings. These steels are preferred due to their high ductility, easy machinability and economy.

There are many experimental and numerical studies investigating the performance of members made of HSS and CCMS materials. A study performed by Outinen et. al. (2001) focused on steel structures in fire conditions. It involves simulating steel and steel-composite constructions under fire as well as material testing. Cold-formed sections and steel grades S350GD+Z, S355, and S460M were subjected to

experimental testing. It also covered how to use the finite element code for structural analysis of steel and steel-concrete composite frames, along with validation studies and thermal load application techniques. Different cooling techniques are crucial for steel post-fire (P-F) behavior. Steel samples are often cooled in various ways once they have reached the appropriate temperature. Common methods include cooling in air, water, foam, a furnace, or using a blanket. While research may be done using only one of these cooling techniques, some studies attempt all of them at once and compare the outcomes. (Ren et al., 2020; Yin et al., 2023; Kiran and Sajid 2019; Lu et al., 2016; Glassman et al., 2020; Zhang et al., 2020; Molkens et al., 2021; Sajid and Kiran 2018). Shi et al. (2021) tested Q235 base metal and weld coupons to determine their mechanical performance after being exposed to fire using CIA and CIW cooling procedures. Ren et al. (2020) examined the effects of fire and two distinct cooling techniques (air and water) on the mechanical characteristics of Q235 cold-formed steel. Tensile coupon tests were carried out at room temperature to evaluate the qualities of the steel after the fire. Coupon samples with thicknesses of 1 mm and 2 mm were utilized. The mechanical characteristics of S355J2W bridge weathering steel after fire were studied by Yin et al. (2023). They found that while cooling techniques (air, foam, water) and temperature increases have little influence on the material's elastic modulus, they have a major impact on its ultimate strength, yield strength, and ductility. Sajid and Kiran (2019) investigated the P-F mechanical response of ASTM A572 Gr. 50 steels under high stress triaxiality when they were cooled from high temperatures using air-cooling and water-cooling techniques. The P-F mechanical characteristics of hot-rolled Q235, Q345, and Q420 steels and also cold-formed Q235 steels that were subjected to temperatures reaching as high as 1000 °C and cooled with either air or water were examined by Lu et al. (2016). Glassman et al. (2020) assessed the mechanical characteristics of weathering steel (A588) at different temperatures and with different cooling techniques in comparison to non-weathering steel (A709/A992). Their findings show that A588 has a marginally higher reduction in ultimate stress at high temperatures. However, if properly cooled, both steels can maintain similar residual properties; excessive heat and water cooling may cause increased brittleness and unanticipated changes in mechanical properties. Yazıcı (2024) evaluated the impact of elevated temperatures on the mechanical characteristics of S235 cold-formed steel with and without protection, in different thicknesses. According to the study, exposed steel loses a substantial amount of strength at temperatures above 400 °C.

However, by lowering temperature exposure by about 200 °C, intumescent coatings increase the strength of coated specimens between 500 and 900 °C. Up to a particular temperature, thicker steel specimens likewise maintain a higher ultimate strength. In order to help with the design of more fire-resistant steel structures, Yazıcı completed with an approach for determining the ultimate strength of both coated and uncoated steel based on temperature and thickness. Dan et al. (2022) examined the mechanical properties of structural steels Q345, Q460, Q550, and Q690 after exposure to temperatures ranging from 300 °C to 800 °C, followed by air cooling. Their analysis revealed that mechanical properties, such as YS and UTS, decrease significantly when temperatures exceed 600 °C. The residual factors show either exponential or linear relationships with temperature. New predictive equations for these residual factors are proposed based on experimental data, and a stress-strain model is introduced to accurately represent the stages of the stress-strain curve under fire conditions. The P-F mechanical properties of cold-formed steel members, which are essential for a variety of building applications, were examined by Gunalan and Mahendran (2014). Tensile coupons of various grades and thicknesses were subjected to temperatures as high as 800 °C before being cooled to room temperature. The study found that steel exposed to temperatures above 300 °C showed significant reductions in mechanical properties. As a result, they developed new predictive equations for assessing P-F strength, helping engineers evaluate the safety of fire-exposed cold-formed steel structures. Balakrishnan et al. (2022) studied the residual properties of S355 J2 steel joints after fire exposure up to 900 °C. The results showed a slight increase in YS, UTS, and hardness at 300 °C, but significant deterioration above this temperature, with strength reduction linked to microstructural changes in the steel. After studying the P-F mechanical characteristics of Q355 steel, Zhang et al. (2020) discovered that cooling techniques had a major impact on the material's strength and ductility following exposure to temperatures beyond 600 °C. Water cooling boosted strength but decreased ductility, while fire-extinguishing foam cooling resulted in decreased strength and increased ductility. New predictive equations for Q355 steel were developed based on these findings. Molkens et al. (2021) provide recommendations on P-F material properties and safety factors for structural carbon steel, addressing discrepancies between design and P-F assessment methodologies. Their study includes a statistical evaluation of 718 tests from various sources and suggests adjusted safety factors and a reduced reliability index to improve the assessment and retrofitting of

fire-damaged steel structures based on performance data and technical analysis. Outinen and Makelainen (2004) conducted experimental research to investigate the mechanical properties of structural steels S350GD+Z, S355, S460M, and cold-formed S355J2H at elevated temperatures using transient state tensile tests. Their study provided data on temperature-dependent properties such as YS, E, and thermal elongation, comparing these results with the material model outlined in Eurocode 3. Sajid and Kiran (2018) investigated how cooling techniques and stress triaxiality affected the P-F response of ASTM A36 steels. They found that air-cooling from temperatures above 700 °C resulted in a 14% drop in UTS and a 22% increase in fracture strain, while cooling from 600 °C had no effect on mechanical parameters. On the other hand, water cooling at high temperatures increased UTS by up to 146% while decreasing fracture strain by 76%. High stress triaxiality further increased strength while decreasing ductility. Numerous investigations have been carried out on diverse steel types to comprehend the behavior of steel in the presence of fire. Some of these focus on the behavior of steel at elevated temperatures. Other studies have attempted to reveal the differences in the behavior of steel by focusing on different cooling methods. Few research has examined the P-F behavior of steels with varying thicknesses. In the literature, there are widespread studies on Q235 steel, which has a yield strength close to S235JR steel. Although there are studies on Q235, choosing S235JR steel is important due to its compliance with European standards (EN 10025-2), which ensure consistency and reliability in structural performance, especially in European construction projects. Incorporating the S235JR into fire behavior studies provides valuable information regarding its performance under high temperatures, which is necessary to increase structural integrity and meet European safety requirements. Understanding the behavior of S235JR in fire scenarios contributes to improved design guidelines and retrofit strategies for fire-damaged structures. Thus, one of the steel grades considered in this thesis is S235JR.

One of the earliest studies on HSS was performed by Haaijer (1963). Some structural members made of HSS were considered to explore their mechanical behavior. The results of the study showed that utilization of HSS can reduce the number of materials to build lightweight structures. A study performed by Adams (1966) also demonstrated that the use of HSS resulted in lighter and slenderer members. After understanding the applicability of HSS from previous studies, attention was paid to the mechanical

behavior of structural members made of HSS and this was explored in the following categories: instability behavior (Nie et al., 2018; Chen et al., 2022), connection performance (Qiang et al., 2014; Lee, 2017; Jiang et al., 2021; Jiang et al., 2021; Lin et al., 2021) and seismic response (Wang et al., 2014; Hue and Wang 2023) of HSS structures. It should be noted that usage of HS steels is not limited to building type structures. Their superior mechanical properties make them preferred materials in the oil and gas industries. However, cylindrical shell structures such as pressure vessels and pipes are more prone to fire hazards. Likewise, there are times when it is inevitable for the high-strength steel components of buildings of this kind to experience fire incidents. Despite the fact that these steels are widely used in the civil engineering industry, there was limited knowledge of how materials would behave under extreme structural pressures, such as fire (Azhari et al, 2017). While most study has been done on mild steels, very few studies have examined how high strength steel members react to fire. Chen et al. (2006) conducted one of the earliest studies on the behavior of HSS members at high temperatures. It was found that when temperature increased, HSS specimens' yield strength and elastic modulus decreased. It was detected that the behavior of HSSs at temperatures above 540 °C is quite different from that of conventional carbon mild steel (CCMS) samples. The mechanical performance of S690 steel grade was investigated by Qiang et al. (2012) at various temperatures (ranging from ambient temperature to 700 °C), considering both transient state and steady state processes. They claimed that there were no safe criteria for directing the construction of steel structures with high yield strength that would ensure fire resistance. Chiew et al. (2014) examined the behavior of grade S690 HSS at elevated temperatures. It was revealed that HSS has minor degradation in strength at temperatures below 400 °C, while it experiences a major reduction in some mechanical properties at higher temperatures. Their study demonstrated that after a fire event the mechanical performance of HSSs are different from those of CCM steels as stated the study performed by Chiew et al. (2014). Qiang et al. (2012) explored changes in the mechanical behavior of two different HS steels after fire events. It was demonstrated that there was a significant effect of the steel grade on post fire performance of HSS. Qiang et al. (2013) performed an experimental study to assess the structural and material performance of S960 steel after fire. It was detected that there was no change in the behavior of high strength S960 grade steel before a heating temperature of 600 °C. Wang et al. (2013) explored the influence of temperature change on the behavior

of Q460 grade steel. Their studies showed that the deterioration in the stiffness and strength of Q460 HSS was different from that of CCMS at elevated temperatures.

The above-mentioned works mostly concentrated on the performance of HS steels at elevated temperatures. However, the following studies concentrated on the response of HSS after high temperature exposure. Li et al. (2017) evaluated the structural performance of Q690 steel after a fire situation. The material properties of HSS were found to be strongly impacted by the cooling approach as the temperature increased above 500°C. It has been stated that even though the yield strength values for different HSS grades (i.e. Q690 and S690) are the same, there are differences in their P-F behavior. Zhou et al. (2019) used two distinct cooling methods (cooling by air and cooling by water) to examine how the Q690 HSS grade responded to high temperatures. Regardless of the cooling method, a slight loss of strength was observed after the steel was subjected to temperatures up to 600°C. However, when temperatures exceeding 700 °C were applied to the HSS specimens, it was found that the strength deterioration worsened even more. Kang et al. (2021) conducted mechanical and fracture behavior of Q460 steel grade after a fire situation. When the test specimens were subjected to temperature values above 650 °C, strength values started to decrease. However, no significant change in Poisson's ratio and the E of Q460 steel grade was noticed when the heating temperature reached 900 °C. Conversely, specimens that underwent tensile testing subsequent to heating exhibited ductile fracture failure. Zeng et al. (2021) examined the P-F mechanical characteristics of Q890 steel grade while taking water- and air-cooling methods into account. It was shown that temperature variations and cooling techniques both significantly affected the performance of high strength steels. Research on how high-strength steels react to fire was done by Dan et al. (2022). It was determined that when the heating temperature value increased above 600 °C, the deterioration in strength and stiffness became more evident. Zhou et al. (2021) investigated how cooling techniques—such as air, water, and firefighting foam—affect the mechanical properties of Q620 high strength steel. After cooling in air and foam, the similar stress-strain behavior for Q620 high strength steel was observed. Furthermore, they compared their results with other steel grades such as Q460, S460, Q690 and S690. Their studies revealed that although P-F mechanical parameters of Q620 high strength steel are similar to Q460 and S460, there was a difference in these properties between the Q620, Q690 and S690 steel grades. Molkens

et al., (2021) attempted to develop a design guideline to assess and retrofit existing steel buildings which suffered and survived a fire incident. Their study pointed out that there is a difference between approaches utilized in the design phase and evaluation procedures employed after a fire event. Considering the available data in the literature, a reliability-based approach was proposed to predict the future service life of the buildings after a fire incident. After exposing circular bar samples produced of Q690 HSS grade to a range of temperature conditions, Li et al. (2024) conducted experimental research on them. They said that a P-F constitutive model for such steels might be required to assess the service life of the buildings in addition to figuring out the mechanical characteristics of HS steels following fire exposure. An elastoplastic constitutive model that is temperature-dependent was created to approximate the P-F mechanical behavior of high-strength steel Q690. These investigations demonstrate how the mechanical behavior of HSS steel members varies following a fire hazard. While some qualitative conclusions are available in the open literature about the mechanical behavior of fire exposed mild steels, the widely used design specifications British standard BS 5950 (2001) and European Standard EN 1993-1-2 (2007) provide brief information about reuse of these types of steel after a fire event. Furthermore, no detailed recommendation is given for them after P-F exposure in these design standards. In other words, BS 5950 (2001) and EN 1993-1-2 (2007) only address mild steels at elevated temperatures. On the other hand, there are some design treatments to investigate the P-F behavior of high strength steels, but there are no design guidelines regarding P-F response of HS steels. Previous studies (Qiang et al., 2012; Qiang et al., 2016; Azhari et al., 2017; Xiong et al., 2017) also showed that there exists a lack of knowledge about the effects of exposure to fire events on the performance of HS steels. Furthermore, since the present standards' reduction factors are based on test results from mild steel specimens, they should be revised when determining the material properties of various HS steels at elevated temperatures, according to studies on HS steels (Shakil et al., 2020). Previous research on the P-F mechanical characteristics of high-strength steels has mostly focused on a yield strength of 690 MPa. Researchers studied different steel grades such as S690, S690QL, Q690 and RQT 690. All these grades have a minimum yield strength of 690 MPa. The experimental study conducted by Li et al., (2017) revealed that the P-F mechanical behaviors of Chinese Q690 HSS S690 HSS were quite different even though they both have the same nominal yield strength ($f_y=690$ MPa). Another widely used HSS grade is S700 MC. It is also a high

strength low-alloy steel grade like the abovementioned family of constructional steel (S690, S690QL, Q690 and RQT 690) having yield strength of 690 MPa. Although their yield strength values are close, there are significant differences between them, such as chemical composition, mechanical properties and applications. S700 MC is commonly preferred in good formability and high strength demand applications such as cranes, trucks and bridges due to excellent weldability and high impact resistance properties, while S690QL steed grade is widely used in energy, mining applications such as load-carrying structures and lifting equipment since it has superior toughness and high strength properties. Furthermore, S700 MC is resistant to heavy loads (static and dynamic) and severe conditions, making it a popular choice for demanding applications such as offshore platforms, pipelines and other critical infrastructure applications. However, there are no studies on the P-F behavior of S700 MC steel grade. Thus, an attempt has been done to explore the mechanical behavior of S700 MC (minimum nominal yield strength of 700 MPa) high strength steel after exposure to fire. As mentioned before, S700 MC steel grade was selected because there is almost no research in the open literature investigating the P-F behavior of this grade. Thus, the reuse of these materials after cooling down from the fire should be assessed by taking into account reliable and rational approaches. This study is motivated by the lack of a design standard for the reuse of HS steel members after a fire incident.

In this thesis, two different steel grades (S235JR and S700 MC) above-mentioned were selected to investigate their mechanical performance after a fire accident. As mentioned before, S235 is a low carbon structural conventional steel commonly used in construction and machinery manufacturing, S700 MC is a high-strength low-alloy steel employed in a wide variety of industries. The evaluation of their post-fire performance is an important subject from the standpoint of safety. Pursuant to this aim, a combined experimental and parametric study was performed to examine the post fire response of HSS members.

While specimens with thicknesses ranging from 2.5 mm to 15 mm were selected for S700 MC steel grade, specimens with thicknesses ranging from 6 mm to 12 mm were selected for S235 JR steel grade. For P-F mechanical behavior, the following heating temperatures were considered: 24 °C (ambient temperature), 200 °C, 400 °C, 600 °C, 800 °C, 1000 °C and 1200 °C, respectively.

Each group of test specimens was first placed in the furnace. Then, these specimens were exposed to the target heating value. When the specimens reached the expected temperature, they were kept for 30 minutes to distribute the temperature evenly over the steel surface. After ensuring uniform temperature distribution, the specimens were taken from the furnace and left to cool. Then, they were cooled down naturally to normal room. In the next phase of the study, a tensile test was performed on coupon samples to assess the mechanical behavior of high strength and conventional low carbon steels after exposure to high temperatures. For the parametric study, considering findings of the experimental part and data obtained from the literature, a statistical analysis was conducted. Finally, empirical formulas were proposed to estimate the changes in the mechanical parameters of both steel grades.

2. EXPERIMENTAL STUDY

The experimental investigation consisted of three main stages, i.e. heating, cooling and tensile tests. 9 different thicknesses tensile coupon specimens for S700MC and 4 different thicknesses tensile coupon specimens for S235JR were considered. Figure 2.1 depicts a representative test specimen of 2.5 mm and 8 mm for S700MC steel, while Figure 2.2 shows specimens of S235JR steel in various sizes. Different thicknesses for S235JR and S700MC steel grades were selected to examine the effect of thickness change on mechanical behavior. Test specimens from each group were kept at room temperature, while the remaining test specimens were heated to desired temperatures to mimic the fire event.

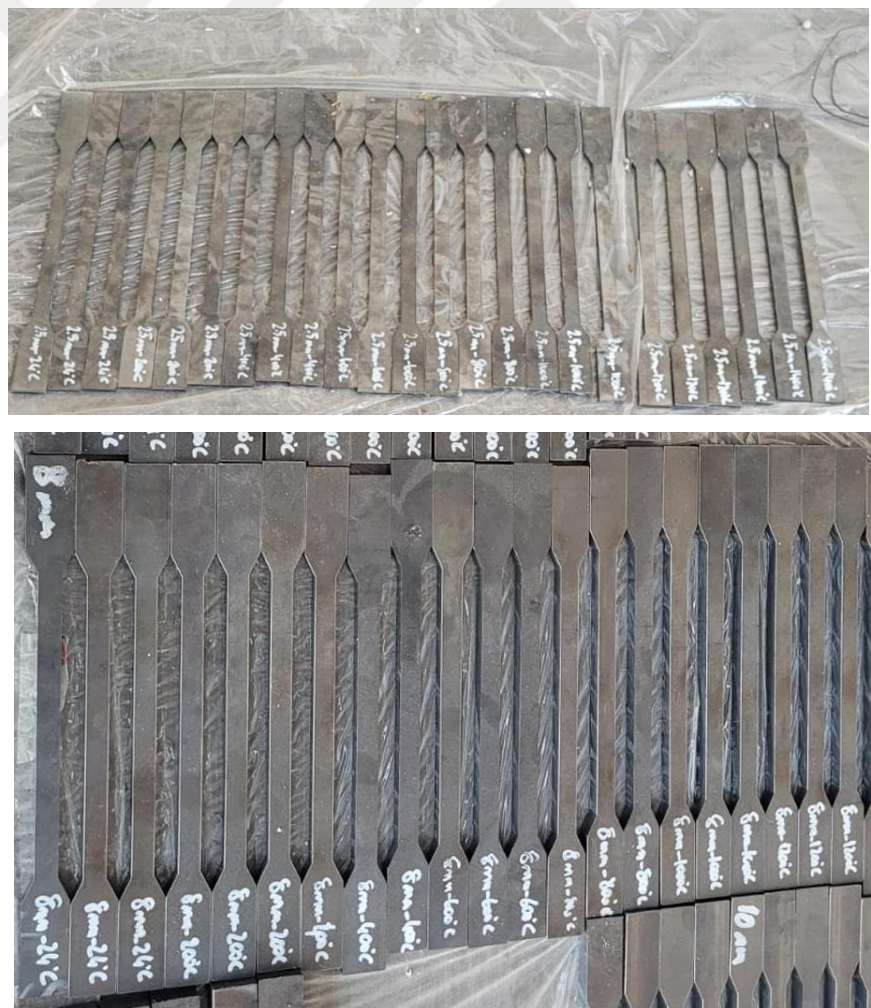


Figure 2.1. Test specimens with plate thicknesses of 2.5 mm and 8 mm for S700MC.



Figure 2.2. Test specimens with different thicknesses for S235JR.

2.1. Test Specimens

2.1.1. High strength steel S700MC

The S700MC steel grade was considered to investigate changes in mechanical behavior of HS steels. S700MC is a high-strength structural steel produced in accordance with EN 10149-2 (2013). The chemical composition of the S700MC steel grade is given in Table 2.1. The test samples were cut from steel sheets made from S700MC steel grade. To explore the effect of thickness on behavior, nine different thickness were chosen, from 2.5 mm to 15.0 mm, which are frequently used in applications.

Table 2.1. Chemical composition of high strength S700MC steel

C	Mn	Si	P	S	Al	V	Ti	Nb	Mo	B
0.12	2.10	0.60	0.025	0.015	0.015	0.20	0.22	0.09	0.5	50

2.1.2. Conventional carbon mild steel S235JR

The investigation focused on evaluating the P-F mechanical performance of CCM steels, employing S235JR steel as the test material. S235JR, renowned for its high

ductility, is widely employed in various construction applications. S235JR is a conventional structural steel produced in accordance with EN 10149-2 (2013), the European Standard for hot-rolled flat products made from low carbon component thermo-mechanically rolled steels for cold forming. Detailed chemical composition data for the S235JR grade is presented in Table 2.2.

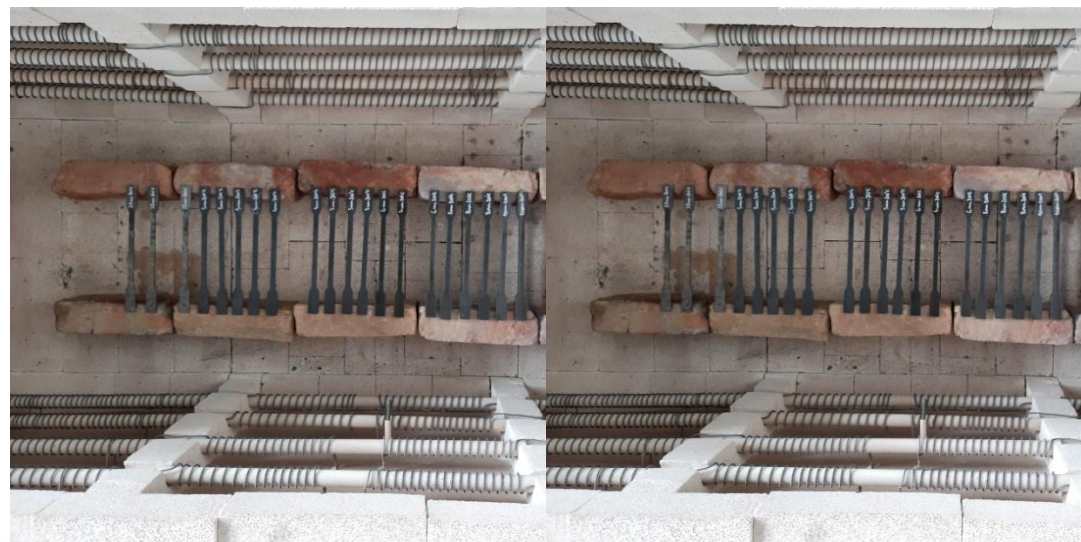
Test specimens were meticulously extracted from steel sheets of the S235JR grade to ensure consistency in material properties. The study aimed to elucidate how varying thicknesses, ranging from 6 mm to 12 mm, impact the mechanical behavior of the steel P-F. These thicknesses were chosen based on their frequent utilization across different practical applications, aiming to provide insights into structural performance under fire conditions.

Table 2.2. Chemical composition of conventional carbon mild steel S235JR

Element	C	Mn	Si	P	S	N
Min-max	0.0-0.12	0.0-1.4	0.0-0.30	0.0-0.045	0.0-0.045	0.0-0.009

2.2. Test Setup and Instrumentation

After the tensile test specimens were prepared, the heating process was initiated to imitate the fire event. In the first phase of the study, the heating process was conducted through a temperature-controlled furnace as shown in Figure 2.3.



a) View of heating furnace for S700MC



b) View of heating furnace for S235JR

Figure 2.3. View of heating furnace

For the heat treatment, a Nevola series temperature-controlled electric furnace with a heating capacity of up to 1200 °C was employed. Test samples were positioned at

the center of the furnace. In the study, six different heating temperatures, i.e. 200 °C, 400 °C, 600 °C, 800 °C, 1000 °C, 1200 °C were selected with a heating rate of 10 °C/ min. These test samples were heated from an ambient temperature to the designated temperature.

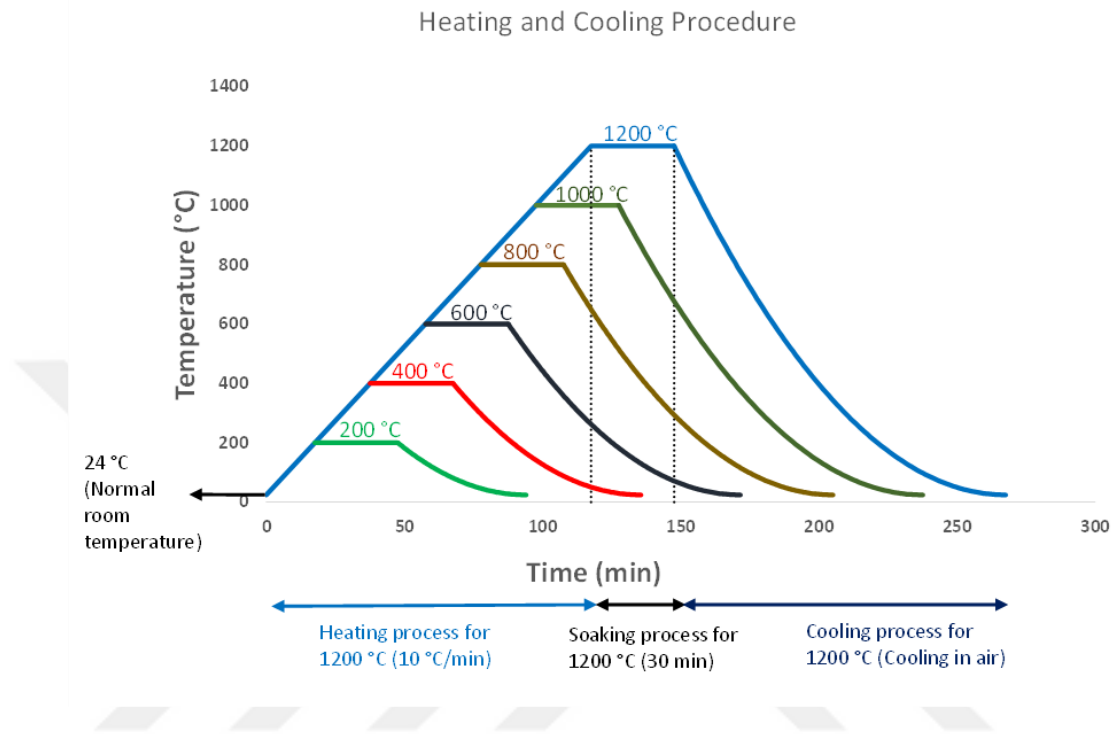
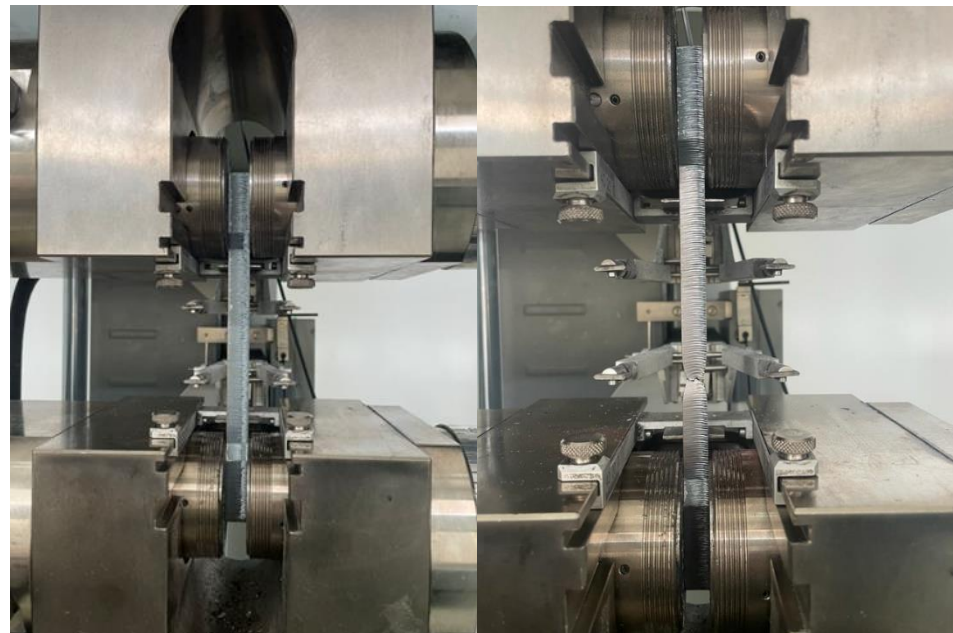
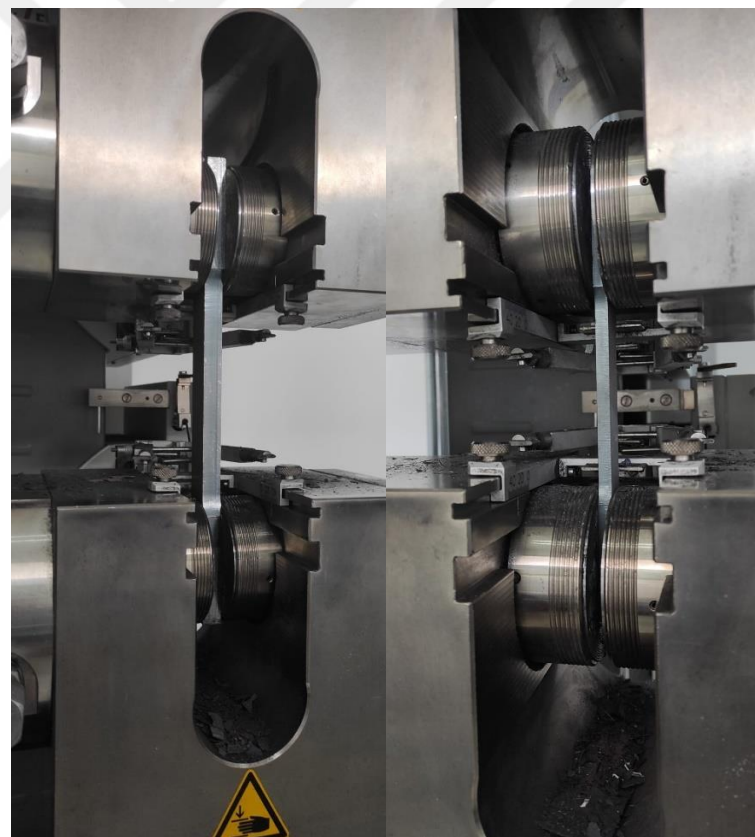


Figure 2.4. Heating and cooling procedures

After heating, as shown in Figure 2.4. they were held in the furnace for 30 minutes at the desired temperatures to render them stable. After that, they were removed from the furnace to cool in the air. The test samples cooled down to room temperature on their own. Tensile tests were performed at room temperature upon cooling. For this purpose, a Zwick/Roell Z250 materials testing machine with a capacity of 250 kN was employed as depicted in Figure 2.5. All the tests were carried out at ambient temperature with the loading strain rate of 0.002/sec. To identify the mechanical behavior of specimens, the testing machine recorded stress-strain values for each specimen.



a) Tensile testing machine for S700MC

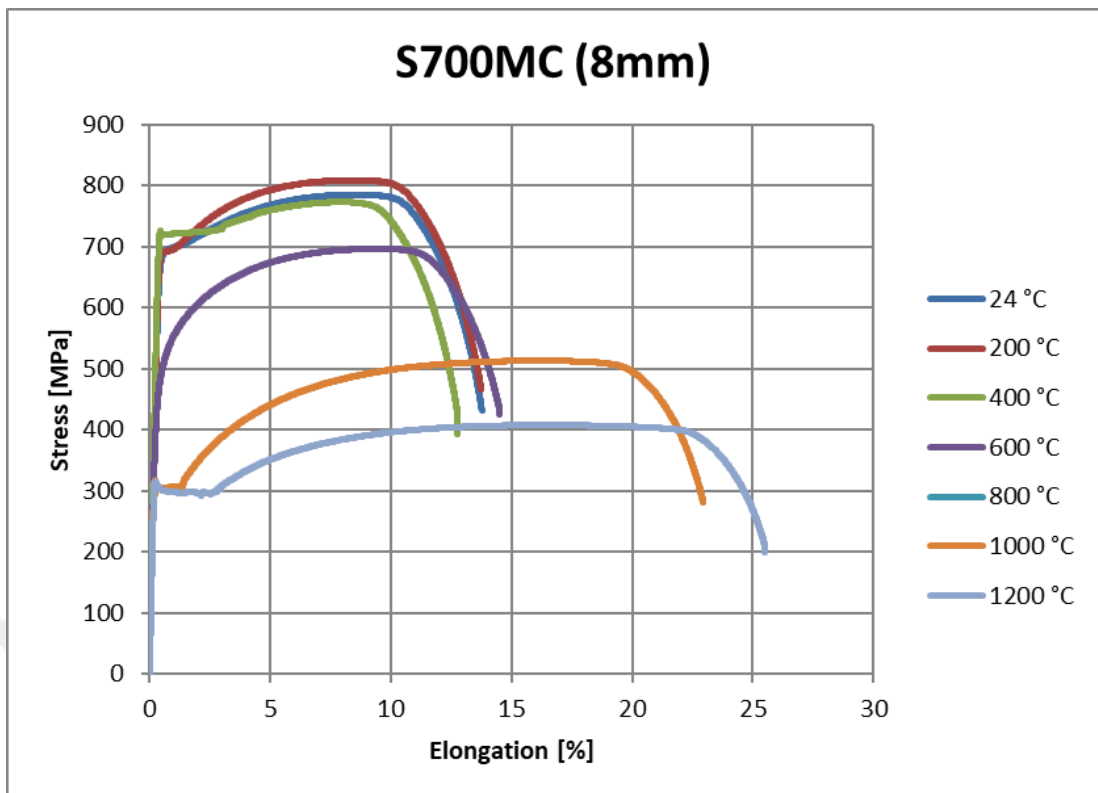


b) Tensile testing machine for S235JR

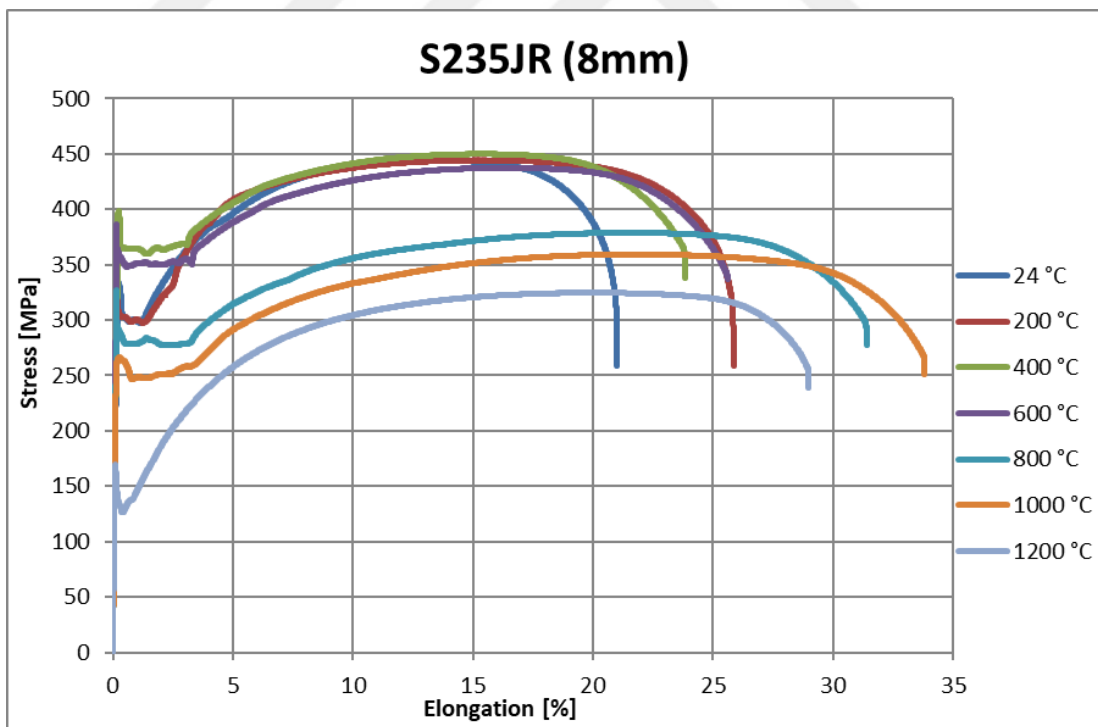
Figure 2.5. Tensile testing machine

3. EXPERIMENTAL RESULTS

After being subjected to elevated temperatures, the mechanical behavior of S700MC and S235JR specimens was determined by conducting tensile tests. A representative stress-strain curve for S700MC and S235JR test specimens was plotted as shown in Figure 3.1. Changes in strength and elastic modulus values were then determined by considering these curves. Test results of both steel grade showed that when the specimens are subjected to temperatures below to 600 °C, the effect of temperature on the P-F stress-strain curve is slight. However, the impact of temperature on stress-strain behavior is more pronounced when the heating temperature exceeds 600 °C. Furthermore, a better ductility was detected with increasing temperature for the high temperature treatment ($T>600$ °C). To identify changes in the strength, different strain levels were considered. As depicted in Figure 3.2. strength values for S700MC were identified by considering different strain levels, i.e., 0.2%, 0.5%, 1.5% and 2.0%. It should be noted that the 0.2% yield strength ($f_y,0.2$) was determined by using the offset strength and it was calculated from the stress-strain curve which is intersected by a line that has a slope equal to the modulus of elasticity of the steel material and starts at a strain of 0.2%. The yield strengths of $f_{y,0.5}$, $f_{y,1.5}$ and $f_{y,2.0}$ at the strain levels of 0.5%, 1.5% and 2.0% were determined using the proof strength. These values are the stresses on stress-strain curves at their intersection with the indicated vertical lines at the above-mentioned strain levels. In the same manner, the ultimate strength (f_u) values were determined as depicted in Figure 3.2. Similarly, f_y , f_u and E values for S235JR steel were determined as in figure 3.3. Furthermore, failure modes of the test samples are presented in Figure 3.4.



a) Stress-strain curves for S700MC steel grade.



b) Stress-strain curves for S235JR steel grade.

Figure 3.1. Stress-strain curves for 8 mm specimen.

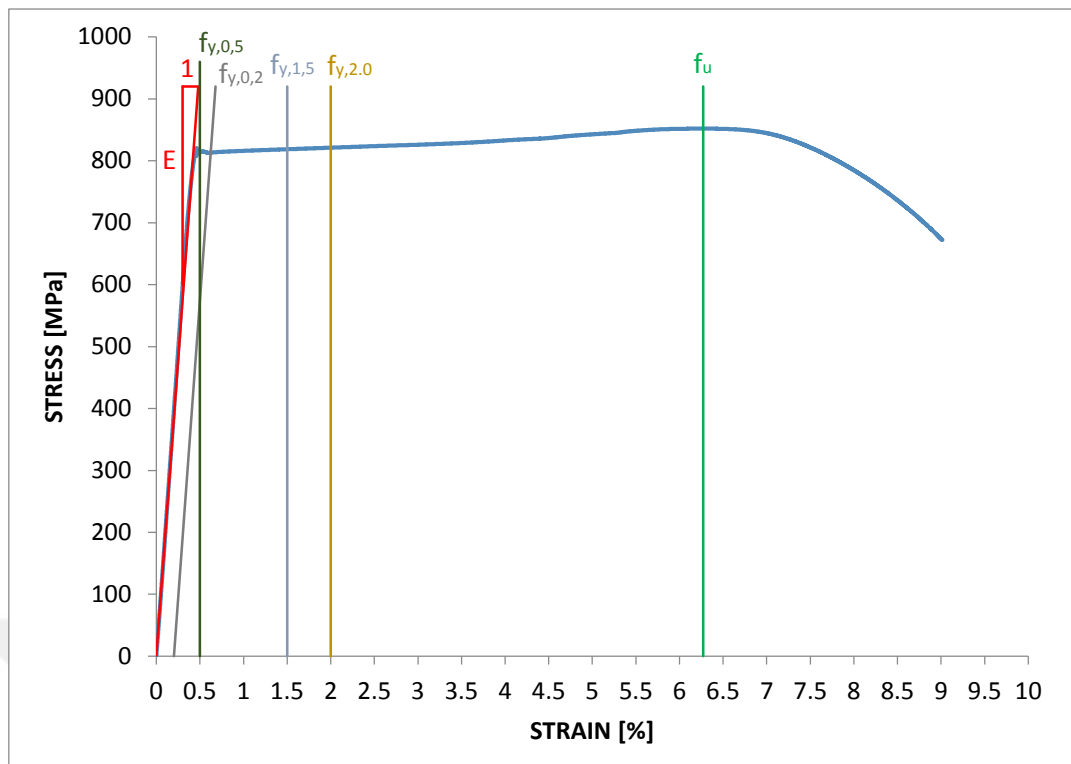


Figure 3.2. Symbols to identify mechanical properties of S700MC.

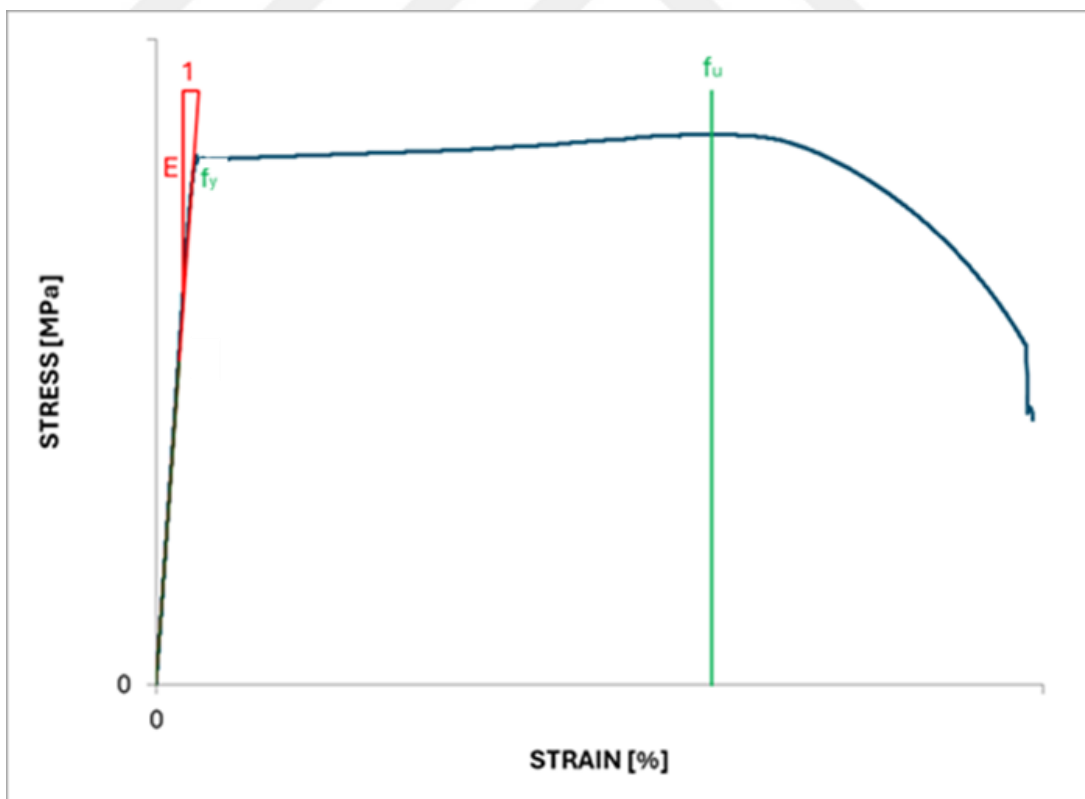


Figure 3.3. Symbols to identify mechanical properties of S235JR.



a) Failure modes of tension test specimens for S700MC steel grade



b) Failure modes of tension test specimens for S235JR steel grade

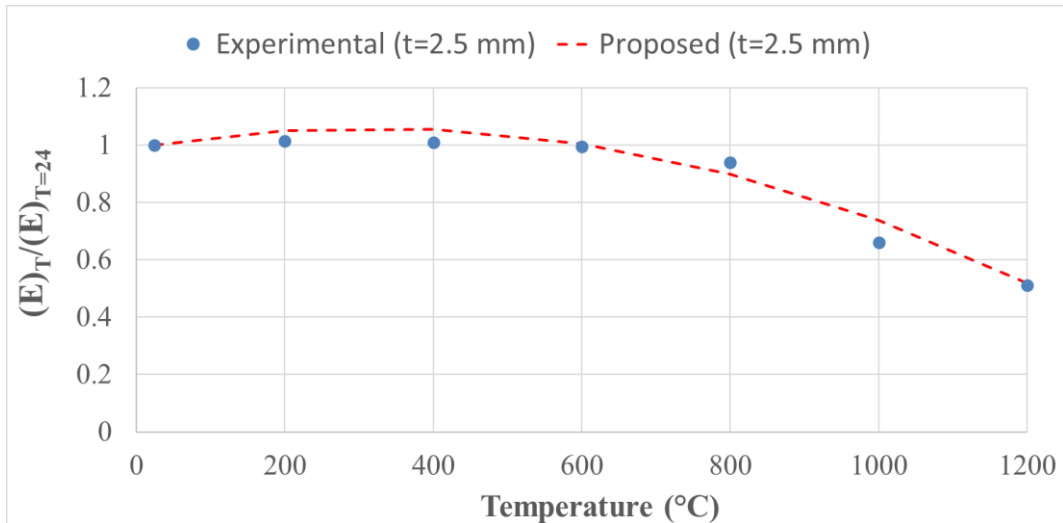
Figure 3.4. Failure modes of tension test specimens

3.1. Modulus of Elasticity

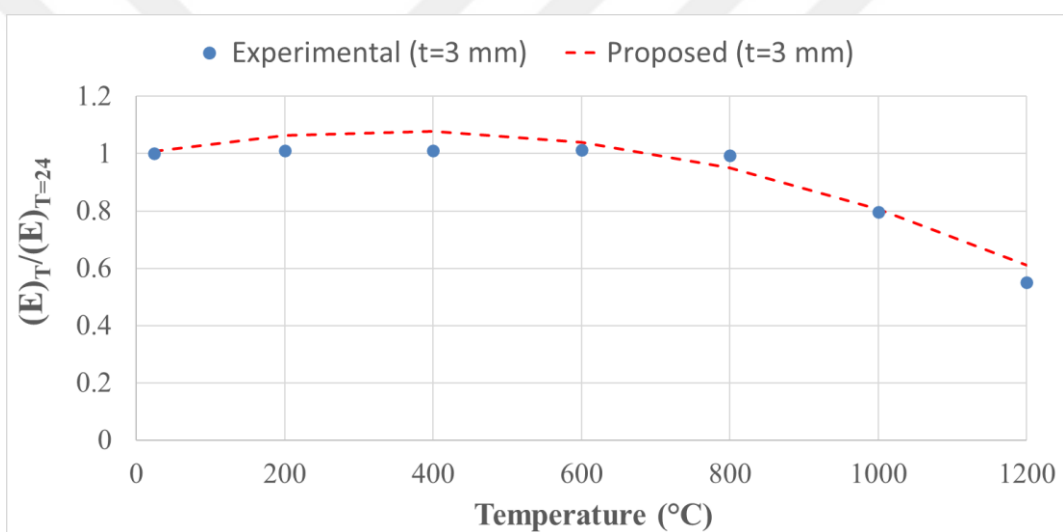
Based on the measured stress-strain diagram, the modulus of elasticity, one of the most important parameters representing load-bearing capacity, can be estimated. In addition to the ambient temperature (24°C), the Young's modulus of steels after being subjected to fire (200°C-1200°C) was determined by considering the slope of linear region of the stress-strain curves. The tangent modulus of the initial linear-elastic part is equal to the elastic modulus. Elastic modulus values recorded from steels exposed to different temperatures ($(E)_T$) were compared with values in ambient temperature cases ($(E)_{T=24}$). In this way, changes in the elastic modulus were calculated. Based on temperature variation, the normalized value $((E)_T/(E)_{T=24})$ for each specimen of S700MC is shown in Figure 3.5, and for each specimen of S235JR is shown in Figure 3.6. It should be noted that the Resonance Frequency and Damping Analysis (RFDA) widely used experimental technique was employed to measure elastic modulus of S235JR steel. Rectangular samples were prepared according to ASTM E1876-15. Test samples and RFDA are presented in Figure 3.5.



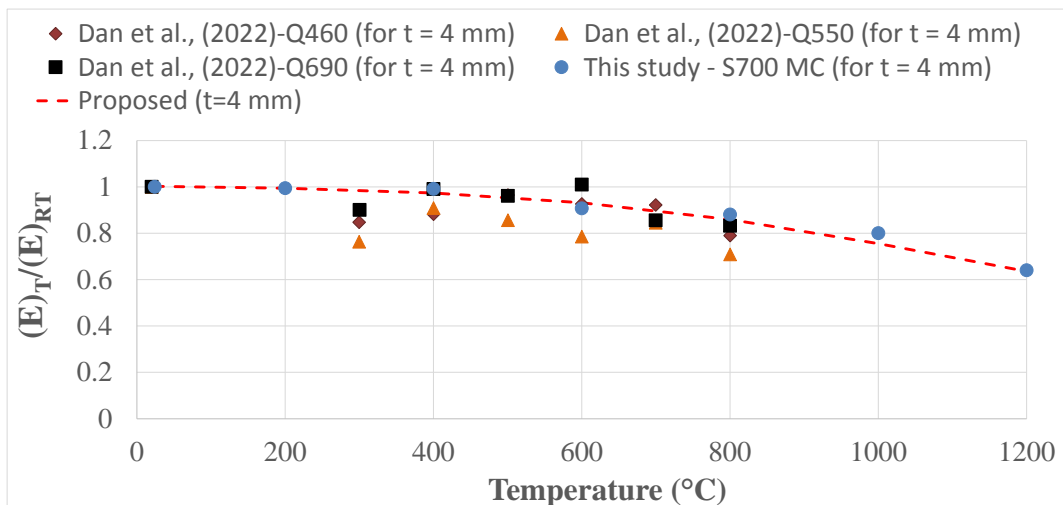
Figure 3.5. RFDA machine and test samples for S235JR steel grade



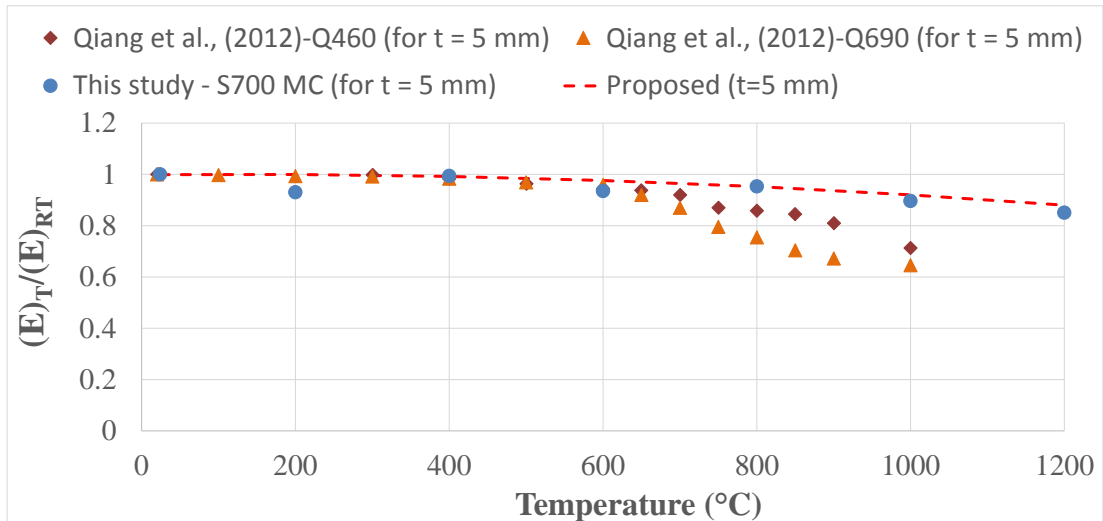
a) Assessment of elastic modulus properties of test samples with a thickness of 2,5 mm



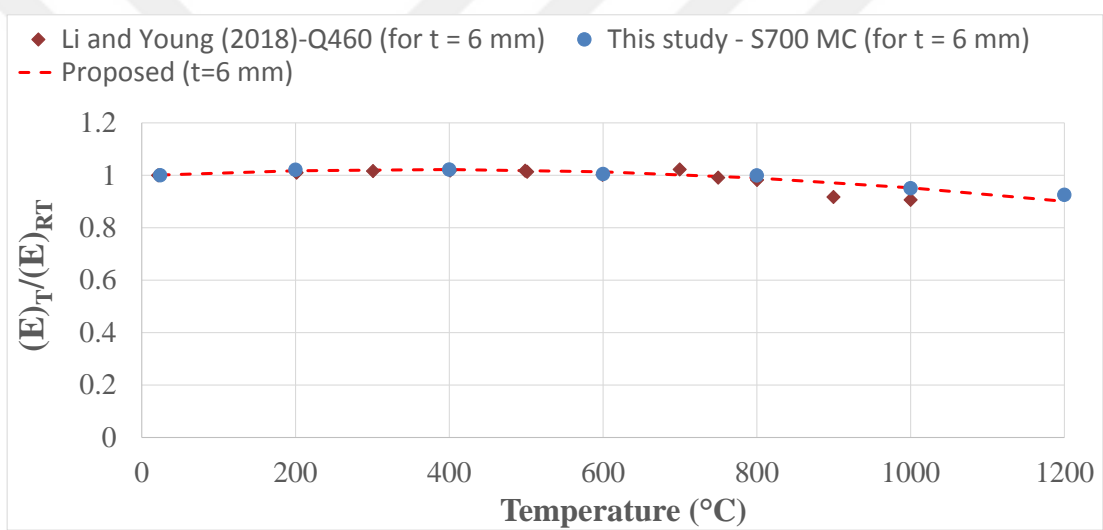
b) Assessment of elastic modulus properties of test samples with a thickness of 3 mm



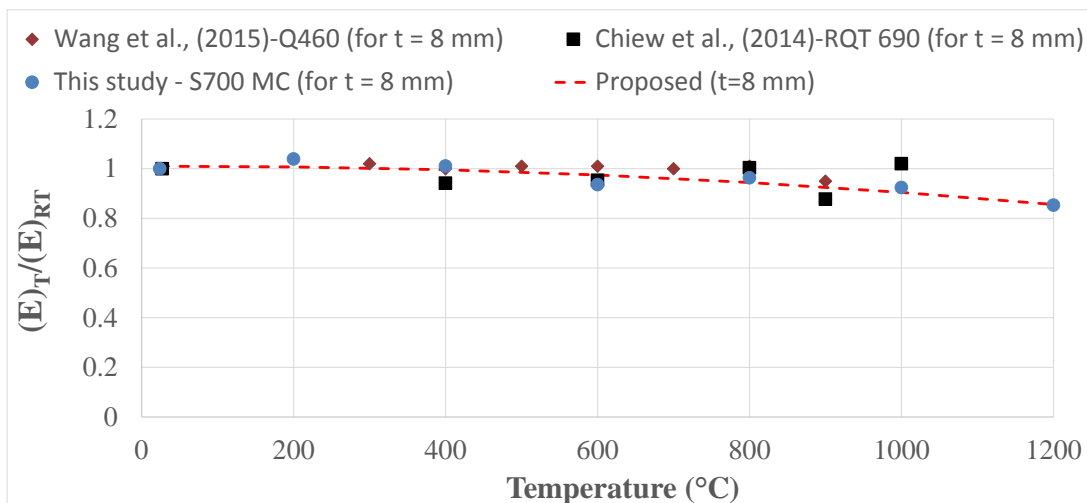
c) Assessment of elastic modulus properties of test samples with a thickness of 4 mm



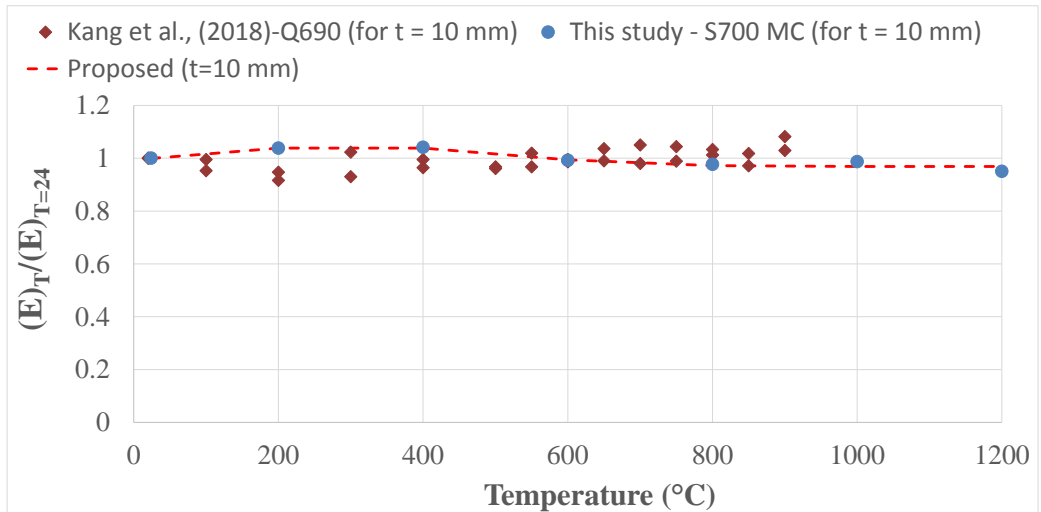
d) Assessment of elastic modulus properties of test samples with a thickness of 5 mm



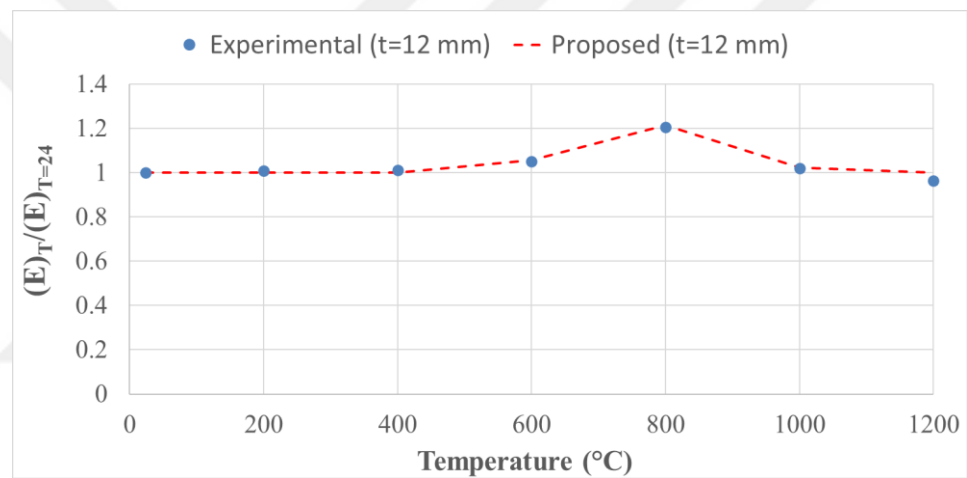
e) Assessment of elastic modulus properties of test samples with a thickness of 6 mm



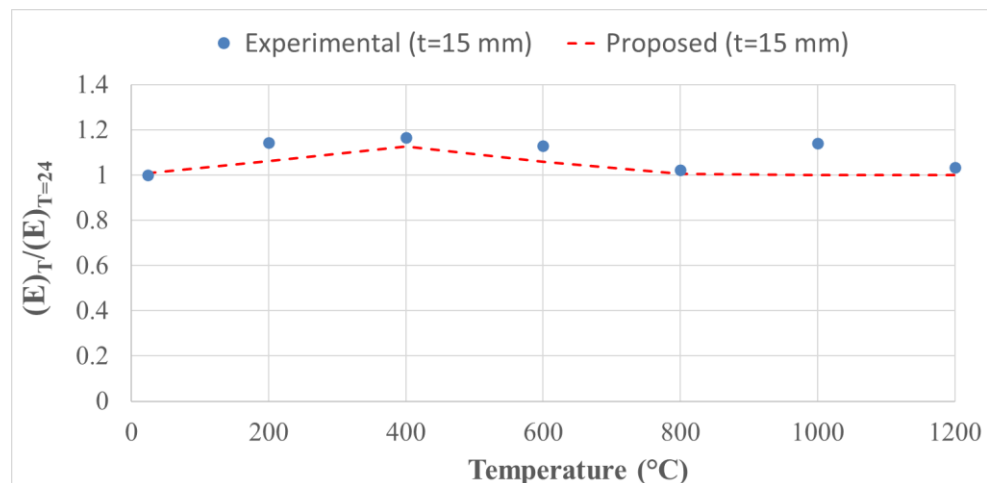
f) Assessment of elastic modulus properties of test samples with a thickness of 8 mm



g) Assessment of elastic modulus properties of test samples with a thickness of 10 mm

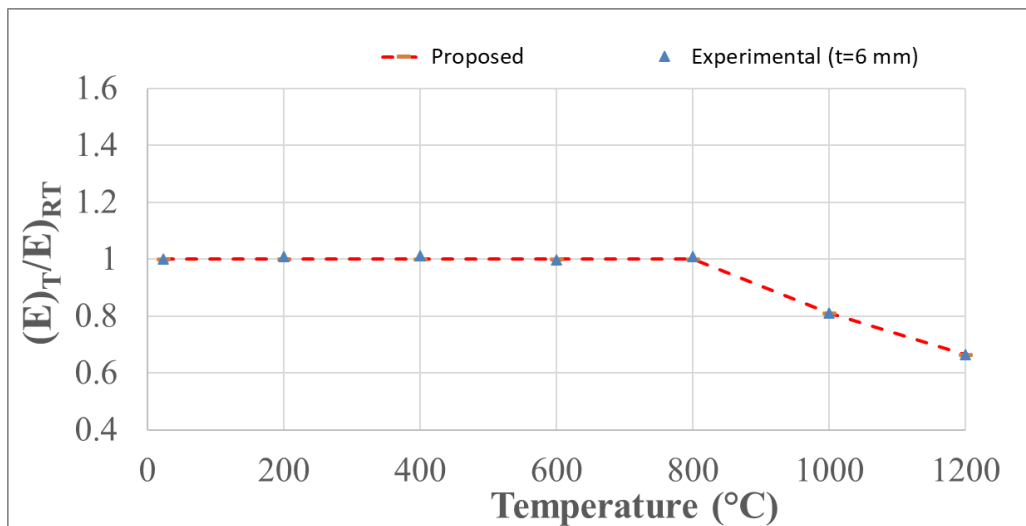


h) Assessment of elastic modulus properties of test samples with a thickness of 12 mm

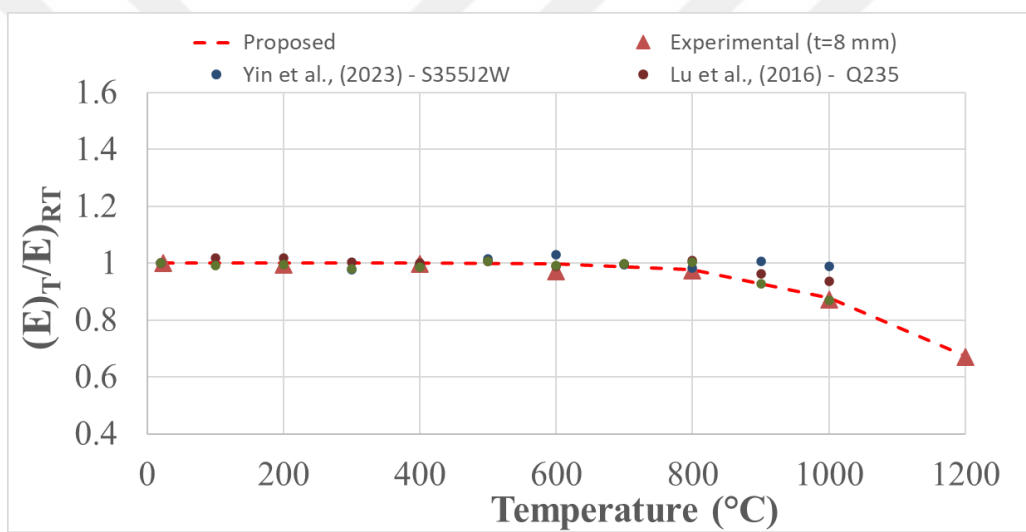


i) Assessment of elastic modulus properties of test samples with a thickness of 15 mm

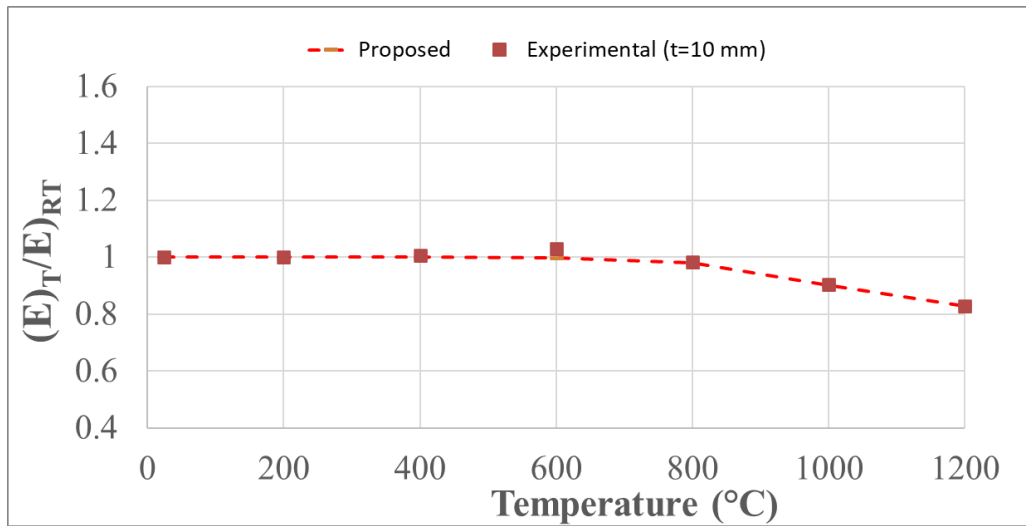
Figure 3.6. Changes in the modulus of elasticity of HSS S700MC at different temperatures



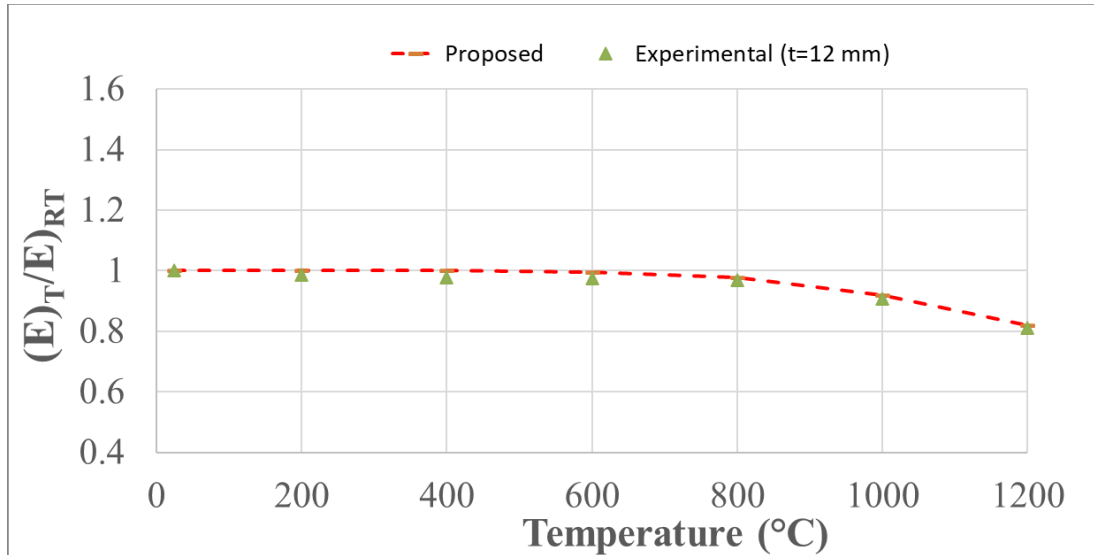
a) Elastic modulus properties of test samples with a thickness of 6 mm



b) Elastic modulus properties of test samples with a thickness of 8 mm



c) Elastic modulus properties of test samples with a thickness of 10 mm



d) Elastic modulus properties of test samples with a thickness of 12 mm

Figure 3.7. Changes in the modulus of elasticity of CCMS S235JR at different temperatures

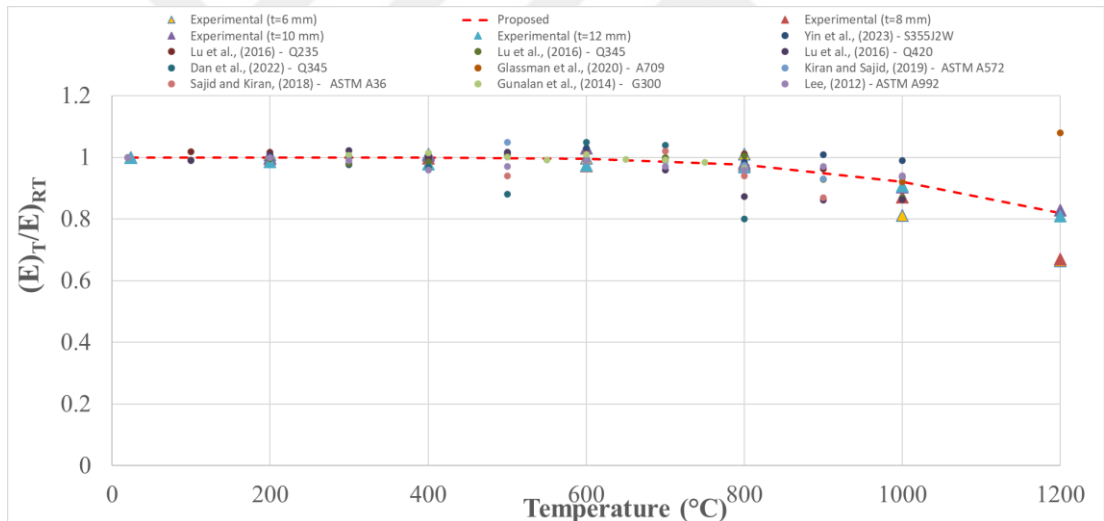


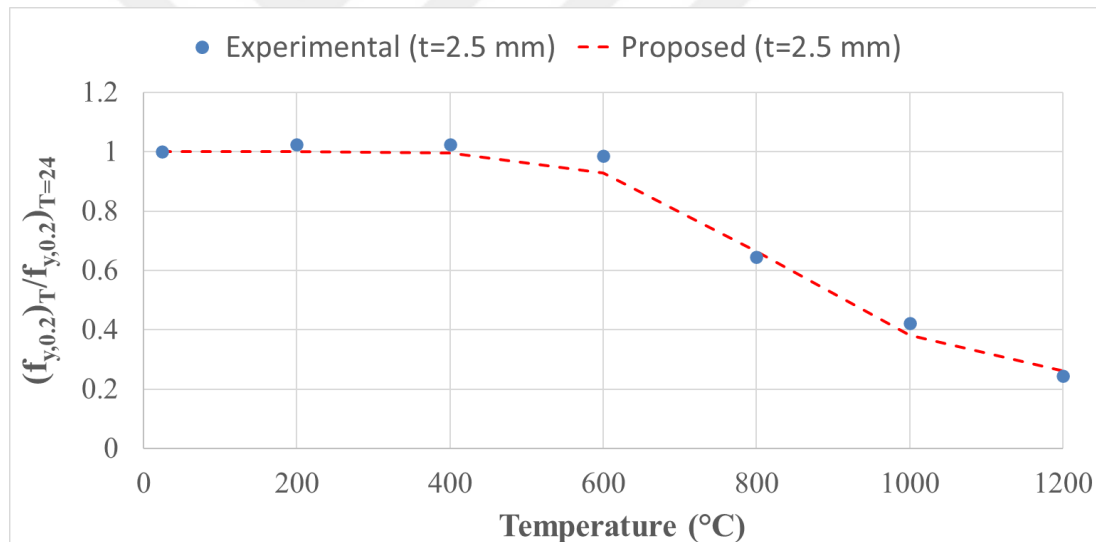
Figure 3.8. Assessment of modulus of elasticity of different CCM steels at different temperatures

Figure 3.6 - Figure 3.8. depict the changes in the E of steels with different thicknesses after exposure to a variety of different temperatures up to 1200°C. As depicted in Figure 3.6. a minor change in the modulus of elasticity of the S700MC test specimens was detected when the specimens were heated to 600°C. As shown in Figure 3.6. It is observed that when the S235JR samples are heated, there is no significant change in the modulus of elasticity up to 800°C. After this temperature, E values for S235JR started to decrease. Furthermore, these decreases are more evident in thinner specimens for both steel grades.

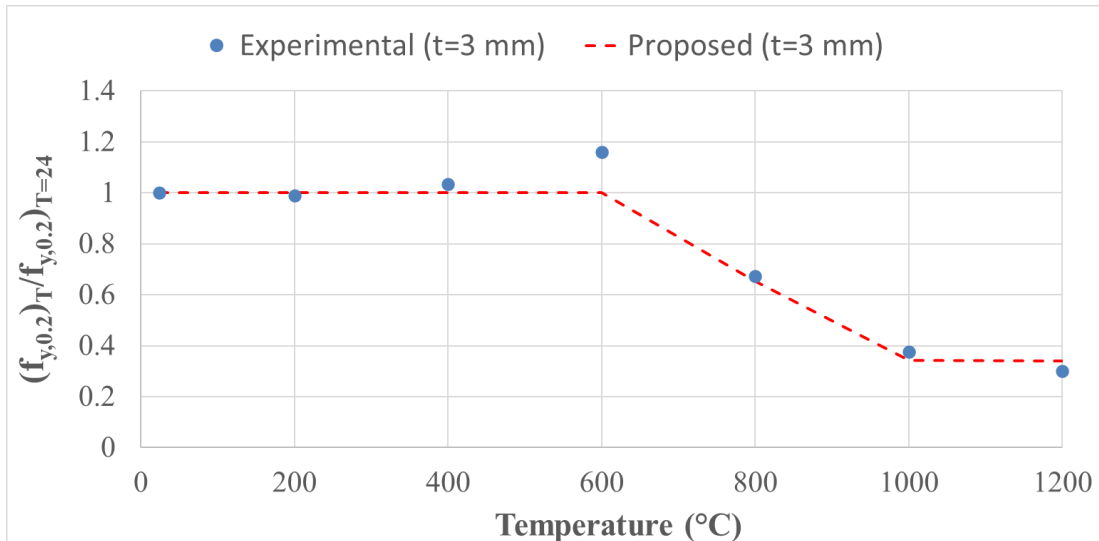
3.2. Yield Strength and Ultimate Tensile Strength

3.2.1. Yield strength for S700MC

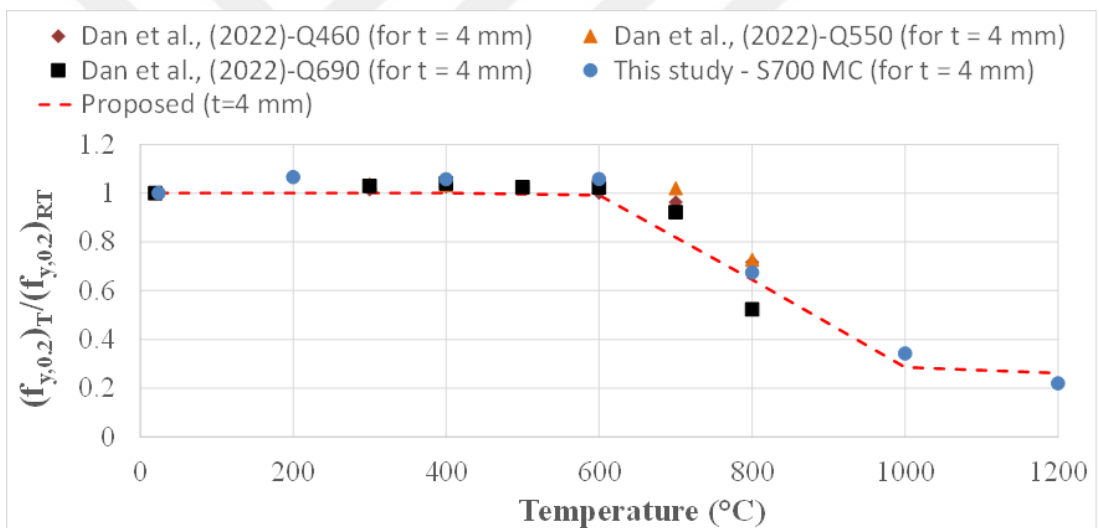
As mentioned earlier, the YS at different strain points, i.e., 0.2%, 0.5%, 1.5% and 2.0% were examined considering stress-strain curves. These parameters at different strain points are presented in Figure 3.2. For comparison, yield strength values for four strain levels were determined by considering the stress-strain behavior of different test samples. Subsequently, these values were compared with values at normal room temperature. The relation between four yield strength values obtained from elevated temperatures and the values at normal room temperature (RT) was examined. The normalized values $((f_{y,0.2})_T / (f_{y,0.2})_{RT}, (f_{y,0.5})_T / (f_{y,0.5})_{RT}, (f_{y,1.5})_T / (f_{y,1.5})_{RT}, (f_{y,2.0})_T / (f_{y,2.0})_{RT})$ for test specimens of each thickness have been presented in Figure 3.9- Figure 3.12 as a function of temperature.



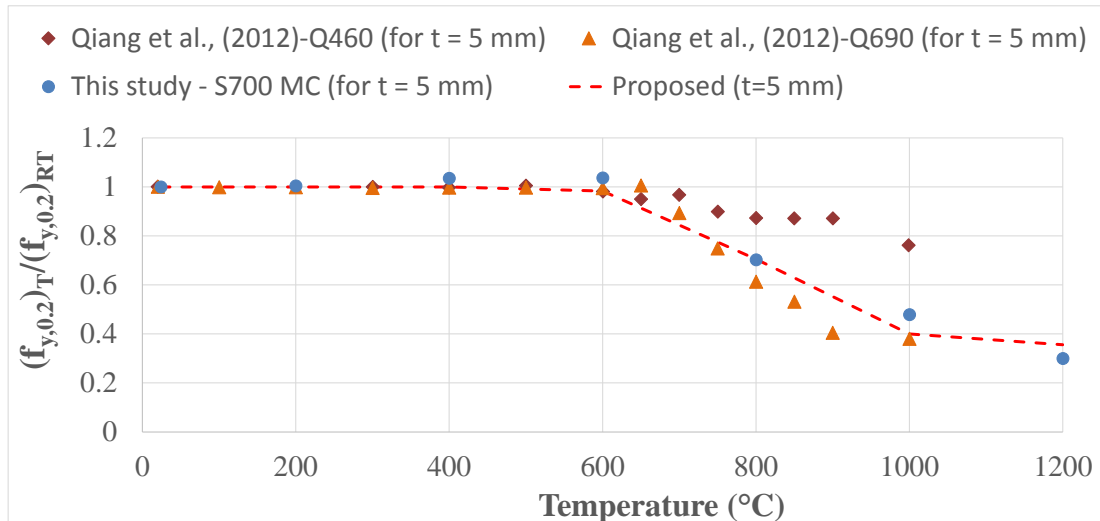
a) Assessment of the YS (or 0.2% proof strength) properties of test samples with a thickness of 2.5 mm



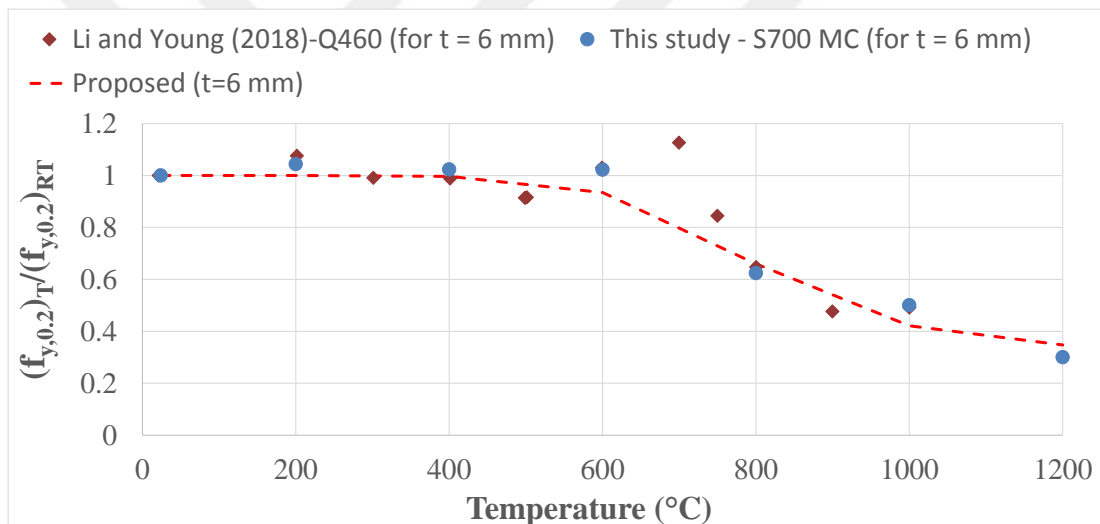
b) Assessment of the YS (or 0.2% proof strength) properties of test samples with a thickness of 3 mm



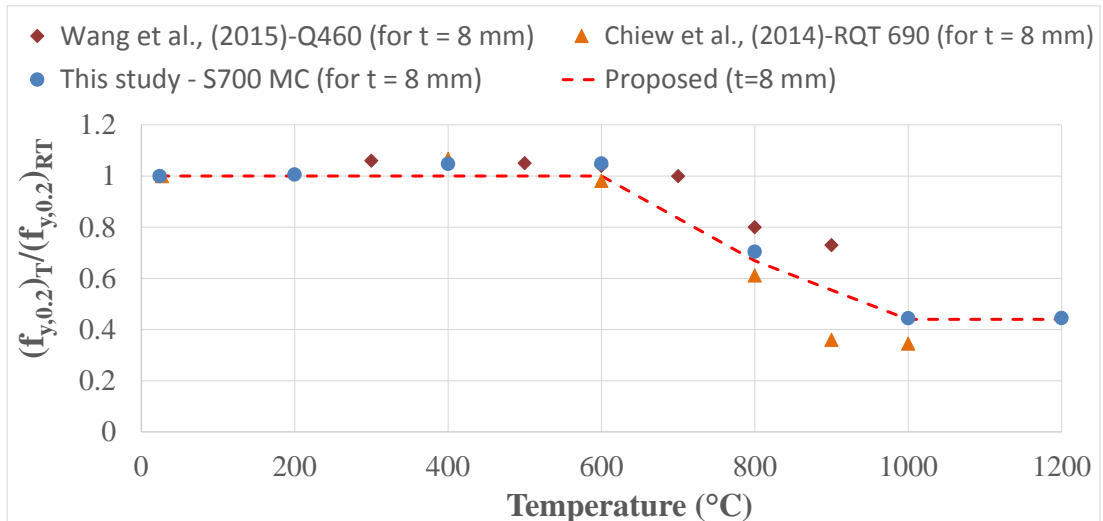
c) Assessment of the YS (or 0.2% proof strength) properties of test samples with a thickness of 4 mm



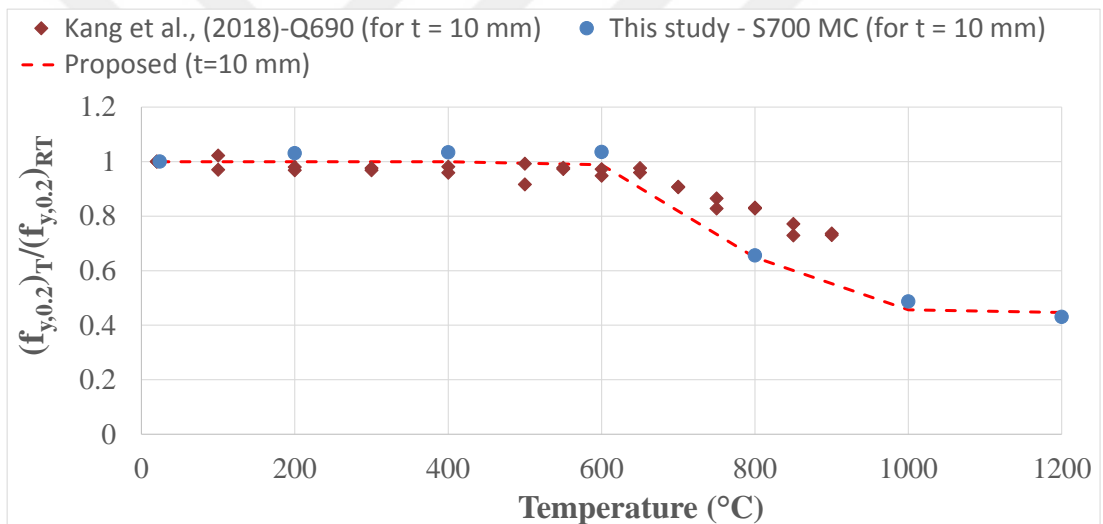
d) Assessment of the YS (or 0.2% proof strength) properties of test samples with a thickness of 5 mm



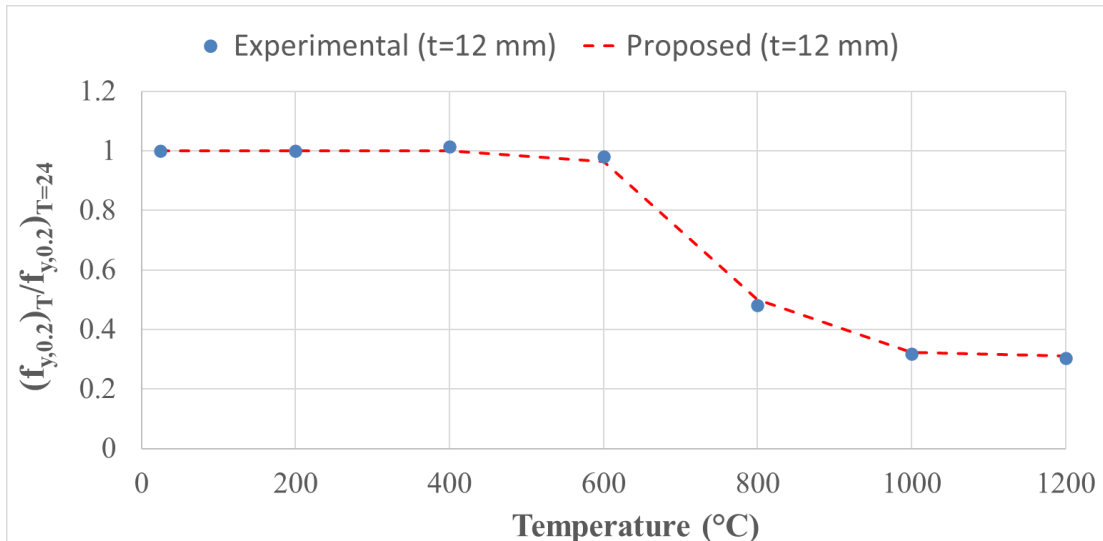
e) Assessment of the YS (or 0.2% proof strength) properties of test samples with a thickness of 6 mm



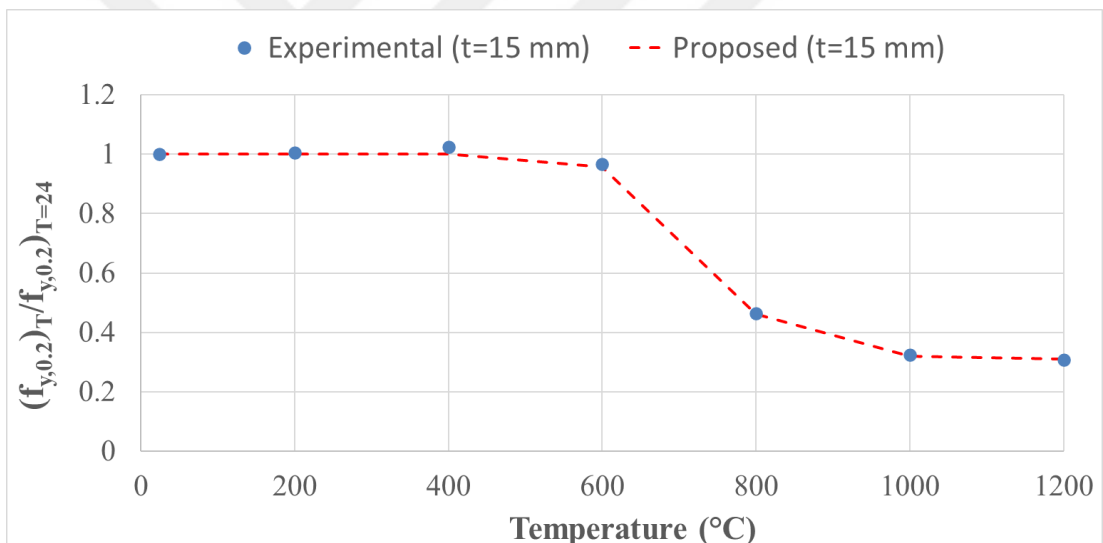
f) Assessment of the YS (0.2% proof strength) properties of test samples with a thickness of 8 mm



g) Assessment of the YS (0.2% proof strength) properties of test samples with a thickness of 10 mm

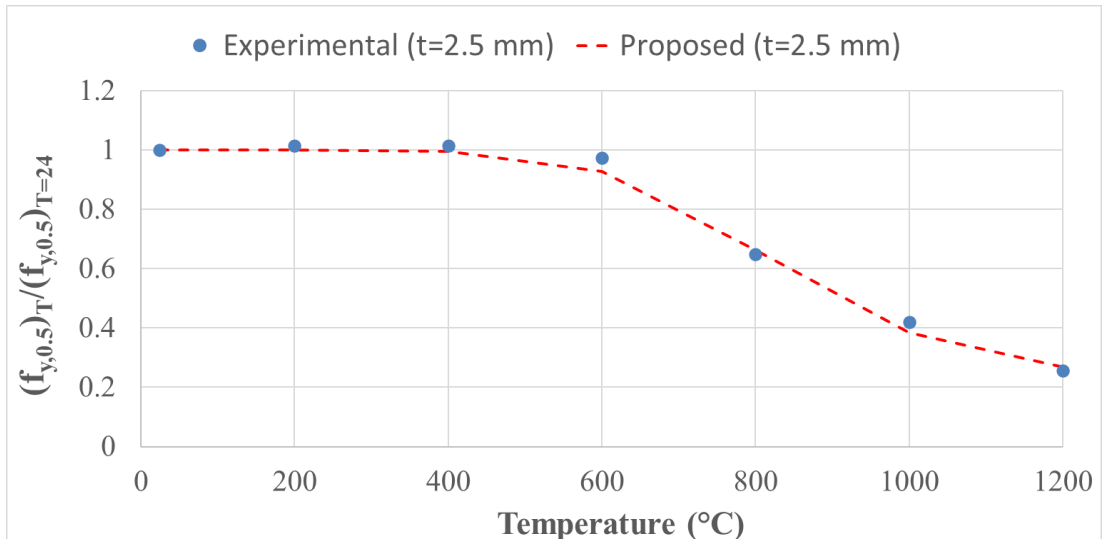


h) Assessment of the YS (or 0.2% proof strength) properties of test samples with a thickness of 12 mm

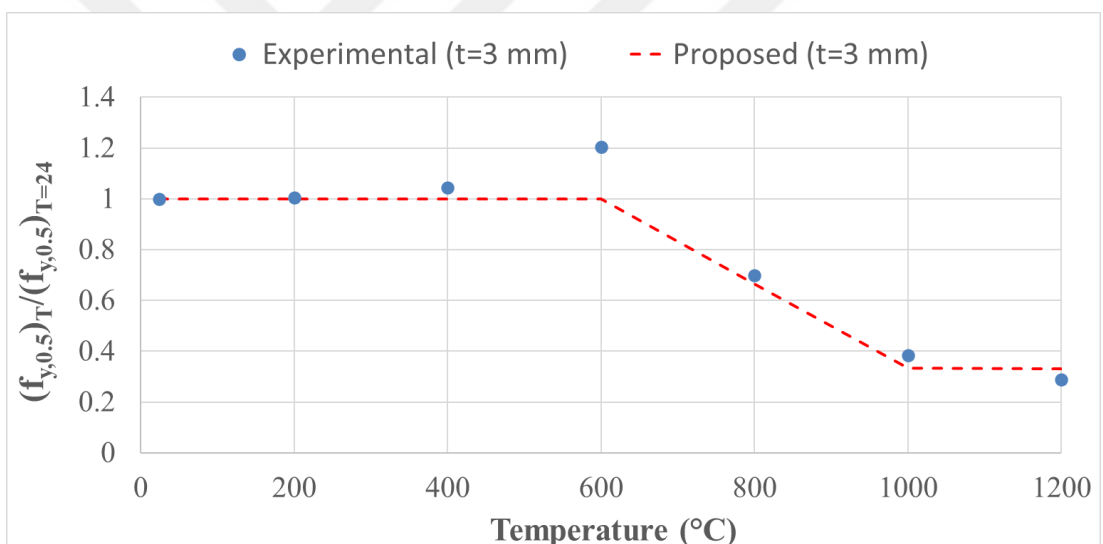


i) Assessment of the YS (or 0.2% proof strength) properties of test samples with a thickness of 15 mm

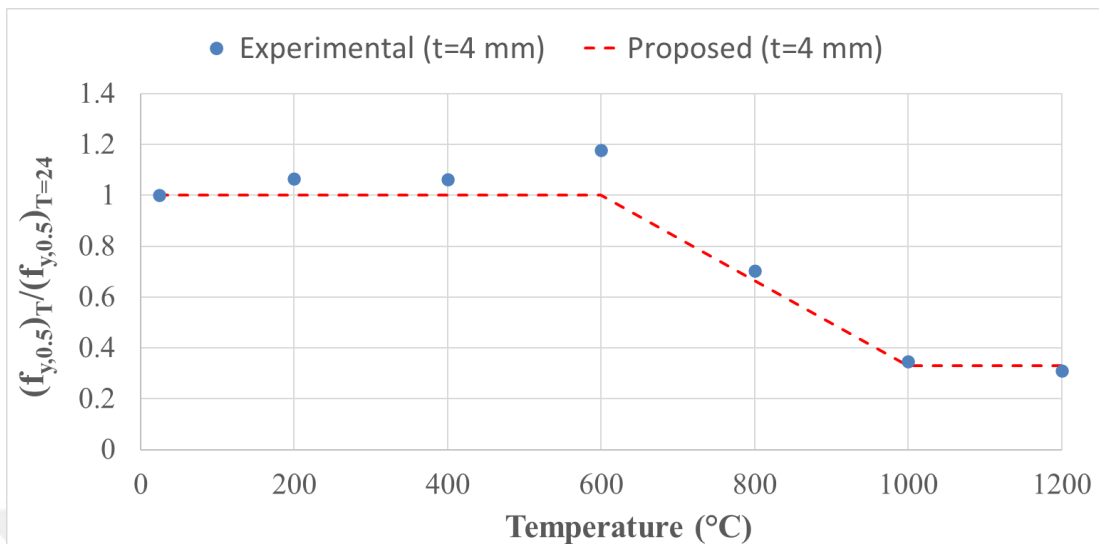
Figure 3.9. Assessment of YS (or 0.2% proof strength) of different HSS



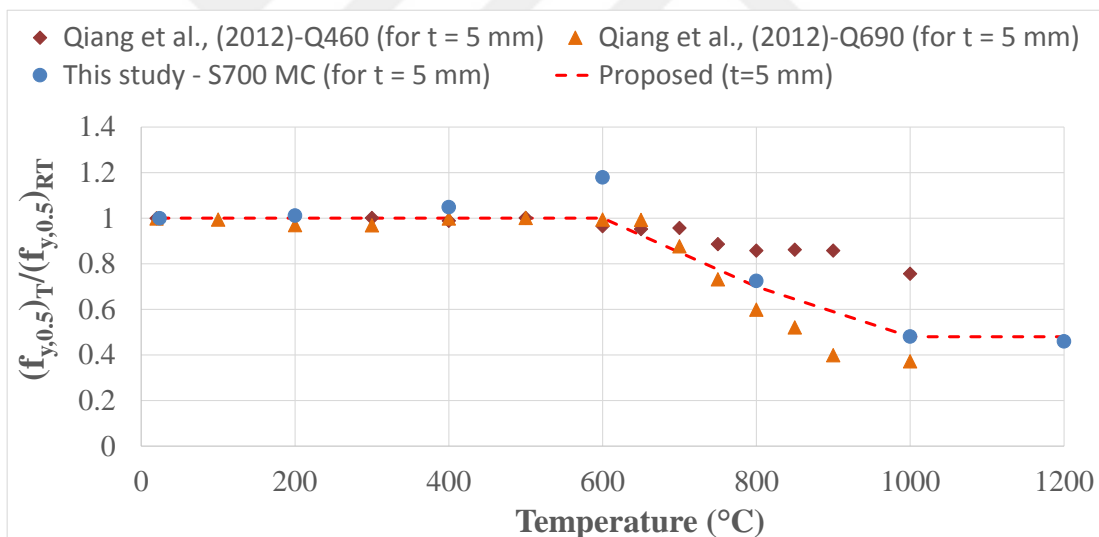
a) Assessment of the YS (0.5% proof strength) properties of test samples with a thickness of 2.5 mm



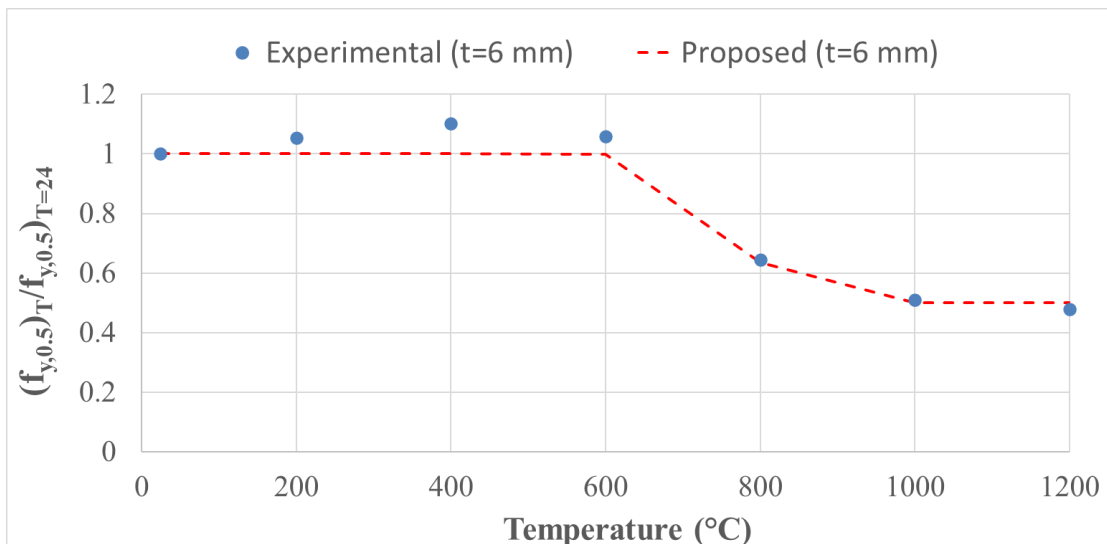
b) Assessment of the YS (0.5% proof strength) properties of test samples with a thickness of 3 mm



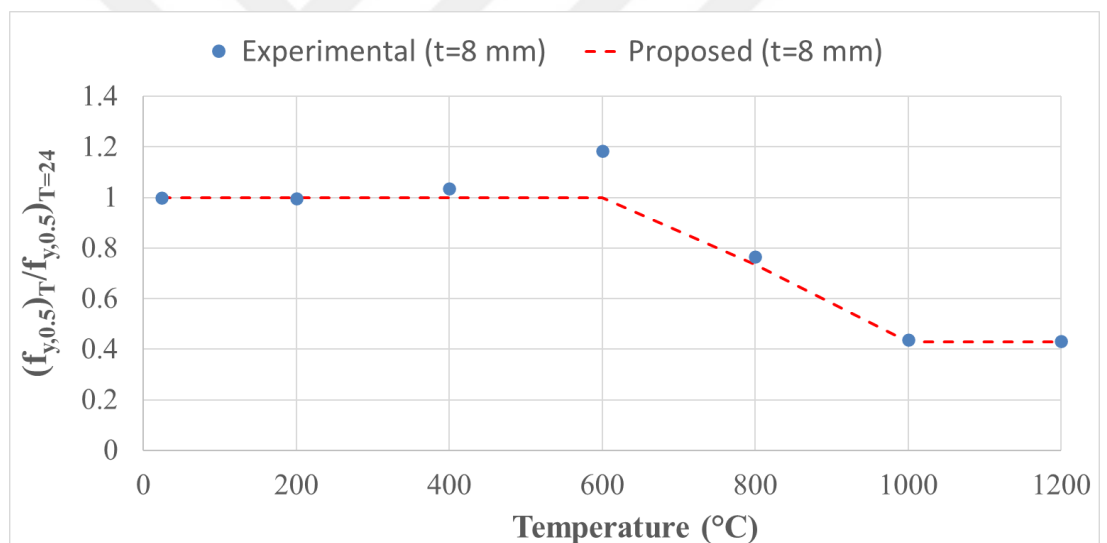
c) Assessment of the YS (0.5% proof strength) properties of test samples with a thickness of 4 mm



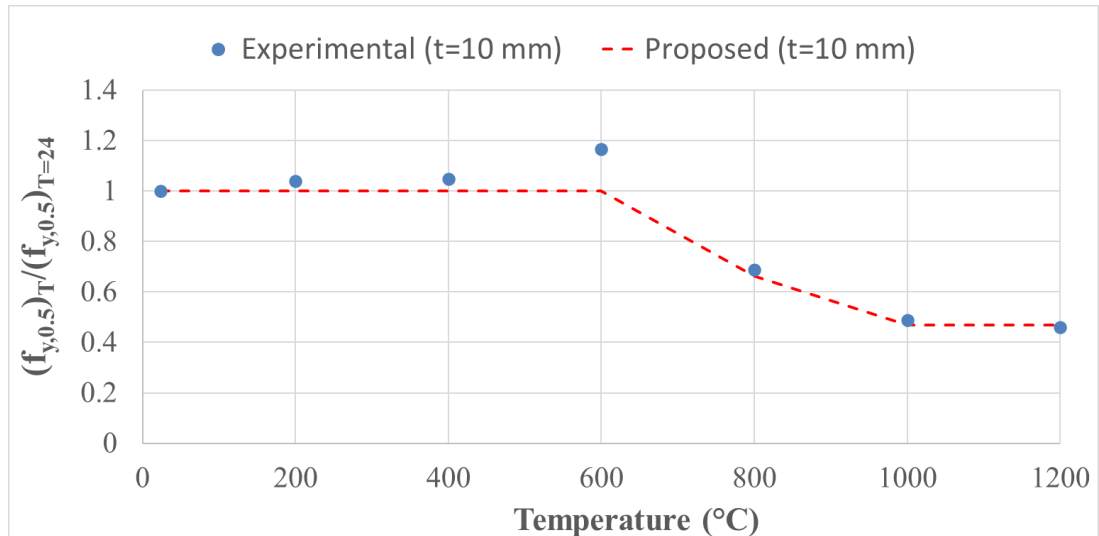
d) Assessment of the YS (0.5% proof strength) properties of test samples with a thickness of 5 mm



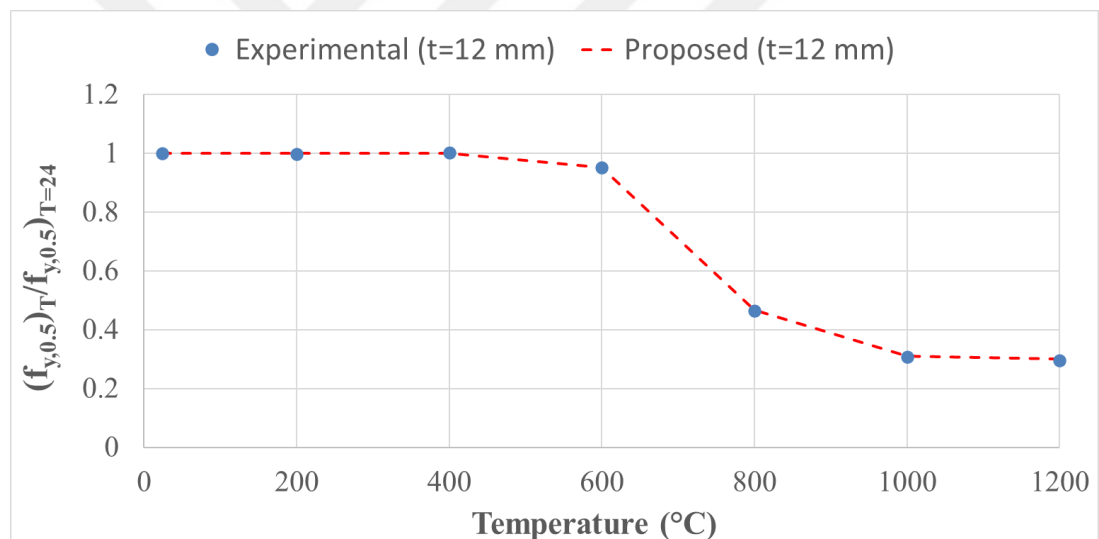
e) Assessment of the YS (0.5% proof strength) properties of test samples with a thickness of 6 mm



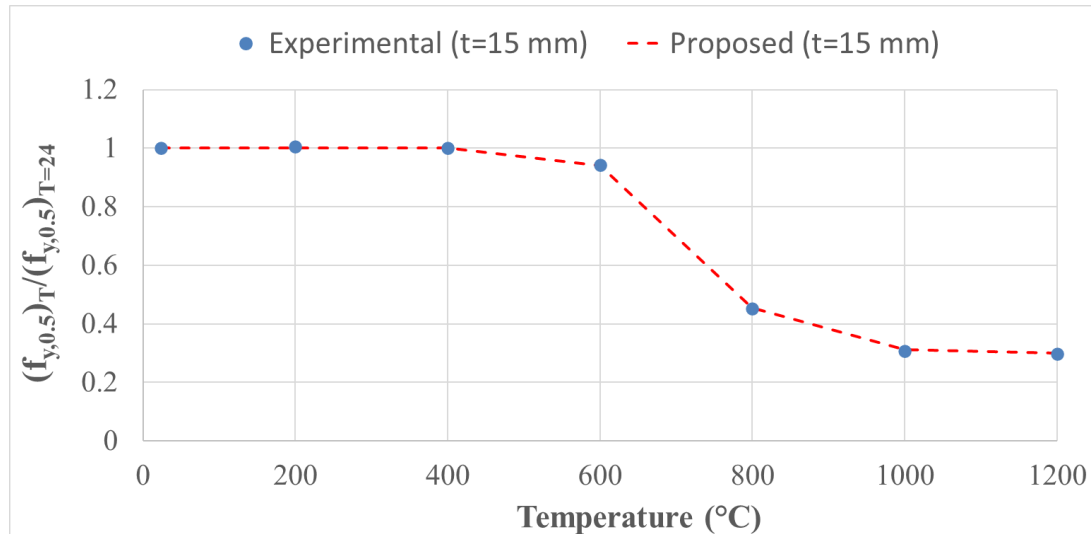
f) Assessment of the YS (0.5% proof strength) properties of test samples with a thickness of 8 mm



g) Assessment of the YS (0.5% proof strength) properties of test samples with a thickness of 10 mm

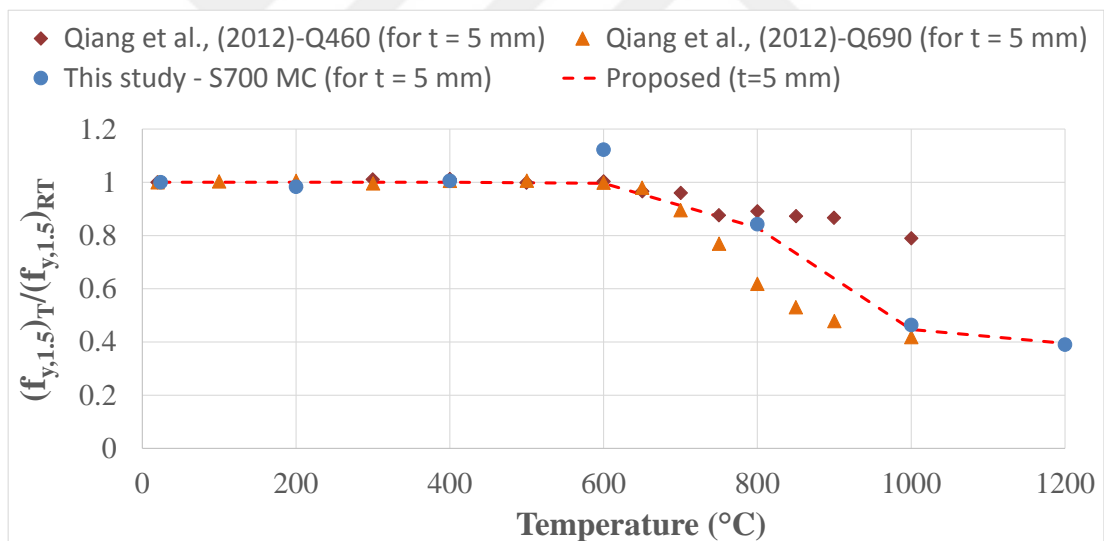


h) Assessment of the YS (0.5% proof strength) properties of test samples with a thickness of 12 mm



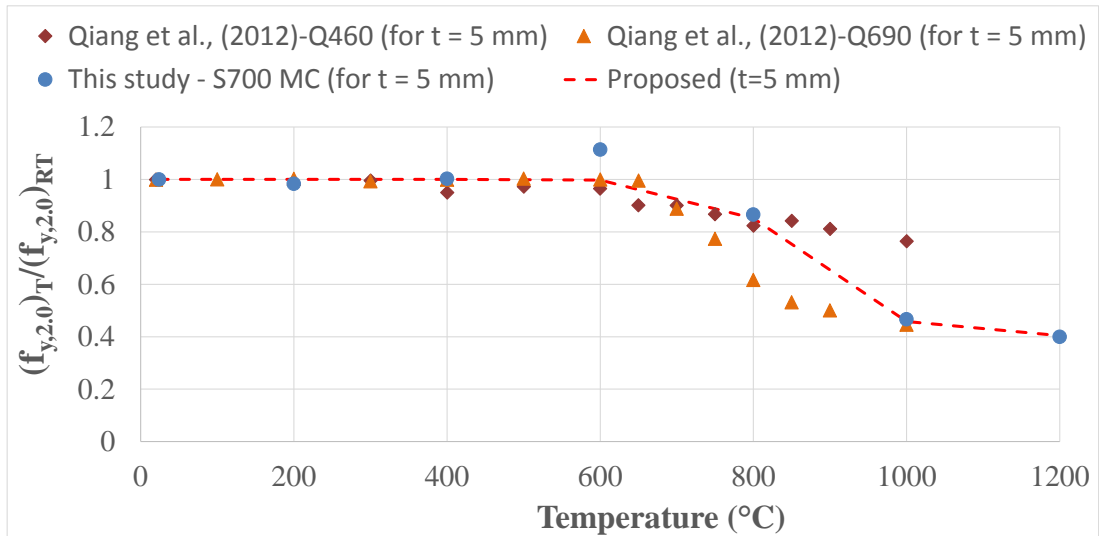
i) Assessment of the YS (0.5% proof strength) properties of test samples with a thickness of 15 mm

Figure 3.10. Assessment of YS of different (0.5% proof strength) HSS

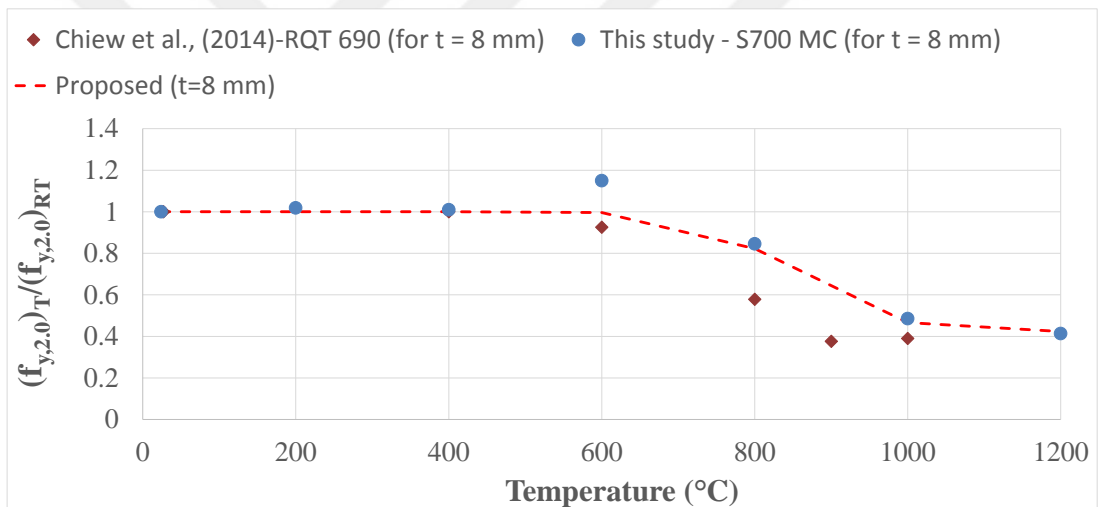


a) Assessment of the YS (1.5% proof strength) properties of test samples with a thickness of 5 mm

Figure 3.11. Assessment of the YS of different (1.5% proof strength) HSS



a) Assessment of the YS (2.0% proof strength) properties of test samples with a thickness of 5 mm

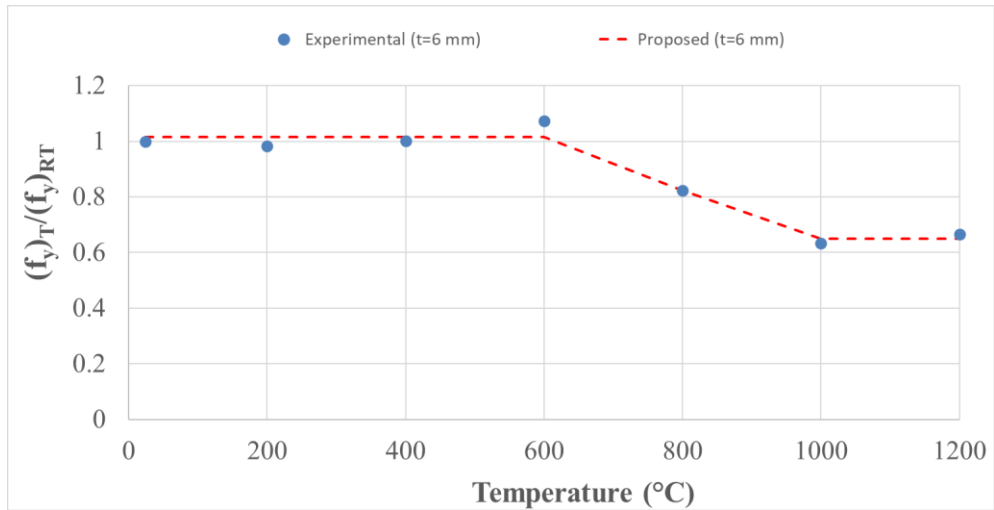


b) Assessment of the YS (2.0% proof strength) properties of test samples with a thickness of 8 mm

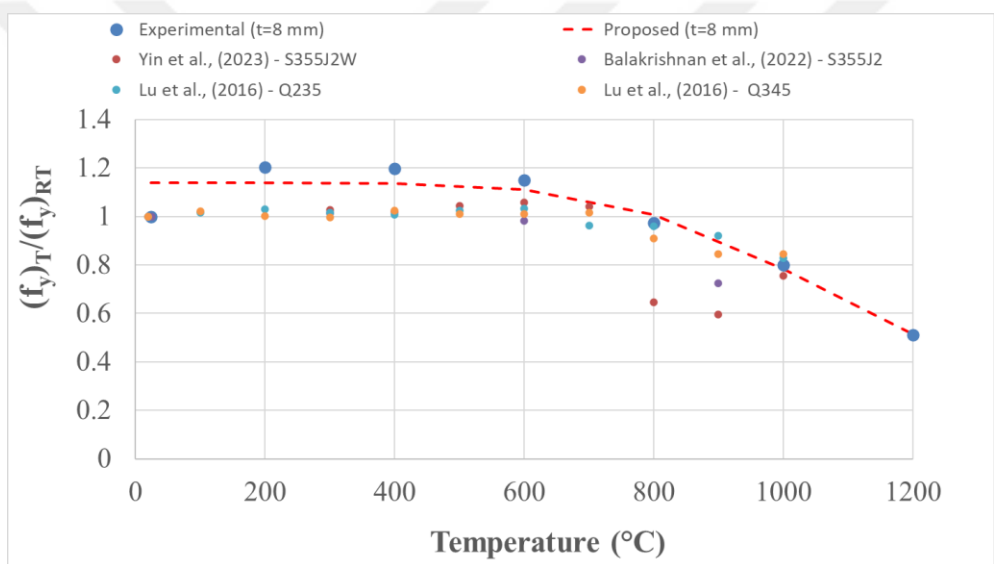
Figure 3.12. Assessment of the YS of different (2.0% proof strength) HSS

3.2.2. Yield strength for S235JR

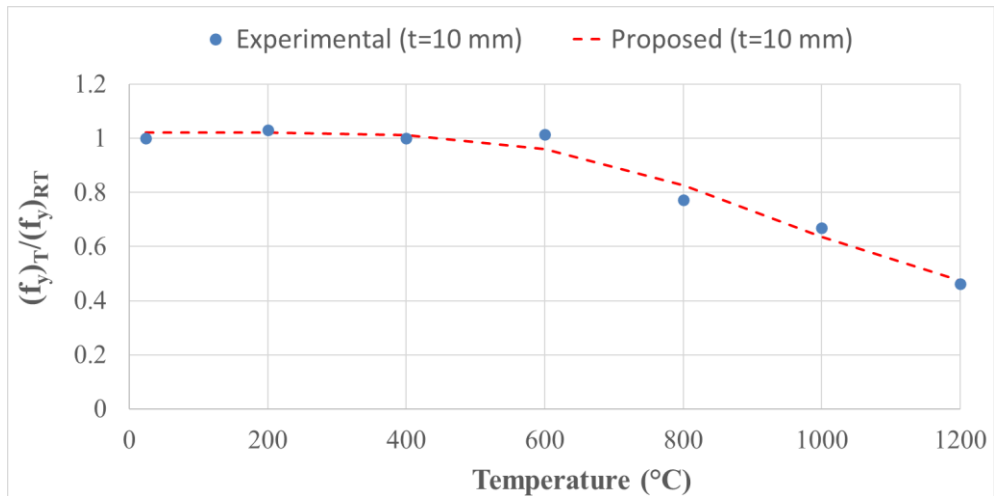
The determination of the YS of the S235JR steel, selected to represent CCM steels, is shown in Figure 3.2. The YS changes of S235JR steel at different temperatures for thicknesses ranging from 6 mm to 12 mm, are shown in Figures 3.13. The assessment of yield strength of different CCM steels at different temperatures is shown in Figures 3.14.



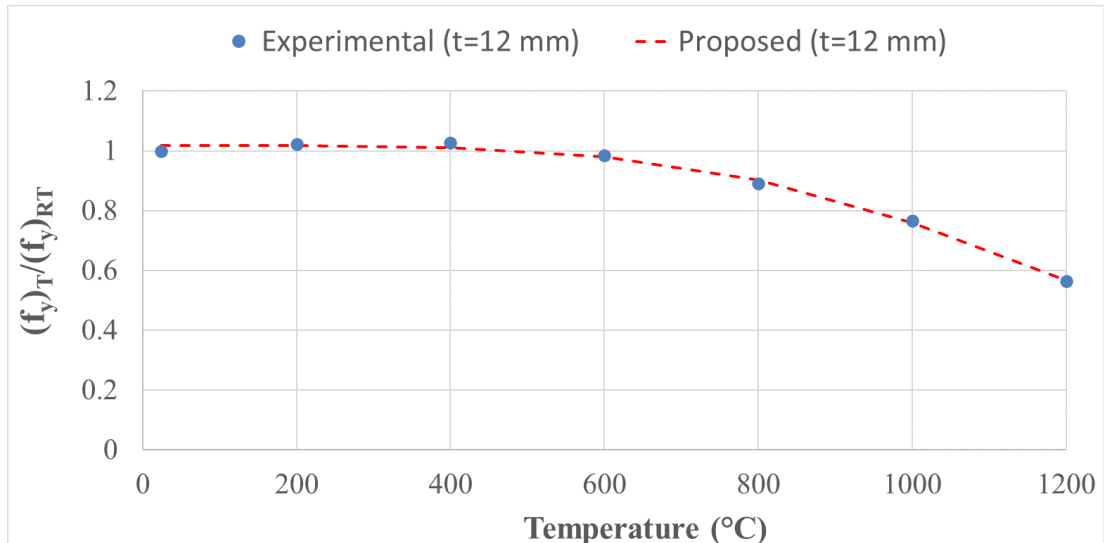
a) Assessment of the YS properties of test samples with a thickness of 6 mm



b) Assessment of the YS properties of test samples with a thickness of 8 mm



c) Assessment of the YS properties of test samples with a thickness of 10 mm



d) Assessment of the YS properties of test samples with a thickness of 12 mm

Figure 3.13. Assessment of the YS of conventional carbon mild steel

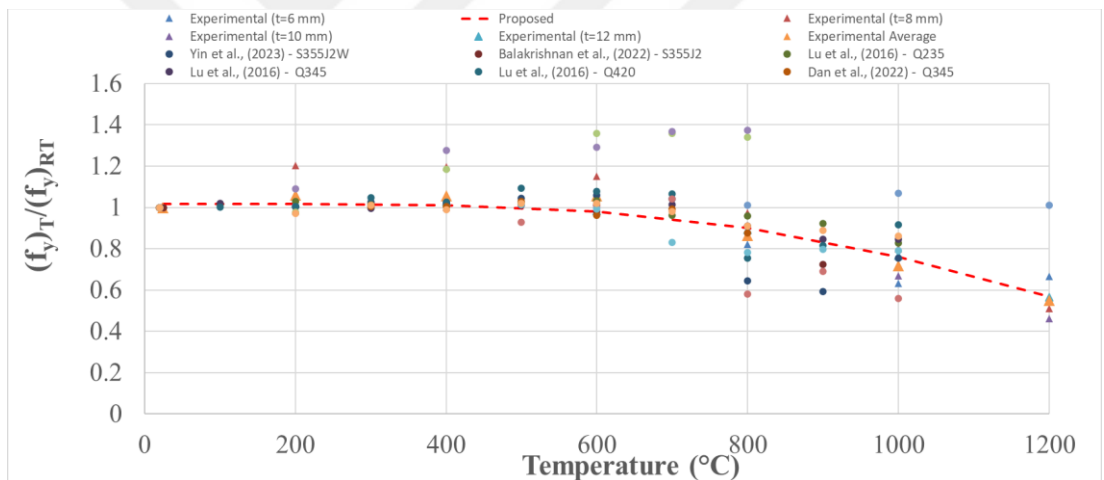
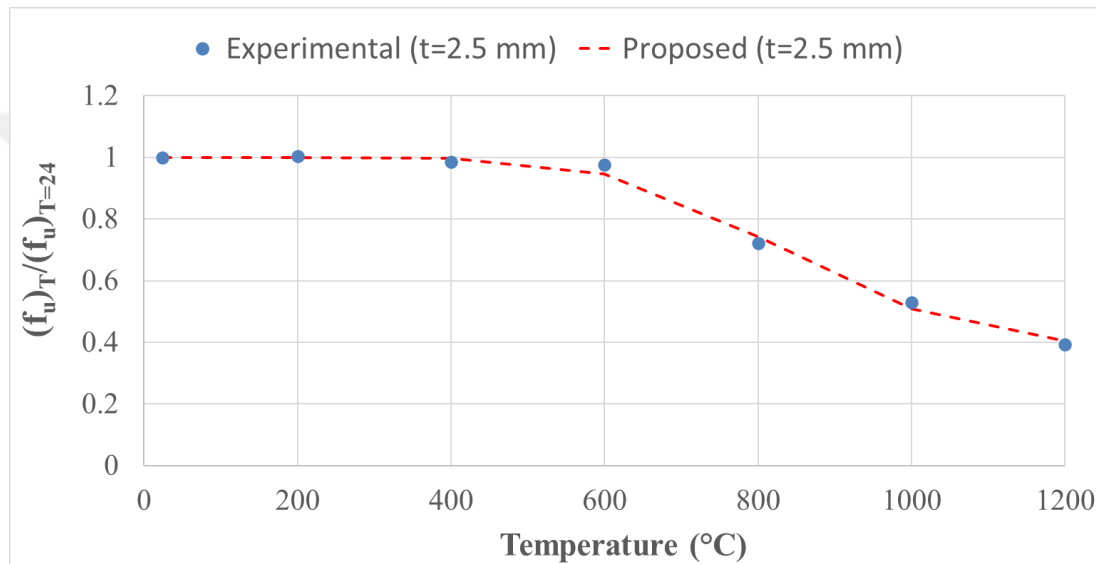


Figure 3.14. Assessment of YS of different CCM steels at different temperatures

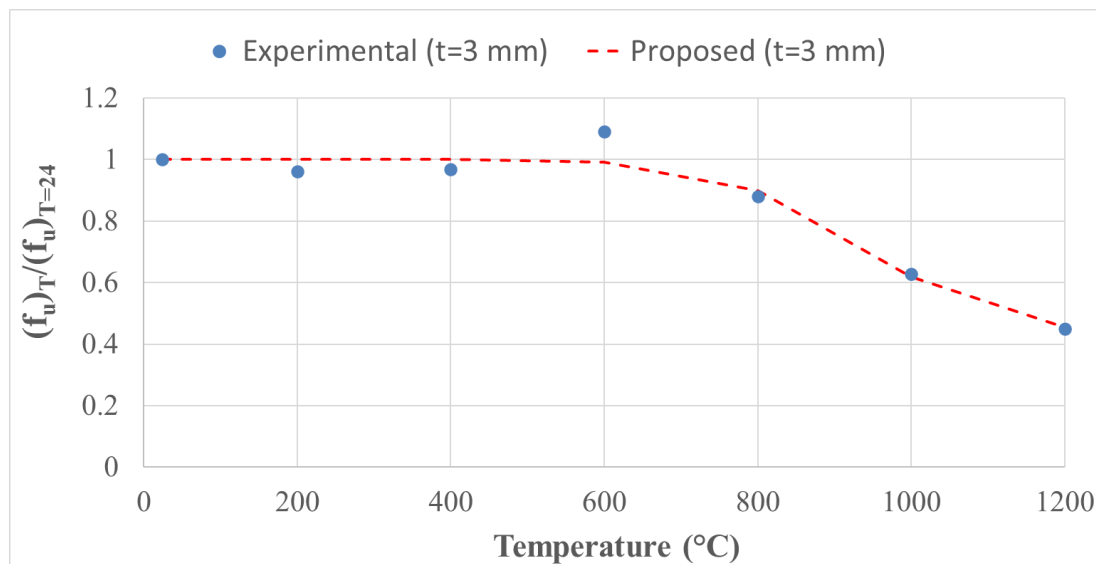
As shown in Figure 3.6. – Figure 3.14. it has been observed that the YS of most test samples is not affected when the heating temperature does not exceed 600°C in both S700MC and S235JR test samples. This result thereby confirmed a study conducted by Qiang et al. (2012). However, the deterioration in strength was more pronounced at temperatures above 600°C.

3.2.3. Ultimate strength for S700MC

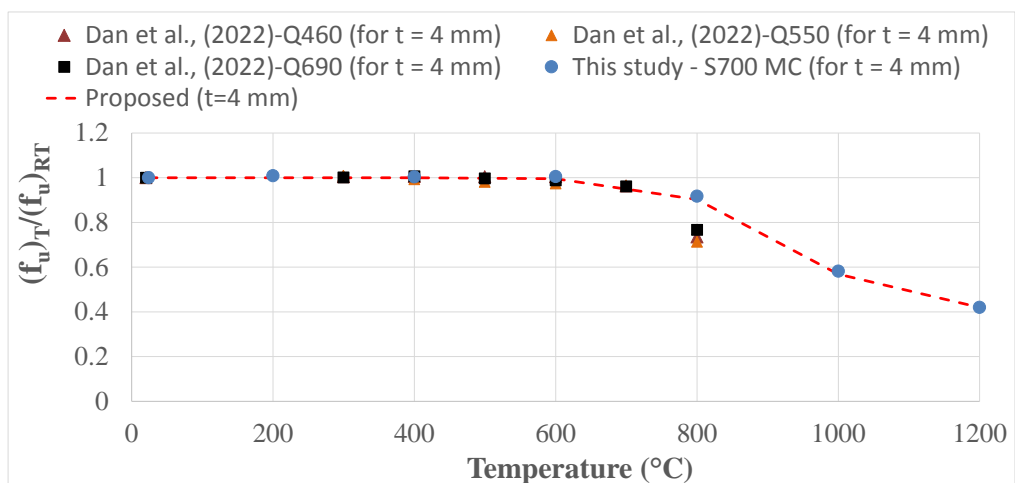
Changes in the ultimate tensile strength values after specimens were subjected to high temperatures were calculated. In order to find the ultimate tensile strength (UTS) of test samples, a tensile test was carried out until fracture. The UTS values of the test samples after fire exposure were identified. The relation between yield strength values obtained from high temperatures and the values at normal room temperature was examined. The normalized values $((f_u)_T/(f_u)_{T=24})$ for each thick specimens are shown in Figure 3.15.



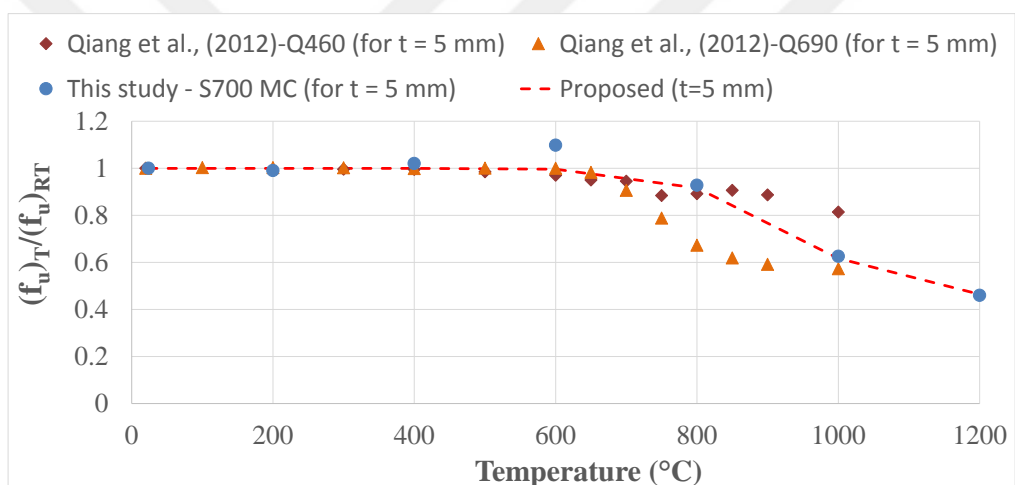
a) Assessment of ultimate strength properties of test samples with a thickness of 2.5 mm



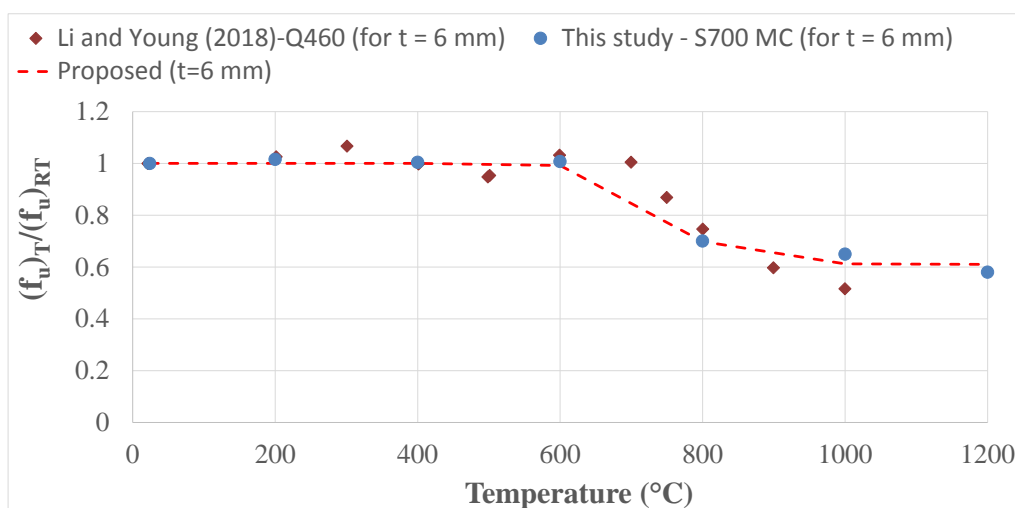
b) Assessment of ultimate strength properties of test samples with a thickness of 3 mm



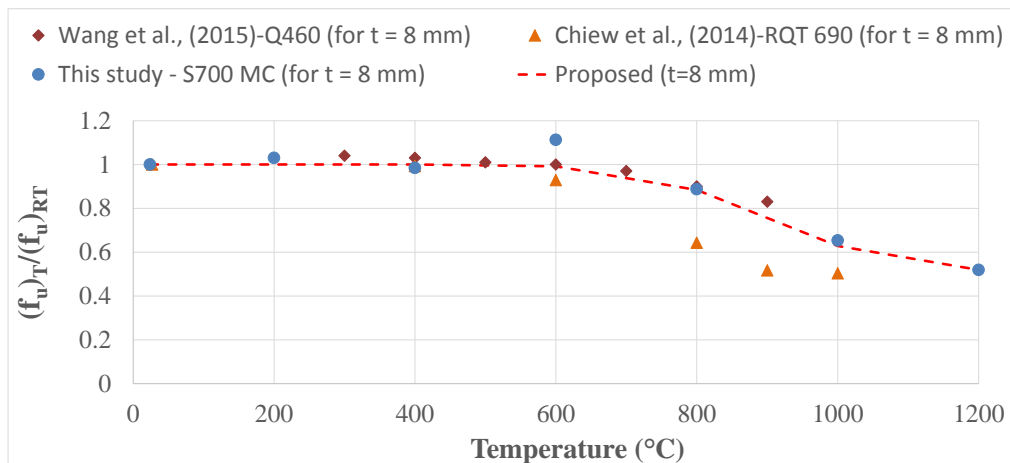
c) Assessment of ultimate strength properties of test samples with a thickness of 4 mm



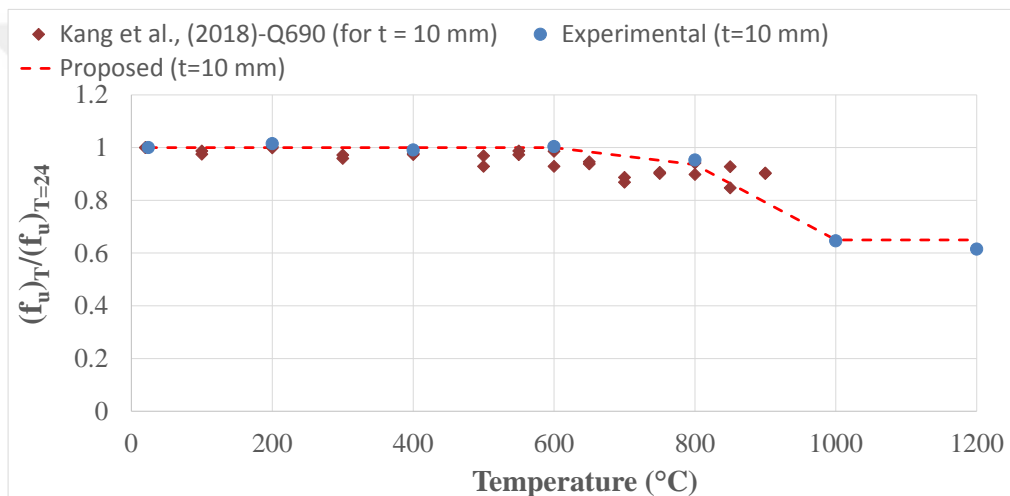
d) Assessment of ultimate strength properties of test samples with a thickness of 5 mm



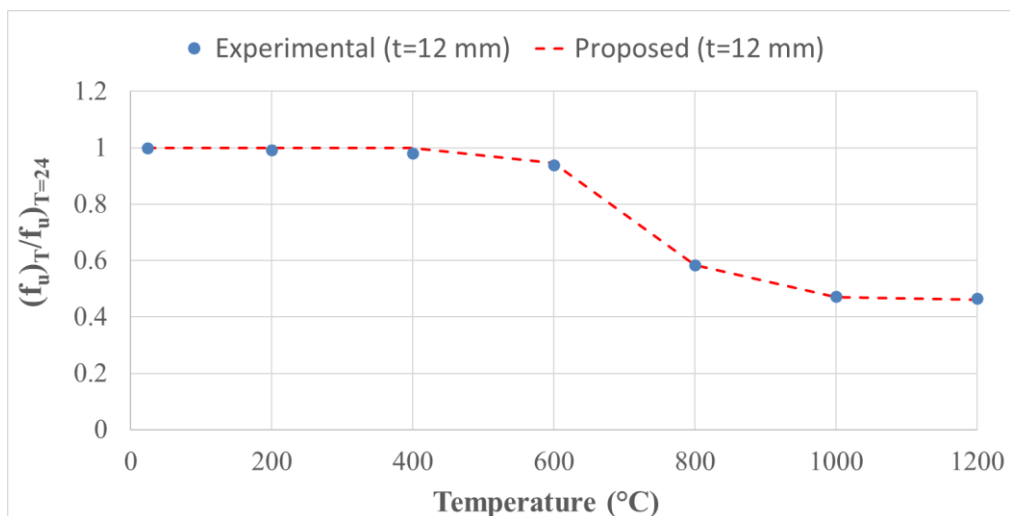
e) Assessment of ultimate strength properties of test samples with a thickness of 6 mm



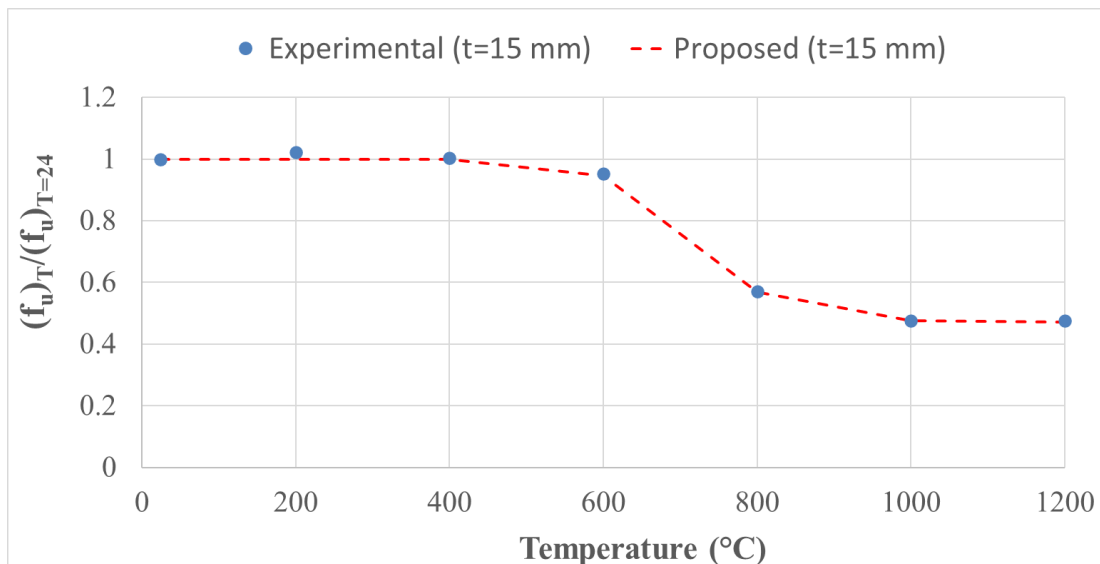
f) Assessment of ultimate strength properties of test samples with a thickness of 8 mm



g) Assessment of ultimate strength properties of test samples with a thickness of 10 mm



h) Assessment of ultimate strength properties of test samples with a thickness of 12 mm



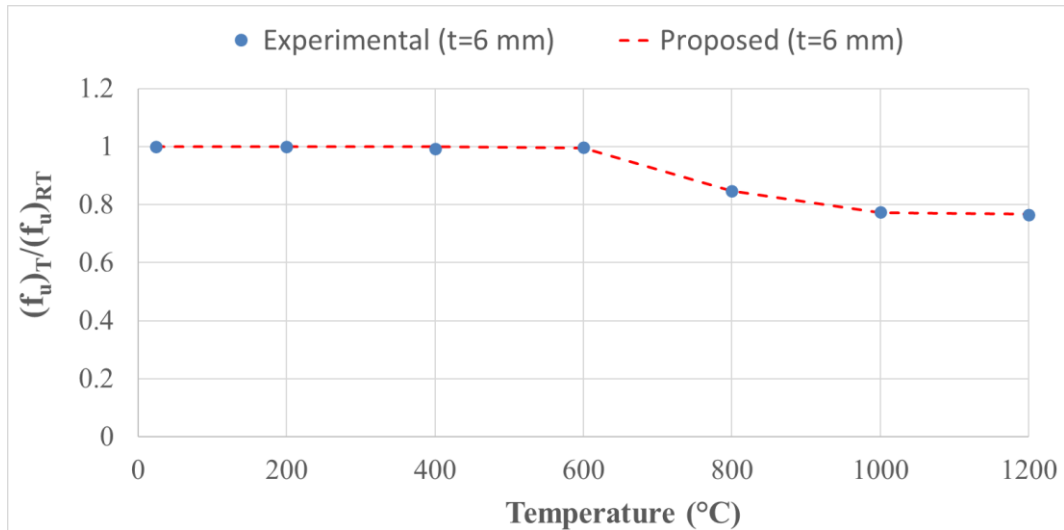
i) Assessment of ultimate strength properties of test samples with a thickness of 15 mm

Figure 3.15. Assessment of Ultimate Tensile Strengths of Different HSS

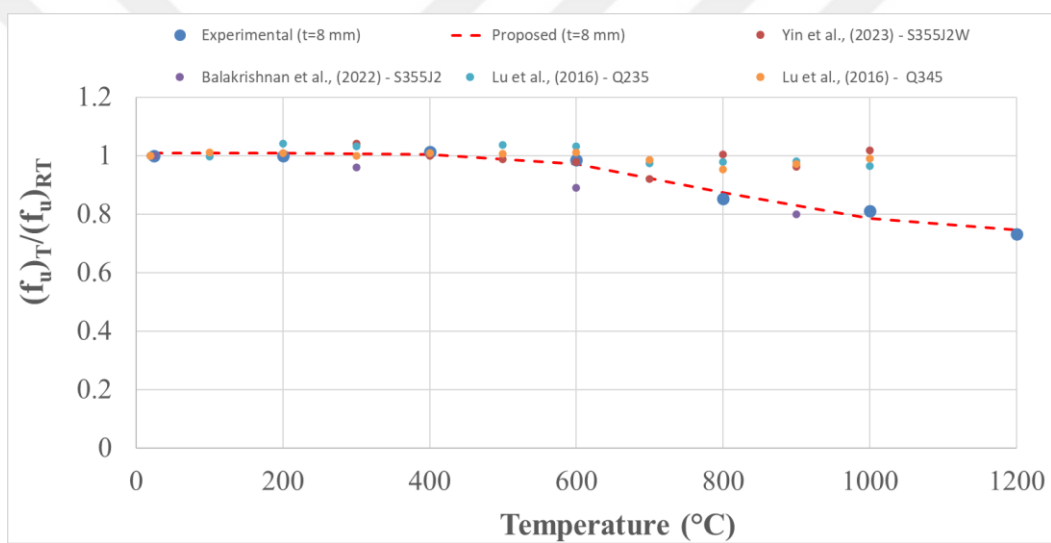
As shown in Figure 3.15. the UTS of most test specimens was not affected until the temperature reached 600°C . However, a decrease in the UTS of the test samples was observed when the heating temperature exceeded 600°C .

3.2.4. Ultimate strength for S235JR

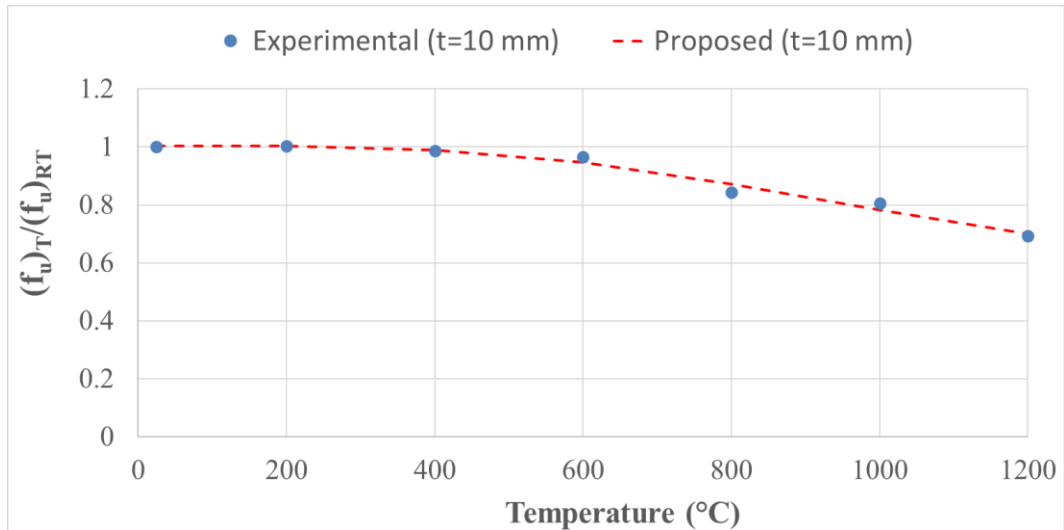
As shown in Figure 3.16. in experiments using S235JR steel samples, the UTS value starts to decrease mostly at 400°C , but the rate of decrease is sharper at 600°C . When figure 3.16 is examined, as the thickness of S235JR steel coupon samples increases, the UTS of the steel tends to decrease even when heated at low temperatures. For example, as can be seen in figure 3.16.a, although the UTS of 6 mm samples does not show a meaningful change when heated to 600°C , it can be observed in figure 3.16.d that the UTS of 12 mm samples decreases even though they are heated at low temperatures. In figure 3.17, a comparison of the results of this study with the studies carried out on CCM steels related to UTS can be seen.



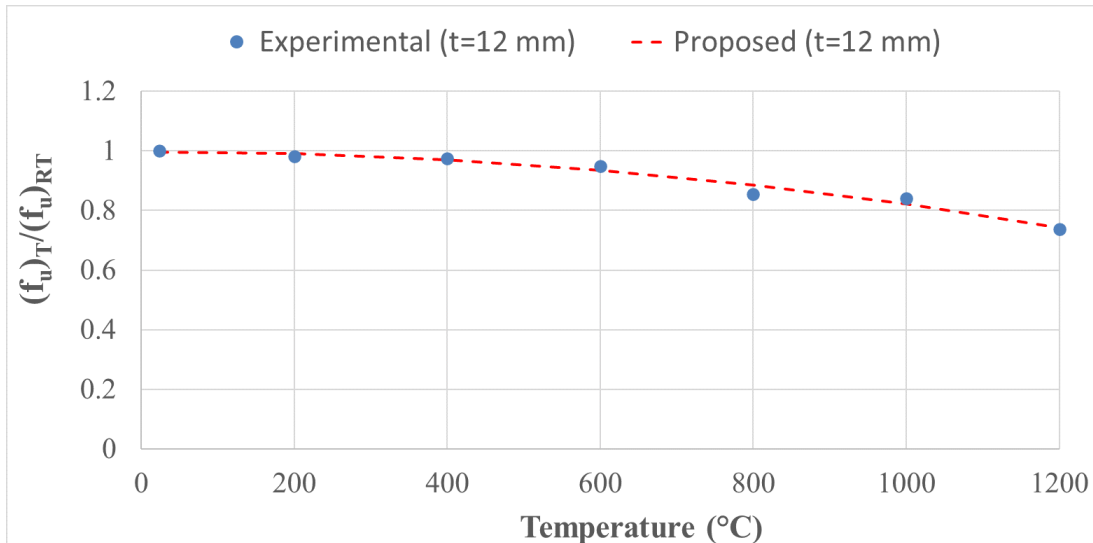
a) Assessment of ultimate strength properties of test samples with a thickness of 6 mm



b) Assessment of ultimate strength properties of test samples with a thickness of 8 mm



c) Assessment of ultimate strength properties of test samples with a thickness of 10 mm



d) Assessment of ultimate strength properties of test samples with a thickness of 12 mm

Figure 3.16. Assessment of Ultimate Tensile Strengths of CCMS

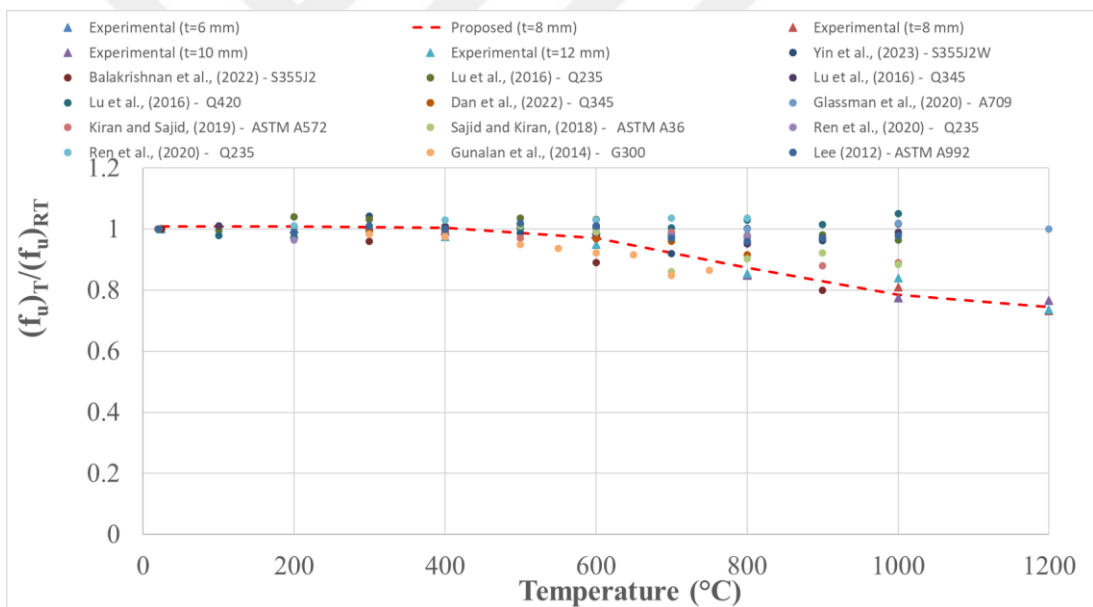


Figure 3.17. Assessment of ultimate strength of different CCM steels at different temperatures

4. COMPARISON OF EXPERIMENTAL RESULTS WITH AVAILABLE RESULTS IN THE LITERATURE AND PROPOSED PREDICTIVE EQUATIONS

In order to evaluate the experimental test results conducted in this study, mechanical parameters obtained from other researchers were considered. Pursuant to this goal, test data on different high strength steels such as Q235, Q345, S355J2, Q420, A709, A36, A572, A992, G300, Q460, Q550, Q690 and RQT-690 was collected. The test results of CCMS conducted by Yin et al. (2023), Balakrishnan et al. (2022), Lu et al. (2016), Dan et al. (2022), Glassman et al (2020), Kiran and Sajid (2019), Sajid and Kiran (2018), Ren et al. (2020), Gunalan et al. (2014), and Lee et al. (2012), as well as the test results of HSS conducted by Qiang et al. (2012), Chiew et al. (2012), Wang et al. (2015), Dan et al. (2022), and Li and Young (2018), were compared with the results from the present study. Based on the test specimen thickness, Figure 3.5 - Figure 3.16. represents the comparison of mechanical properties between different HS and CCM steels as a function of temperature. It should be noted that the S235JR and S700MC steel grades were used in this study. S235JR test specimens with thicknesses ranging from 6 mm to 12 mm and S700MC test specimens with thicknesses ranging from 2.5 mm to 15 mm were heated up to 1200 °C, but in the available literature studies, the exposure temperature of the test specimens, which were prepared considering a single thickness, was mostly below 1000 °C. As shown in Figure 3.5 - Figure 3.16. data representing P-F mechanical properties mostly follow similar trends. The data points for the elastic modulus, yield and ultimate strengths each fall within a narrow band. The changes in the response quantities can be accurately and directly represented as a function of the temperature. By applying curve-fitting to the data presented in Figure 3.5 - Figure 3.16. the following relationship between response quantities and temperature (T) has been developed:

$$(E)_T = \left\{ C_1 + C_2 \times \text{EXP} \left\{ -0.5 \times \left[(T - C_3) / C_4 \right]^2 \right\} \right\} \times (E)_{RT} \quad (4.1)$$

where C1, C2, C3 and C4 = the coefficients given in Table 4.1 for S700MC.

Table 4.1. Constants for the S700MC modulus of elasticity used in Equation (4.1)

	Thickness of plate (mm)	C_1	C_2	C_3	C_4
$(E)_T$	2.5	-848.74	849.8	318	24730
	3	-185.22	186.3	354.7	11914
	4	1.007	-0.53	1647.7	530.3
	5	-28.3	29.3	120	11900
	6	-488.58	489.6	370	37241
	8	-8.7	9.71	47	6447
	10	0.969	0.079	299.5	198.86
	12	1	0.22	775	106
	15	0.92	0.265	690	407.7

$$(f)_T = \left\{ C_5 + \frac{C_6}{\left[1 + \left(\frac{T}{C_7} \right)^{C_8} \right]} \right\} \times (f)_{RT} \quad (4.2)$$

where C5, C6, C7 and C8 are the coefficients given in Table 4.2 - Table 4.9.

Eqs. (4.1) indicate that expressions for the P-F mechanical properties were derived considering four different coefficients given in Table 4.1 - Table 4.9. As shown in Eq. (4.1), the P-F modulus of elasticity $(E)_T$ is given as a function of the temperature (T), E value at room temperature $(E)_{RT}$ and exposure temperature (T in °C) value of the HSS. It should be noted that Equation (4.2) provides changes in the elasticity modulus of CCMS, as well as changes in the yield strength and ultimate strength of HSS and CCMS after exposure to fire. As shown in Eq. (4.2), P-F yield strength values $(f_{y,0.2})_T$, $(f_{y,0.5})_T$, $(f_{y,1.5})_T$, $(f_{y,2.0})_T$, $(f_y)_T$ and P-F ultimate tensile strength $(f)_{RT}$ values are given as a function of the temperature (T in °C), and corresponding strength values at

room temperature ($(f)_{RT}$). The coefficients C_5 , C_6 , C_7 and C_8 are given in Table 4.2 - Table 4.9. The elasticity modulus of S235JR steel does not show significant changes until it reaches 800°C. However, after heating to temperatures above 800°C, the elastic modulus decreases, with a loss reaching up to 35% at 1200°C for 6 mm and 8 mm thicknesses. The maximum modulus of elasticity loss is about 20% at 1200°C for 10 mm and 12 mm thicknesses. This indicates that the elasticity modulus loss is higher at elevated temperatures for smaller thicknesses. As mentioned earlier, these values were measured by RFDA.

Table 4.2. Constants for the S235JR modulus of elasticity used in Equation (4.2)

	Thickness of plate (mm)	C_5	C_6	C_7	C_8
$(E)_T$	6	0.664	0.336	996.9	87.8
	8	0.415	0.585	1167	8.58
	10	0.8	0.2	1000	9.68
	12	0.535	0.465	1290	6.21

Table 4.3. Constants for the S700MC yield strength of $(f_{y,0.2})_T$ used in Equation (4.2)

	Thickness of plate (mm)	C_5	C_6	C_7	C_8
$(f_{y,0.2})_T$	2.5	0.20	0.80	838	6.91
	3	0.34	0.66	796.8	34.9
	4	0.26	0.74	804.3	15.3
	5	0.35	0.65	812.5	12
	6	0.32	0.68	800	7.8
	8	0.44	0.56	798	148.5
	10	0.446	0.554	772.05	15.4
	12	0.31	0.69	744	13.3
	15	0.39	0.61	738	12

Table 4.4. Constants for the S700MC yield strength of $(f_{y,0.5})_T$ used in Equation (4.2)

	Thickness of plate (mm)	C_5	C_6	C_7	C_8
$(f_{y,0.5})_T$	2.5	0.20	0.80	838	6.91
	3	0.34	0.66	796.8	34.9
	4	0.26	0.74	804.3	15.3
	5	0.35	0.65	812.5	12
	6	0.32	0.68	800	7.8
	8	0.44	0.56	798	148.5
	10	0.45	0.55	787	41
	12	0.31	0.69	744	13.3
	15	0.39	0.61	738	12

Table 4.5. Constants for the S700MC yield strength of $(f_{y,1.5})_T$ used in Equation (4.2)

	Thickness of plate (mm)	C_5	C_6	C_7	C_8
$(f_{y,1.5})_T$	2.5	0.20	0.80	838	6.91
	3	0.34	0.66	796.8	34.9
	4	0.26	0.74	804.3	15.3
	5	0.35	0.65	812.5	12
	6	0.32	0.68	800	7.8
	8	0.44	0.56	798	148.5
	10	0.45	0.55	787	41
	12	0.31	0.69	744	13.3
	15	0.39	0.61	738	12

Table 4.6. Constants for the S700MC yield strength of $(f_{y,2.0})_T$ used in Equation (4.2).

	Thickness of plate (mm)	C_5	C_6	C_7	C_8
$(f_{y,2.0})_T$	2.5	0.20	0.80	838	6.91
	3	0.34	0.66	796.8	34.9
	4	0.26	0.74	804.3	15.3
	5	0.35	0.65	812.5	12
	6	0.32	0.68	800	7.8
	8	0.44	0.56	798	148.5
	10	0.45	0.55	787	41
	12	0.31	0.69	744	13.3
	15	0.39	0.61	738	12

Table 4.7. Constants for the S235JR yield strength of $(f_y)_T$ used in Equation (4.2).

	Thickness of plate (mm)	C5	C6	C7	C8
$(f_y)_T$	6	0.6488	0.3652	799	83.28
	8	0.05975	1.08025	1134	5.64
	10	0.2389	0.7821	1006	4.815
	12	-0.309	1.327	1409	4.14

Table 4.8. Constants for the S700MC ultimate tensile strength of $(f_u)_T$ used in Equation (4.2).

	Thickness of plate (mm)	C_5	C_6	C_7	C_8
$(f_u)_T$	2.5	0.35	0.65	850	6.9
	3	0.40	0.60	944.4	9.8
	4	0.39	0.61	925.6	11.4
	5	0.43	0.57	937.3	11.1
	6	0.61	0.39	746	17.6
	8	0.49	0.51	905	9.9
	10	0.65	0.35	820	60.25
	12	0.46	0.54	722	11.9
	15	0.60	0.40	688.6	12.64

Table 4.9. Constants for the S235JR ultimate tensile strength of $(f_u)_T$ used in Equation (4.2).

	Thickness of plate (mm)	C_5	C_6	C_7	C_8
$(f_u)_T$	0.76833	0.23014	769.3	16.27	83.28
	0.72	0.288	818.3	6.17	5.64
	0.47	0.534	1107.75	3.45	4.815
	-8.087	9.084	6667.2	2.07	4.14

The statistical measures of the predicted quantities, normalized by the test results, are given in Table 4.10- Table 4.18 for S700MC steel and Table 4.19- Table 4.22 for S235JR steel.

Table 4.10. Statistics for the ratio of estimated to test values for $t = 2.5$ mm specimens

	P-F Mechanical Properties					
	$f_{y,0.2}$	$f_{y,0.5}$	$f_{y,1.5}$	$f_{y,2.0}$	f_u	E
Average	0.98	0.98	1.00	1.00	1.00	1.02
Standard deviation	0.05	0.06	0.04	0.05	0.03	0.05
Maximum	1.07	1.08	1.06	1.07	1.03	1.11
Minimum	0.91	0.90	0.93	0.93	0.96	0.96

Table 4.11. Statistics for the ratio of estimated to test values for $t = 3.0$ mm specimens

	P-F Mechanical Properties					
	$f_{y,0.2}$	$f_{y,0.5}$	$f_{y,1.5}$	$f_{y,2.0}$	f_u	E
Average	0.98	0.96	0.98	0.99	1.00	1.03
Standard deviation	0.09	0.10	0.05	0.06	0.04	0.05
Maximum	1.13	1.14	1.05	1.05	1.04	1.11
Minimum	0.86	0.83	0.88	0.88	0.91	0.95

Table 4.12. Statistics for the ratio of estimated to test values for $t = 4.0$ mm specimens

	P-F Mechanical Properties					
	$f_{y,0.2}$	$f_{y,0.5}$	$f_{y,1.5}$	$f_{y,2.0}$	f_u	E
Average	0.97	0.96	0.97	0.98	0.99	0.99
Standard deviation	0.11	0.07	0.04	0.05	0.01	0.03
Maximum	1.19	1.06	1.00	1.04	1.00	1.03
Minimum	0.83	0.85	0.88	0.89	0.98	0.94

Table 4.13. Statistics for the ratio of estimated to test values for $t = 5.0$ mm specimens

	P-F Mechanical Properties					
	$f_{y,0.2}$	$f_{y,0.5}$	$f_{y,1.5}$	$f_{y,2.0}$	f_u	E
Average	0.99	0.97	0.98	0.98	0.98	1.03
Standard deviation	0.10	0.06	0.04	0.04	0.04	0.03
Maximum	1.19	1.04	1.02	1.02	1.01	1.07
Minimum	0.83	0.85	0.89	0.90	0.91	1.00

Table 4.14. Statistics for the ratio of estimated to test values for $t = 6.0$ mm specimens

	P-F Mechanical Properties					
	$f_{y,0.2}$	$f_{y,0.5}$	$f_{y,1.5}$	$f_{y,2.0}$	f_u	E
Average	0.99	0.97	0.98	0.98	0.99	1.00
Standard deviation	0.10	0.04	0.06	0.01	0.03	0.01
Maximum	1.16	1.04	1.09	1.00	1.05	1.01
Minimum	0.84	0.91	0.91	0.96	0.94	0.97

Table 4.15. Statistics for the ratio of estimated to test values for $t = 8.0$ mm specimens

	P-F Mechanical Properties					
	$f_{y,0.2}$	$f_{y,0.5}$	$f_{y,1.5}$	$f_{y,2.0}$	f_u	E
Average	0.98	0.96	0.97	0.97	0.98	1.00
Standard deviation	0.02	0.06	0.05	0.05	0.04	0.02
Maximum	1.00	1.00	1.02	1.02	1.02	1.04
Minimum	0.95	0.83	0.86	0.87	0.89	0.97

Table 4.16.. Statistics for the ratio of estimated to test values for $t = 10.0$ mm specimens

	P-F Mechanical Properties					
	$f_{y,0.2}$	$f_{y,0.5}$	$f_{y,1.5}$	$f_{y,2.0}$	f_u	E
Average	0.98	0.96	0.96	0.98	1.01	1.00
Standard deviation	0.03	0.05	0.06	0.03	0.02	0.01
Maximum	1.04	1.02	1.01	1.02	1.06	1.02
Minimum	0.94	0.86	0.87	0.92	0.98	0.98

Table 4.17. Statistics for the ratio of estimated to test values for $t = 12.0$ mm specimens

	P-F Mechanical Properties					
	$f_{y,0.2}$	$f_{y,0.5}$	$f_{y,1.5}$	$f_{y,2.0}$	f_u	E
Average	1.01	1.00	1.00	1.00	1.00	1.00
Standard deviation	0.02	0.01	0.01	0.01	0.01	0.02
Maximum	1.04	1.02	1.01	1.02	1.02	1.04
Minimum	0.98	0.98	0.98	0.98	0.99	0.99

Table 4.18. Statistics for the ratio of estimated to test values for $t = 15.0$ mm specimens

	P-F Mechanical Properties					
	$f_{y,0.2}$	$f_{y,0.5}$	$f_{y,1.5}$	$f_{y,2.0}$	f_u	E
Average	1.00	1.00	0.97	1.00	1.00	1.00
Standard deviation	0.02	0.01	0.09	0.02	0.01	0.02
Maximum	1.03	1.03	1.08	1.04	1.02	1.03
Minimum	0.97	0.98	0.80	0.96	0.98	0.97

Table 4.19. Statistics for the ratio of estimated to test values for $t = 6.0$ mm specimens of CCMS S235JR

	P-F Mechanical Properties	
	f_y	f_u
Average	1	1
Standard deviation	0.03	0.00
Maximum	1.01	1
Minimum	0.95	0.99

Table 4.20. Statistics for the ratio of estimated to test values for $t = 8.0$ mm specimens of CCMS S235JR

	P-F Mechanical Properties	
	f_y	f_u
Average	1	1
Standard deviation	0.07	0.02
Maximum	1.04	1.02
Minimum	0.95	0.97

Table 4.21. Statistics for the ratio of estimated to test values for $t = 10.0$ mm specimens of CCMS S235JR

	P-F Mechanical Properties	
	f_y	f_u
Average	1	1
Standard deviation	0.04	0.02
Maximum	1.07	1
Minimum	0.95	0.97

Table 4.22. Statistics for the ratio of estimated to test values for $t = 12.0$ mm specimens of CCMS S235JR

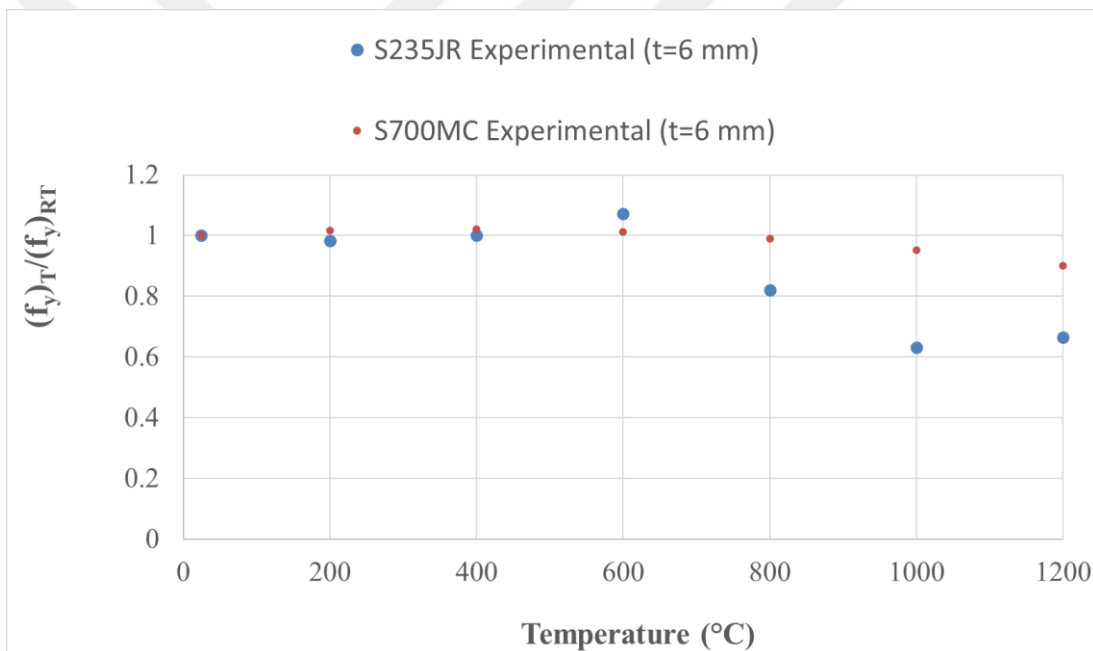
	P-F Mechanical Properties	
	f_y	f_u
Average	1	1
Standard deviation	0.00	0.02
Maximum	1.01	1.03
Minimum	0.98	0.98

The normalized value averages are generally near unity, suggesting the viability of the suggested models. The range of standard deviations is 0.02 to 0.11. All normalized values lie between 0.80 and 1.19, which shows that the proposed models give an accurate model for practical design purposes. These results show that developed expressions can accurately describe experimental results.

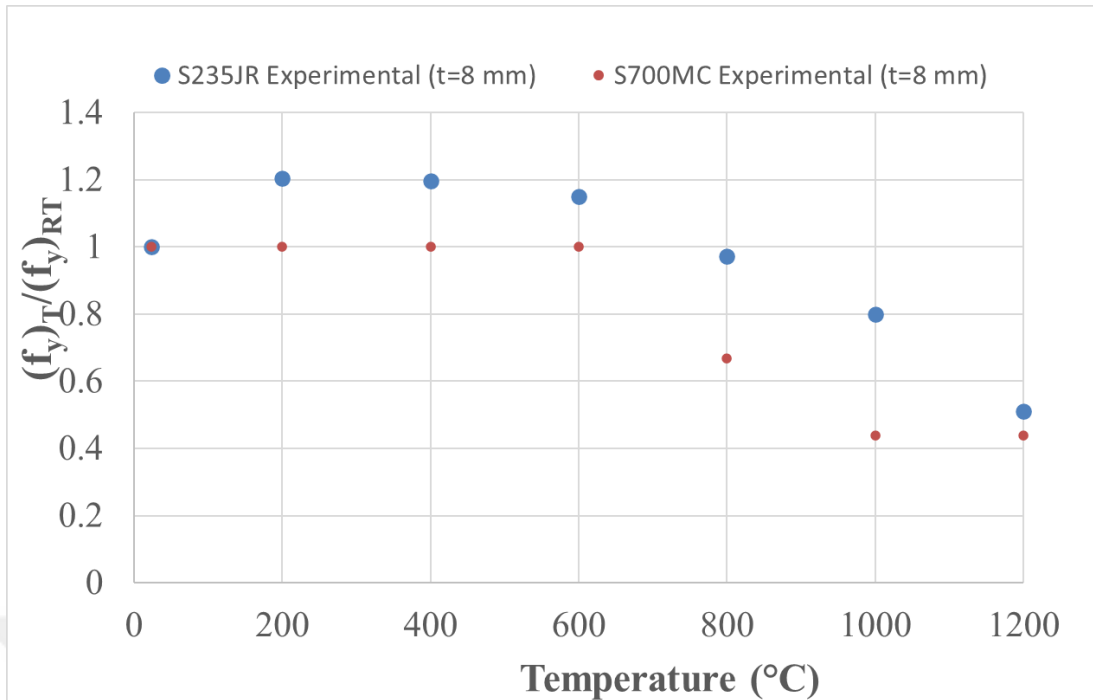
These newly proposed expressions based on experimental investigation and previous results conducted by other researchers can be employed to estimate changes in the mechanical parameters of HSS and CCMS after experiencing high temperatures. These equations are valid when HS steels with yield strengths up to 700 MPa and CCM steels with yield strengths up to 420 MPa are exposed to temperatures of 1200 °C and lower.

As shown in Figure 4.1, no significant changes occur in the yield strength of both S235JR and S700MC steels when heated to temperatures up to 600 °C and cooled in air. However, when temperatures exceed 600 °C, the yield strength loss becomes significant. For a thickness of 6 mm, S235JR steel experiences a strength loss of up to 40%, while S700MC steel experiences a strength loss of up to 10%. It can be observed that the yield strength loss of S700MC steel tends to increase with thickness. Specifically, for a thickness of 12 mm, the strength loss of S235JR steel remains around 40%, whereas the strength loss of S700MC steel can reach up to 70%. When Figure 4.2 is examined, a similar situation is observed for ultimate strength. It can be observed that although the yield strength loss of S700MC steel tends to increase with thickness, thickness has no significant effect on S235JR steel. The highest yield strength loss for S235JR steel was measured as 50% for 8 mm thickness and 1200 °C temperature, and for S700MC steel it was measured as 70% for 12 mm thickness and 1200 °C temperature. There are no significant changes in ultimate strength up to 600 °C, but temperatures exceeding 600 °C cause significant damage to the steel. The

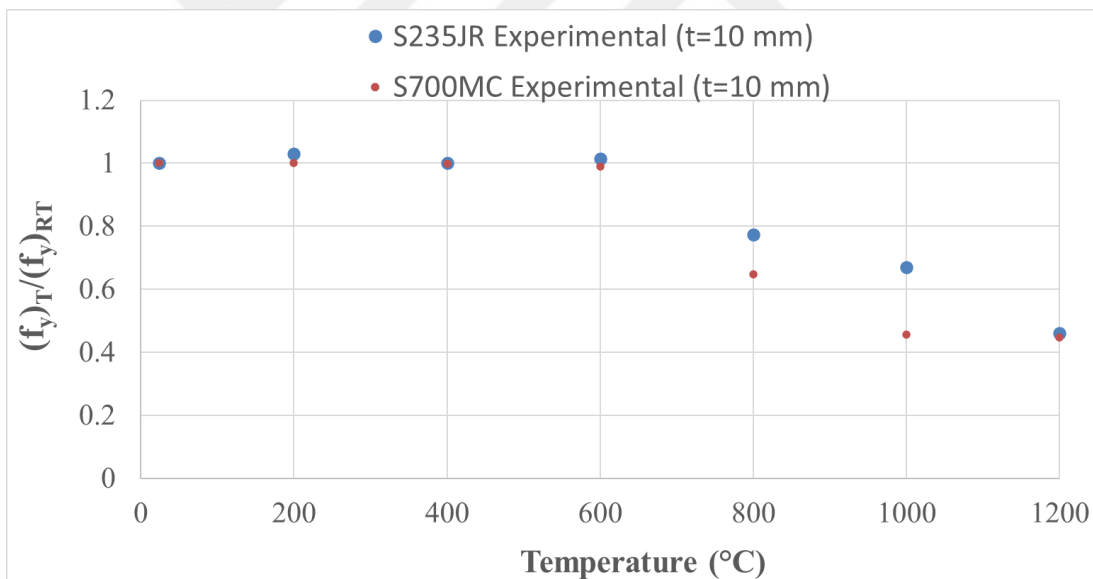
effect of thickness on ultimate strength loss is limited. In the case of exposure to high temperatures, the ultimate strength loss is generally around 30% for S235JR steel, while for S700MC steel, it varies but can reach up to 50%. When Figure 4.3 is examined, it can be seen that the damage caused by high temperatures to the YS and UTS values does not occur in the modulus of elasticity. The change in the modulus of elasticity (E) is limited until 800°C for S235JR steel, whereas for S700MC, it remains limited until 600°C but then linearly decreases above this temperature for both steels. The maximum loss in the modulus of elasticity for S235JR is approximately 20% for 10 mm and 12 mm thicknesses, and about 35% for 6 mm and 8 mm thicknesses at 1200°C. For S700MC, the maximum loss in the modulus of elasticity reaches up to 40% for smaller thicknesses (2.5 mm, 3 mm, 4 mm) at 1200°C, while for larger thicknesses, the maximum loss does not exceed 20%.



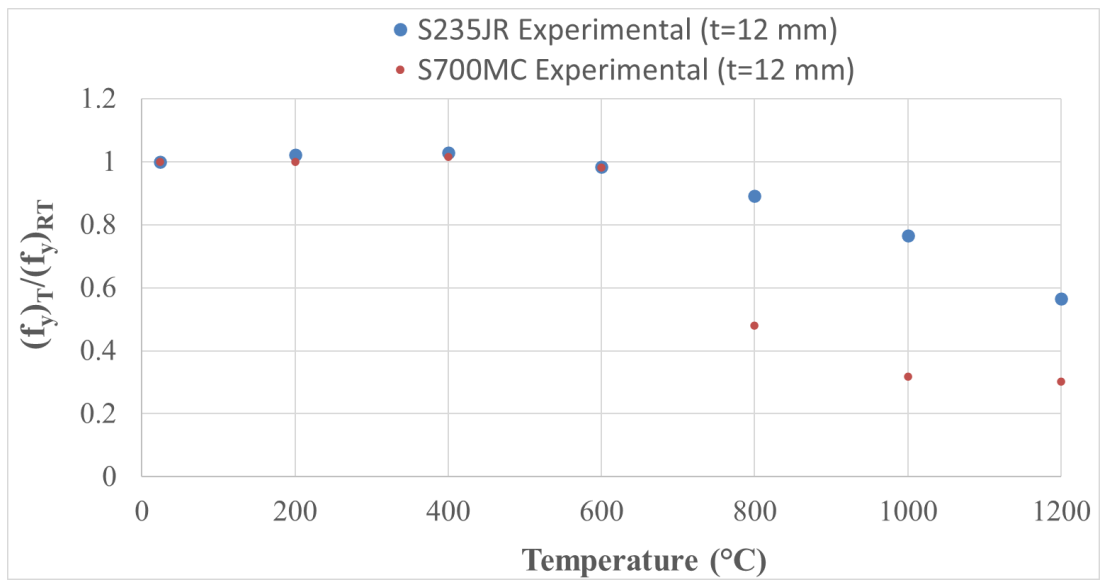
a) Comparison of yield strength of S235JR and S700MC for t=6 mm



b) Comparison of yield strength of S235JR and S700MC for $t=8$ mm

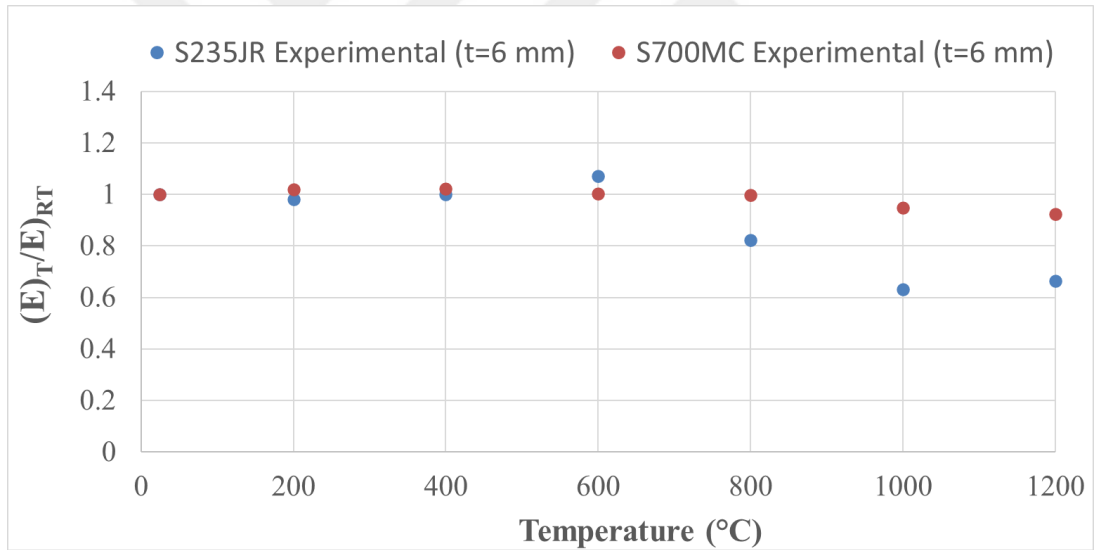


c) Comparison of yield strength of S235JR and S700MC for $t=10$ mm

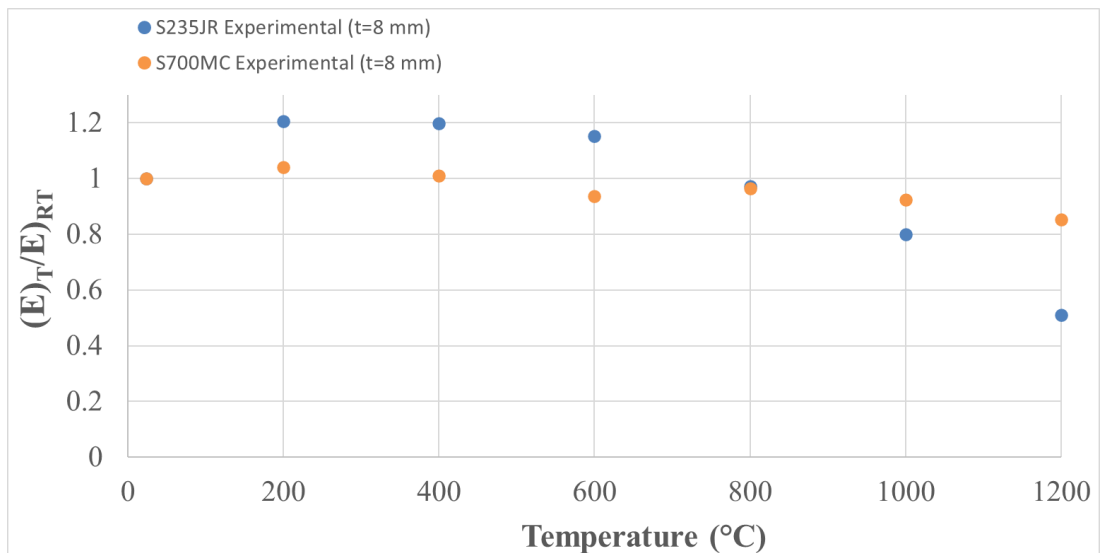


d) Comparison of yield strength of S235JR and S700MC for $t=12$ mm

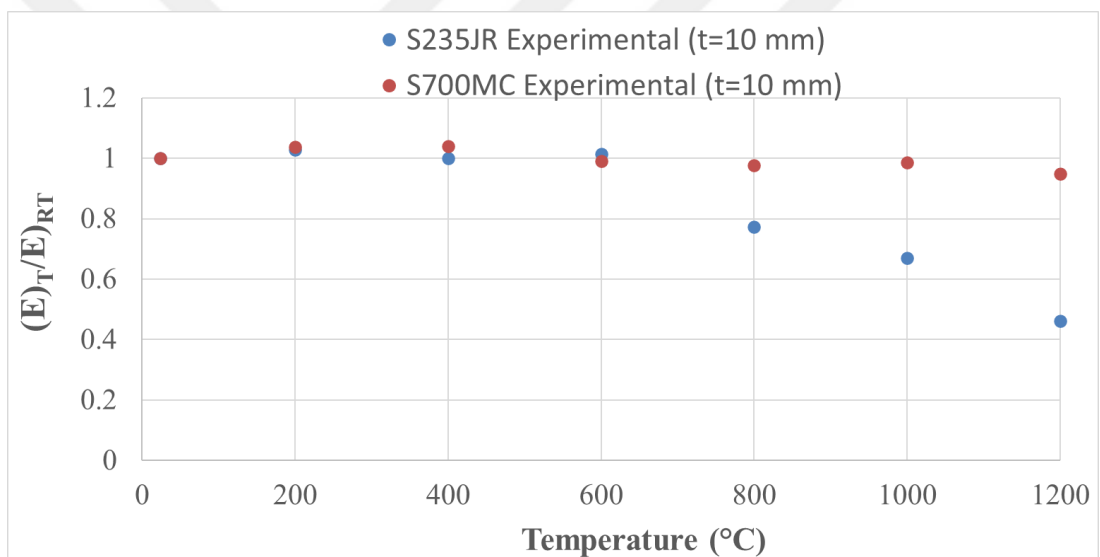
Figure 4.1. Comparison of yield strength of S235JR and S700MC for different thickness



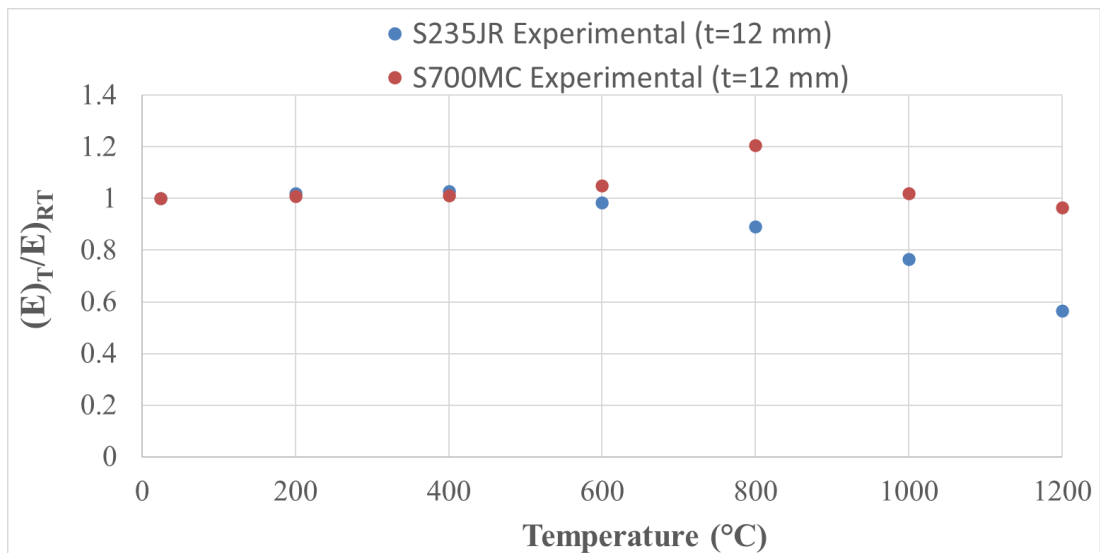
a) Comparison of ultimate strength of S235JR and S700MC for $t=6$ mm



b) Comparison of elasticity modulus of S235JR and S700MC for t=8 mm

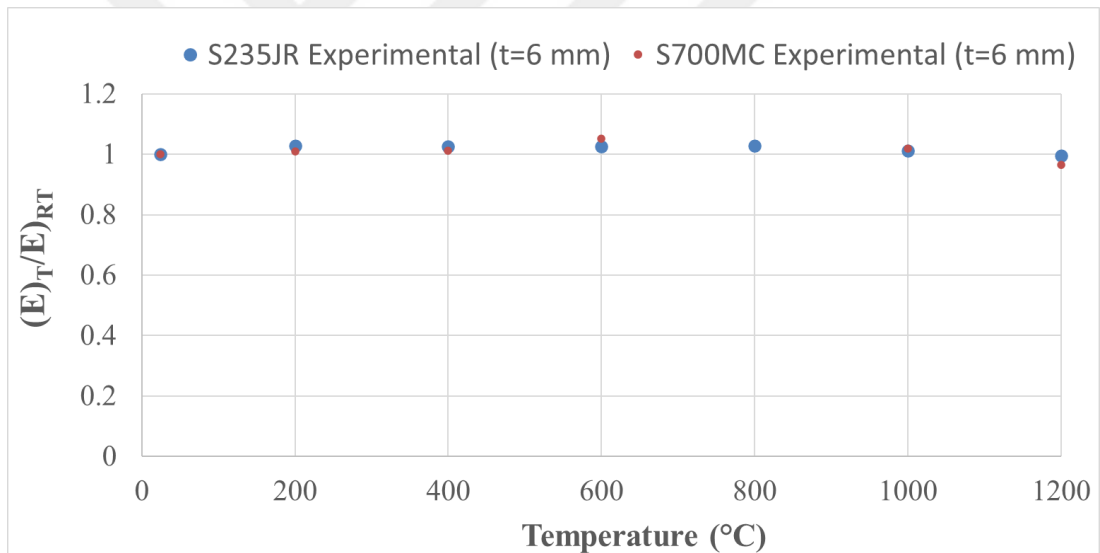


c) Comparison of elasticity modulus of S235JR and S700MC for t=10 mm

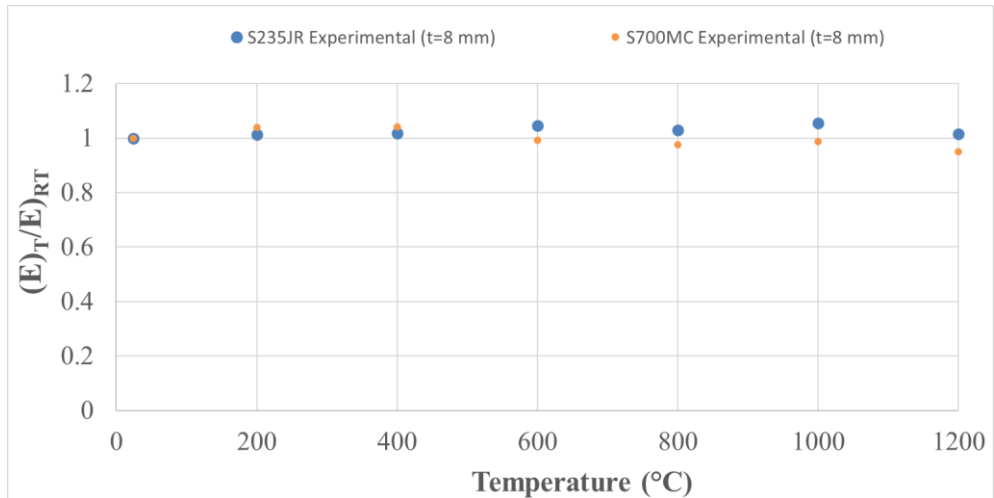


d) Comparison of elasticity modulus of S235JR and S700MC for $t=12$ mm

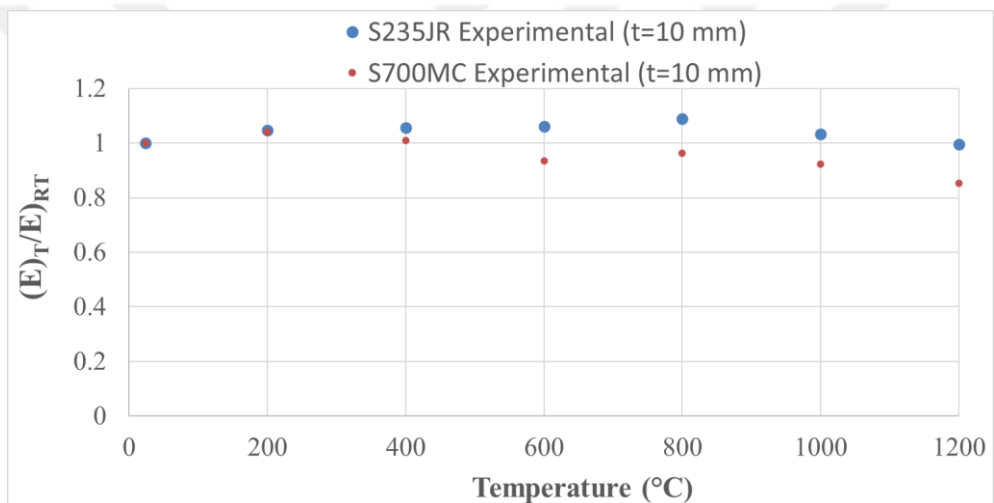
Figure 4.2. Comparison of elasticity modulus of S235JR and S700MC for different thickness



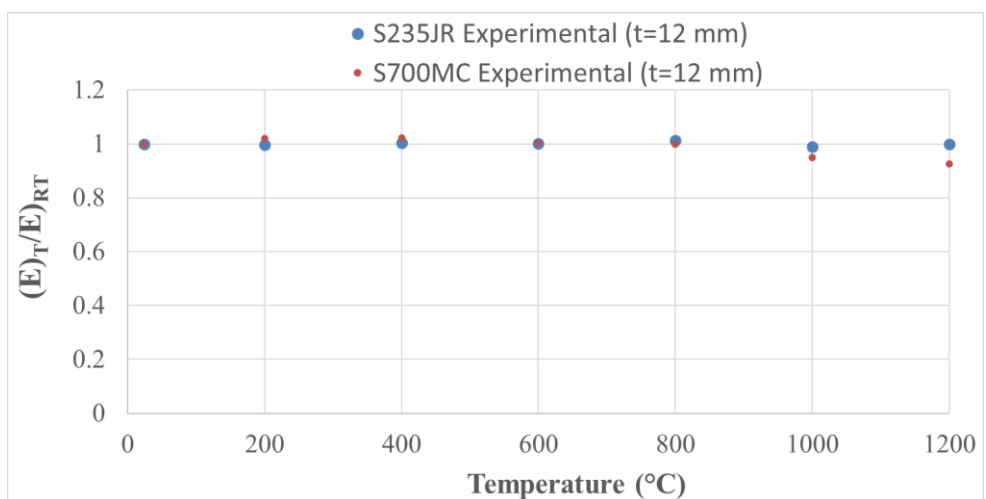
a) Comparison of elasticity modulus of S235JR and S700MC for $t=6$ mm



b) Comparison of elasticity modulus of S235JR and S700MC for $t=8$ mm



c) Comparison of elasticity modulus of S235JR and S700MC for $t=10$ mm



a) Comparison of elasticity modulus of S235JR and S700MC for $t=12$ mm

Figure 4.3. Comparison of elasticity modulus of S235JR and S700MC for different thickness

5. CONCLUSIONS AND FUTURE RESEARCH NEEDS

A combined experimental and parametric research study on the response of the S700MC and S235JR steel grade subjected to different high temperatures was performed. The experimental study consisted of S700MC tensile test coupons extracted from steel plates with thicknesses ranging from 2.5 mm to 15 mm and S235JR tensile test coupons extracted from steel plates with thicknesses ranging from 6 mm to 12 mm. These specimens were subjected to different high temperatures up to 1200 °C and then permitted to cool to normal room temperature by natural air cooling. The mechanical behavior of each test sample was identified by tensile tests. The results indicated that the strength and stiffness of most S700MC test specimens was not affected much until the temperature reached 600°C. However, the exposure temperature dramatically influences the behavior of S700MC when the temperature exceeds 600 °C. According to the research, it has been observed that YS and UTS may decrease even at low temperatures as the sample thickness increases in S235JR steel. It has been observed that after exposure to elevated temperatures (600 °C and higher), the strength values decrease, but the ductility increases. The yield strength of S235JR and S700MC steels remains stable up to 600°C. Beyond this temperature, significant yield strength loss occurs. For S235JR steel with a 6 mm thickness, the loss is up to 40%, and for S700MC, it is up to 10%. At 12 mm thickness, S235JR's strength loss remains around 40%, but S700MC's loss can reach up to 70%. Ultimate strength shows similar trends, with significant loss beyond 600°C. S235JR steel loses about 30% of its ultimate strength, while S700MC's loss can reach up to 50%. The elasticity modulus for both steels shows negligible changes. P-F mechanical properties of the high-strength S700MC and conventional carbon mild S235JR steels are mostly different from each other depending on the specimen thickness. In the second phase of the study, a parametric study was conducted to propose more generalized assessment criteria for the HS and CCM steels after experiencing the fire event. A novel set of empirical expressions was developed to accurately predict the yield strength, ultimate tensile strength, and elastic modulus of tested steels after exposure to fire. Good agreement

was observed between the developed expressions and the tensile test results. The simple expressions developed for high strength S700 MC and conventional carbon mild S235JR steels can be employed to assess the fire resistance of buildings constructed with HSS with a yield strength of up to 700 MPa and CCMS with a yield strength of up to 420 MPa. Since the proposed expressions are quite general, they are suitable for direct adoption into design specifications.

This study is limited to HSS with nominal yield strengths up to 700 MPa and CCMS with nominal yield strengths up to 420 MPa. There is a lack of information on the mechanical properties of ultra-high strength steels (UHSs) with a yield strength greater than 700 MPa. Future studies need to focus on UHSs, as other steels with YSs above 700 MPa have different chemical compositions. On the other hand, it was observed that different cooling methods had also different effects on the P-F mechanical properties of HS and CCM steels. In this study, natural air cooling was utilized to mimic the P-F state, and therefore different cooling techniques such as water, foam and CO₂ fire extinguisher should also be the subject of future research. Although it is important to determine the mechanical properties of HS and CCM steels after fire in order to evaluate the service life of buildings more rationally, the next phase of this work will address the constitutive models of such steels after exposure to fire.

REFERENCES

Adams, P. F. G. (1966) Plastic design in high strength steel, *Lehigh University*.

ASTM E1876-15 Standard (2015) Test method for dynamic Young's Modulus, shear Modulus, and Poisson's ratio by impulse excitation of vibration. ASTM International, West Conshohocken, PA.

Azhari, F., Tan, K. H., Zhao, O., & Tan, J. (2017) Post-fire mechanical response of ultra-high strength (Grade 1200) steel under high temperatures: Linking thermal stability and microstructure, *Thin-Walled Struct.*, 119: 114-125.

Balakrishnan, M., Leitão, C., Craveiro, D., Rodrigues, D. M., Santiago, A., da Silva, L. S., & Subramanian, C. (2022). Post-fire tensile properties of S355 J2 structural steel welded connections for construction industrial applications. *Metall. Res. Technol.*, 119, 511.

Chen, J., Young, B., & Uy, B. (2006) Behavior of high strength structural steel at elevated temperatures, *J. Struct. Eng.*, 132(12): 1948-1954.

Chen, S., Gao, S., Zhou, Q., & Wang, L. (2022) Design for local buckling behaviour of welded high strength steel I-sections under bending, *Thin-Walled Struct.*, 172: 108792.

Chiew, S. P., Zhao, M. S., & Lee, C. K. (2014) Mechanical properties of heat-treated high strength steel under fire/post-fire conditions, *J. Constr. Steel Res.*, 98: 12-19.

Code, P. (2007) Eurocode 3: Design of steel structures-part 1-2: *General rules-structural fire design*, London: European Committee for Standardisation.

Collin, P., & Johansson, B. Eurocode for high strength steel and applications in construction, *Associazione Italiana di Metallurgia*.

Dan, W.-J., Gou, R.-B., Yu, M., Ge, Y.-B., & Li, T.-J. (2022). Experimental study on the post-fire mechanical behaviours of structural steels. *J. Constr. Steel Res.*, 199, 107629.

Din, E. N. (2013) 10149-2: 2013: Hot rolled flat products made of high yield strength steels for cold forming—Part 2: *Technical delivery conditions for thermomechanically rolled steels*; German version, Deutsches Institut für Normung eV.

EN (2007) Eurocode 3. Design of steel structures. Part 1-12. *Additional rules for the extension of EN 1993 up to steel grades S 700*.

Glassman, J. D., Gomez, A., Garlock, M. E. M., & Ricles, J. (2020). Mechanical properties of weathering steels at elevated temperatures. *J. Constr. Steel Res.*, 168, 105996.

Haaijer, G. (1963) Economy of high strength steel structural members, *Trans. Am. Soc. Civ. Eng.*, 128(2): 820-842.

Gunalan, S., & Mahendran, M. (2014). Experimental investigation of post-fire mechanical properties of cold-formed steels. *Thin-Walled Struct.*, 85, 166–175.

Hu, F., & Wang, Z. (2023) Seismic behaviour of high-strength steel bolted extended end-plate connections, *ce/papers*, 6(3-4): 639-644.

Jiang, K., Tan, K. H., & Zhao, O. (2021) Block tearing of S700 high strength steel bolted connections: Testing, numerical modelling and design, *Eng. Struct.*, 246: 112979.

Jiang, K., Tan, K. H., & Zhao, O. (2021) Net section fracture of S700 high strength steel staggered bolted connections, *Thin-Walled Struct.*, 164: 107904.

Kang, L., Sun, F., & Li, Z. (2021) Experimental study on post-fire mechanical performances of high strength steel Q460, *Adv. Struct. Eng.*, 24(12): 2791-2808.

Kiran, R., & Sajid, H. U. (2019). Post-fire mechanical behavior of ASTM A572 steels subjected to high stress triaxialities. *Eng. Struct.*, 190, 220–233.

Kuhlmann, U., Braun, M., & Saari, J. (2021) Update on the revision of Eurocode 3: Evolution by improvement and harmonization, *Steel Constr.*, 14(1): 2-13.

Lee, C.-H. (2017) Structural performance of 800 MPa high-strength steel members and application to highrise and mega building structures, *Int. J. High-Rise Build.*, 6(3): 249-259.

Li, G.-Q., Lyu, H., & Zhang, C. (2017) Post-fire mechanical properties of high strength Q690 structural steel, *J. Constr. Steel Res.*, 132: 108-116.

Li, H.-T., & Young, B. Post-fire mechanical properties of high strength steels, *Univ. Politècnica de València*.

Li, W., Zhao, X., Liu, H., & Sun, X. (2024) Post-fire mechanical properties and constitutive model of Q690 high-strength structural steel, *Eng. Fail. Anal.*, 160: 108232.

Lin, X.-M., Ma, C., Wang, Y., & Yan, S. (2021) A study of net-section resistance of high strength steel bolted connections, *Thin-Walled Struct.*, 159: 107284.

Lu, J., Liu, H., Chen, Z., & Liao, X. (2016). Experimental investigation into the post-fire mechanical properties of hot-rolled and cold-formed steels. *J. Constr. Steel Res.*, 121, 291–310.

Molkens, T., Cashell, K. A., & Rossi, B. (2021) Post-fire mechanical properties of carbon steel and safety factors for the reinstatement of steel structures, *Eng. Struct.*, 234: 111975.

Nie, S., He, H., Wang, W., & Yuan, G. (2018) Investigation of residual stresses in Q460GJ steel plates from medium-walled box sections, *J. Constr. Steel Res.*, 148: 728-740.

Outinen, J., Kaitila, O., & Mäkeläinen, P. (2001). High-temperature testing of structural steel and modelling of structures at fire temperatures. *Helsinki Univ. Technol. Lab. Steel Struct. Publ.*, 23.

Outinen, J., & Mäkeläinen, P. (2004). Mechanical properties of structural steel at elevated temperatures and after cooling down. *Fire Mater.*, 28, 237–251.

Qiang, X., Bijlaard, F. S. K., & Kolstein, H. (2012) Dependence of mechanical properties of high strength steel S690 on elevated temperatures, *Constr. Build. Mater.*, 30: 73-79.

Qiang, X., Bijlaard, F. S. K., & Kolstein, H. (2012) Post-fire mechanical properties of high strength structural steels S460 and S690, *Eng. Struct.*, 35: 1-10.

Qiang, X., Bijlaard, F. S. K., & Kolstein, H. (2013) Post-fire performance of very high strength steel S960, *J. Constr. Steel Res.*, 80: 235-242.

Qiang, X., Bijlaard, F. S. K., & Kolstein, H. (2014) Behaviour of beam-to-column high strength steel endplate connections under fire conditions – Part 1: Experimental study, *Eng. Struct.*, 64: 23-38.

Qiang, X., Bijlaard, F. S. K., & Kolstein, H. (2016) Mechanical properties and design recommendations of very high strength steel S960 in fire, *Eng. Struct.*, 112: 60-70.

Ren, C., Dai, L., Huang, Y., & He, W. (2020). Experimental investigation of post-fire mechanical properties of Q235 cold-formed steel. *Thin-Walled Struct.*, 150, 106651.

Sajid, H. U., & Kiran, R. (2018). Influence of stress concentration and cooling methods on post-fire mechanical behavior of ASTM A36 steels. *Constr. Build. Mater.*

Saufnay, L., Jaspart, J. P., & Demonceau, J. F. (2021) Economic benefit of high strength steel sections for steel structures, *ce/papers*, 4(2-4): 1543-1550.

Shakil, S., Lu, W., & Puttonen, J. (2020) Experimental studies on mechanical properties of S700 MC steel at elevated temperatures, *Fire Saf. J.*, 116: 103157.

Shi, G., Hu, F., & Shi, Y. (2014) Recent research advances of high strength steel structures and codification of design specification in China, *Int. J. Steel Struct.*, 14: 873-887.

Standard, B. (2001) BS 5950: Structural use of steel works in building.

Tan, K. H., Zhao, O., Azhari, F., & Tan, J. (2017) Post-fire mechanical response of ultra-high strength (Grade 1200) steel under high temperatures: Linking thermal stability and microstructure, *Thin-Walled Struct.*, 119: 114-125.

Tankova, T., Rodrigues, F., Leitao, C., Martins, C., & Da Silva, L. S. (2021) Lateral-torsional buckling of high strength steel beams: Experimental resistance, *Thin-Walled Struct.*, 164: 107913.

Wang, W., Liu, T., & Liu, J. (2015) Experimental study on post-fire mechanical properties of high strength Q460 steel, *J. Constr. Steel Res.*, 114: 100-109.

Wang, W., Xia, Y., & Li, G.-Q. (2018) Fire resistance studies on high strength steel structures, *Int. J. High-Rise Build.*, 7(4): 287-298.

Wang, W.-Y., Liu, B., & Kodur, V. (2013) Effect of temperature on strength and elastic modulus of high-strength steel, *J. Mater. Civ. Eng.*, 25(2): 174-182.

Yazici, C. (2024). Mechanical properties of S235 steel protected with intumescent coatings under high temperatures: An experimental study. *Buildings*, 14(6), 1597.

Xiong, M.-X., Liew, J. Y. R., & Du, Y. (2017) Effects of heat-treatment methods on mechanical performance of high-tensile strength steel subject to elevated temperatures, in Applications of Fire Eng., CRC Press, pp. 379-384.

Yin, H., Zhao, E., Zhang, X., & Yan, K. (2023). Evaluating post-fire mechanical performance of S355J2W weathering steel with different artificial cooling approaches. *Case Stud. Constr. Mater.*, 18(3), e02101.

Zeng, X., Liu, J., Wu, Y., & Gao, Z. (2021) Residual mechanical properties of Q890 high-strength structural steel after exposure to fire, *Constr. Build. Mater.*, 304: 124661.

Zhang, C., Jia, B., & Wang, J. (2020). Influence of artificial cooling methods on post-fire mechanical properties of Q355 structural steel. *Constr. Build. Mater.*, 252, 119092.

Zhou, H., Xu, W., & Wu, Z. (2019) Mechanical properties deterioration of high strength steels after high temperature exposure, *Constr. Build. Mater.*, 199: 664-675.

Zhou, X., Zhang, Y., Wang, X., & Liu, Q. (2021) Post-fire mechanical properties of Q620 high-strength steel with different cooling methods, *J. Constr. Steel Res.*, 180: 106608.

ÖZGEÇMİŞ VE ESERLER LİSTESİ

ÖZGEÇMİŞ

Adı ve Soyadı: V****| P****

Doğum Tarihi: **.**.****

Doğum Yeri: Batman

Cep Telefonu: +90 (5**) ***** **

**

E-postası: v****@g****.c**

Bildiği Yabancı Diller (Puan ve Yılı): İngilizce **,** Puan (***)

Uzmanlık Alanı:

Derece	Bölüm/Program	Üniversite	Yıl
Lisans	İnşaat Mühendisliği	İzmir Yüksek Teknoloji Enstitüsü	2021
Y. Lisans	İnşaat Mühendisliği	Muğla Sıtkı Koçman Üniversitesi	2024

Yüksek Lisans Tez Başlığı ve Tez Danışmanları: Post-Fire Response Of Different Steel Grade Materials, Öğr. Üyesi Dr. Özer ZEYBEK,

ESERLER

A. Uluslararası hakemli dergilerde yayımlanan makaleler:

A1. The response of high strength S700 MC steel after fire exposure (Journal of Constructional Steel Research 219, 2024, 108790)